

The Potential for Quagga Mussel Survival in Canyon Lake

by

Theresa Lau

A Thesis Presented in Partial Fulfillment
of the Requirements for the Degree
Master of Science

Approved April 2018 by the
Graduate Supervisory Committee:

Peter Fox, Chair
Susanne Neuer
Morteza Abbaszadegan

ARIZONA STATE UNIVERSITY

May 2018

ABSTRACT

Quagga mussels are an aquatic invasive species capable of causing economic and ecological damage. Despite the quagga mussels' ability to rapidly spread, two watersheds, the Salt River system and the Verde River system of Arizona, both had no quagga mussel detections for 8 years. The main factor thought to deter quagga mussels was the stratification of the two watersheds during the summer, resulting in high temperatures in the epilimnion and low dissolved oxygen in the hypolimnion. In 2015, Canyon Lake, a reservoir of the Salt River watershed, tested positive for quagga mussel veligers. In this study, I used Landsat 7 and Landsat 8 satellite data to determine if changes in the surface temperature have caused a change to the reservoir allowing quagga mussel contamination. I used a location in the center of the lake with a root mean squared error (RMSE) of 0.80 and a correlation coefficient (R^2) of 0.82, but I did not detect any significant variations in surface temperatures from recent years. I also measured 21 locations on Canyon Lake to determine if the locations in Canyon Lake were able to harbor quagga mussels. I found that summer stratification caused hypolimnion dissolved oxygen levels to drop well below the quagga mussel threshold of 2mg/L. Surface temperatures, however were not high enough throughout the lake to prevent quagga mussels from inhabiting the epilimnion. It is likely that a lack of substrate in the epilimnion have forced any quagga mussel inhabitants in Canyon Lake to specific locations that were not necessarily near the point of quagga veliger detection sampling. The research suggests that while Canyon Lake may have been difficult for quagga mussels to infest, once they become established in the proper locations, where they can survive through the summer, quagga mussels are likely to become more prevalent.

ACKNOWLEDGMENTS

I would like to thank all the people and the organizations which made this research possible. This project was supported by the Arizona Game and Fish Department and Erin Raney as Director of Aquatic Invasive Species. I am also grateful for support from Salt River Project. This project would not have been possible if not for those at the Regional Water Quality Project, especially Marisa Masles, who was very helpful and provided us with indispensable data for the project's conception. I would like to thank students and staff at Arizona State University for the wonderful support I received in pursuing this project. Not only was I encouraged by faculty in my courses, but other students and faculty were so friendly and helpful, I am forever grateful to have met them all. Thank you, Dr. Nuer for taking me on excursions to Saguaro Lake and teaching me about the biological side of reservoir research. From you, I learned about how to structure my research and procedures. Thank you, Dr. Abbaszadegan. Your enthusiasm for teaching and understanding of topics taught me so much in how to think about not only my own research, but all research I come across. In particular, I'd like to thank Dr. Peter Fox and Andrew Buell for being there for me regularly to handle tasks that I could not do alone. Andrew, thanks for teaching me how to sample quagga mussels, for helping me drive the boat through windy weather, and for being both a great coworker and a good friend. Dr. Fox, I don't know where I would have been without your support. I owe so much to you for bringing in someone who didn't even qualify for graduate school and allowing me to grow into the engineer I had always wished I could be. Finally, I'd like to thank my family and friends, who believed in me, supported me, and kept me sane through exams and deadlines.

TABLE OF CONTENTS

	Page
LIST OF TABLES	v
LIST OF FIGURES	vi
CHAPTER	
1. INTRODUCTION	1
OBJECTIVES	2
2. LITERATURE REVIEW	2
QUAGGA MUSSELS.....	2
Biology.....	2
Ecological Impact.....	4
Economic Impact.....	4
Detection.....	6
Invasion.....	6
History in Arizona.....	7
CANYON LAKE RESERVOIR.....	10
LANDSAT SATELLITE REMOTE SENSING	12
Landsat 7.....	12
Landsat 8.....	16
REGIONAL WATER QUALITY DATA.....	19
ON-SITE DATA COLLECTION	28
3. RESULTS	32

SURFACE TEMPERATURE: SATELLITE DATA COMPARED TO ON-SITE DATA	32
SURFACE TEMPERATURE TRENDS	41
ON-SITE TEMPERATURE AND DISSOLVED OXYGEN DATA	44
QUAGGA MUSSEL SURVIVABILITY IN CANYON LAKE.....	51
4. CONCLUSIONS	52
REFERENCES	55
APPENDIX	
A. ACRONYMS	58
B. ON-SITE TEMPERATURE AND DISSOLVED OXYGEN TRENDS FOR ALL LOCATIONS.....	60
C. APPENDIX C DATES OF QUAGGA-INHOSPITABLE CONDITIONS	103

LIST OF TABLES

Table 1 SRP Daily Water Report..... 32

Table 2 Root Mean Squared Test for Each Location, All Landsat vs Landsat 7 vs Landsat
8..... 34

Table 3 Days of Inhospitable Conditions at Canyon Lake by Location and Depth 51

LIST OF FIGURES

Figure 1. Canyon Lake Reservoir from Google Maps 12

Figure 2. Regional Water Quality Data at Saguaro Lake, Temperature vs Depth 20

Figure 3. Regional Water Quality Data at Saguaro Lake, Dissolved Oxygen vs Depth..... 20

Figure 4. Regional Water Quality Data at Canyon Lake, Temperature vs Depth 21

Figure 5. Regional Water Quality Data at Canyon Lake, Dissolved Oxygen vs Depth..... 21

Figure 6. GloVis Available scenes containing Canyon Lake for August 2017 (Lake in yellow circle)
..... 23

Figure 7. Landsat 7, Band 6, High Gain Product for October 20, 2017 24

Figure 8. Landsat 7, Cropped image of Canyon Lake for August 2017, August 2016, and August
2015 25

Figure 9. Landsat 8, Band 10, Product for June 22, 2017 27

Figure 10. Landsat 8, Cropped image of Canyon Lake for August 2017, August 2016, and August
2015 28

Figure 11. Sampling Points 30

Figure 12. Close up Differences between Surface (Air) temperature and Temperatures Taken in
the Water from 0 to 2m Depths 31

Figure 13. Landsat Temperature vs On-Site Temperature Over Time at L02 35

Figure 14. Landsat Temperature vs On-Site Temperature at L02 Regression 35

Figure 15. Landsat Temperature vs On-Site Temperature Over Time at L07 36

Figure 16. Landsat Temperature vs On-Site Temperature at L07 Regression 37

Figure 17. Landsat Temperature vs On-Site Temperature Over Time at L05 37

Figure 18. Landsat Temperature vs On-Site Temperature at L05 Regression 38

Figure 19. Landsat Temperature vs On-site Temperature vs RWQ data Over Time for L08 38

Figure 20. Landsat Temperature vs On-Site Temperature for L08 Regression..... 39

Figure 21. Canyon Lake On-Site Surface Temperatures for June 14th, 2017 40

Figure 22. Canyon Lake On-Site surface temperatures for August 9th, 2017 40

Figure 23. Yearly Average Temperature from May to October for Canyon Lake 2007-2017 42

Figure 24. Long Term Summer Temperature Trends using Landsat and On-Site Data..... 43

Figure 25. On-Site Temperature Trends for L08 44

Figure 26 Close up Stratified Temperature vs Depth Trends for L08 45

Figure 27. Dissolved Oxygen vs Depth for L08 May and June 46

Figure 28. Dissolved Oxygen vs Depth for L08 July and August 46

Figure 29. Dissolved Oxygen vs Depth for L08 September and October 47

Figure 30. On-Site Temperature Trends for L08 48

Figure 31. Dissolved Oxygen Trends for L08 49

Figure 32 Close up Stratified Dissolved Oxygen vs Depth for Location L08 50

INTRODUCTION

Dreissena rostriformis bugensis, also known as quagga mussels, are an aquatic invasive species that poses a large problem in freshwater bodies. As a high priority aquatic invasive species, quagga mussels pose a threat to both local ecosystems and drinking water infrastructure. Since their initial detection in Lake Erie in 1989, they spread across the country to the Colorado River in just 17 years, threatening Arizona's precious water systems since 2007. Despite their rapid ability to spread, several of Phoenix, Arizona's major freshwater sources remained free of quagga mussels until detection in 2015. In a study conducted by Arizona State University in 2015, lab experiments on Saguaro Lake, of the Salt River system, and Bartlett Lake, of the Verde River system, suggested that summer stratifications, correlated with high surface temperatures, created an inhospitable environment for quagga mussels. During the summer in Saguaro Lake, surface temperatures rose above the quagga mussel's temperature threshold of 28°C, while a drop in dissolved oxygen in the two watersheds prevented infestation in deeper water. Recent detection of quagga mussel veligers in the Salt River system has brought concern that an external factor, impacting the surface temperature of the lake or an internal factor, inherent to the lake itself, may be allowing quagga mussels to survive in these supposedly inhospitable environments.

In lieu of the recent detection of quagga mussel veligers in Canyon Lake in the year 2015, an in-depth investigation was conducted on the reservoir's potential for quagga mussel infestation. Data was collected from 3 primary sources. The first data source was the Regional Water Quality Sampling Project by ASU. In addition, I collected data from Landsat 7 and Landsat 8 provided by the United States Geological Survey (USGS). The third source of data was taken in-situ and was obtained starting in late May, recording the seasonal summer decline in dissolved oxygen, and ending after the fall lake turnover in October. Using these three data sets, I seek to determine the underlying cause for recent detections of quagga mussel veligers in Canyon Lake, Arizona.

OBJECTIVES

1. Find underlying factors for the lack of detection of quagga mussel veligers in Canyon Lake from 2007 to 2015, and the reasons why they were detected in Canyon Lake recently.
2. Determine whether Canyon Lake contains hospitable zones for quagga mussels to survive and potentially thrive.
3. If hospitable, determine where quagga mussels might reside in Canyon Lake.

LITERATURE REVIEW

QUAGGA MUSSELS

Biology. The quagga mussel is a small bivalve mollusk, reaching up to 4cm in length. Named after the now extinct quagga zebra, the characteristic stripes of the quagga mussel typically fade as they get closer to the hinge of the shell (Benson, et al., 2017). They are closely related to another aquatic invasive species, *Dreissena polymorpha*, better known as the zebra mussel. The quagga mussel is typically distinguished from a zebra mussel by its fading stripes, larger adult size, rounder shape and asymmetric valves (Benson, et al., 2017).

Quagga mussels reproduce by broadcast spawning. A single female mussel can produce over one million eggs per year and fertilization, as well as larval development, are initiated in the water column. Compared to other broadcast spawning organisms, quagga mussels are less susceptible to issues in sperm dilution. Clusters of mussels can impact water flow to encourage concentration of eggs and sperm in eddies (Misamore, Barnard, Couch, & Wong, 2015). Sperm are also capable of successful fertilization 2 hours after spawning. While time of spawning for each mussel varies, in infested lakes, veligers can be found in the water column year-round. In the Great Lakes, quagga mussels in the hypolimnion were observed to offset their spawning time up to one week later than the quagga mussels in the epilimnion, with both spawning more abundantly in the spring and fall.

Although the early stages of quagga mussel development have not been closely studied, they are believed to follow similar stages as the zebra mussel. The zebra mussel larvae first begin with the trochophore stage between 6-96 hours post fertilization. Afterwards, the trochophore secretes its first larval shell, thereby becoming a veliger. 7-9 days post fertilization, a second larval shell forms. The second larval shell then grows and as it gets heavier, initiates the next larval stage. In the pediveliger stage, characterized by the growth of a foot and changes in behavior, the organism begins a shift toward the bottom of the water column, using the foot to move until it finds a suitable location to secrete byssal threads and attach. Byssal threads are proteinaceous filaments secreted from the ventral side of the mussel which allow it to firmly attach to surfaces. It is estimated that the pediveliger stage occurs between 18-90 days post fertilization, after which it is considered a post veliger and begins forming a mouth, gills and an adult shell (Misamore, Barnard, Couch, & Wong, 2015). The juvenile mussel takes a few months more to sexually mature. The adult quagga mussels live on average 2-3 years with the oldest known to live about 5 years.

As a result of their extensive ability to reproduce, quagga mussels in infested lakes can be found in dense colonies, even at great depths. In 2010, the density of a quagga mussel colony at Parker Dam in Lake Havasu, Arizona, was reported at 35,000/m². The deepest they have been found is 130m below the surface in the Great Lakes. (Benson, et al., 2017)

The scientific community is just learning about the unique characteristics of quagga mussels. Their tolerance to water qualities are, in many ways, still uncertain. In some research, quagga mussels were closely approximated by their cousin zebra mussels, ignoring that the species could have key differences that would affect their ability to infest. Calcium requirements for quagga mussels to build their shells were once thought to be similar to those of observed zebra mussels and water with 12ppm or lower concentrations of calcium were thought to be uninhabitable. Experiments have shown successful survival, growth and reproduction of quagga mussels in calcium levels that were considered low. Although field observations did not often

place quagga mussels at locations with low calcium, experiments were conducted which found that quagga mussels could survive calcium levels as low as 12ppm for 90 days. Although mussel mortality was high exceeding 170 days, at 15ppm adult mussels were able to survive up to one year (Davis, Emma, Achara, Chandra, & Jerde, 2015). Quagga mussels have also shown the capability to rapidly adapt to their environment. Low dissolved oxygen tolerance was studied using populations from different lakes in Western Europe. Differences in each colony's survival in low dissolved oxygen depended more on their source water than on their species identity (Ventura, Sarpe, Kopp, & Jokela, 2016). This suggests convergent adaptations from different strains to increase tolerance for low dissolved oxygen conditions.

Ecological Impact. In addition to their prolific nature, quagga mussels also heavily impact the waters that they invade. Quagga mussels are filter feeders and a single quagga mussel can filter a liter of water a day. As filter feeders, quagga mussels concentrate substances including many toxins, in their bodies and in the pseudofeces they expel (Benson, et al., 2017). The prey of the quagga mussels, the phytoplankton, are keystone to the local ecology. As the quagga mussels filter phytoplankton from the water column, zooplankton, which feed on the phytoplankton, are starved. In turn, predators that feed on zooplankton have less food, thereby creating a cascade of decreasing predator populations throughout the biome. The effect of quagga mussel filtration also changes the overall quality of the water, making the water clearer and causing imbalances in the local ecosystems that can lead to more intense algal blooms (Nelson & Nibling, 2013). Overall changes in water quality favor certain organisms over others and cause a decline in biodiversity. Invasion by quagga mussels creates a dramatic shift that impacts the aquatic trophic structure, nutrient cycling and biodiversity of the local aquatic ecosystem (Nelson & Nibling, 2013).

Economic Impact. Quagga mussels pose an economic threat as well due to their propensity to cause biofouling in infrastructure. The mussels heavily colonize hard surfaces and their dense, hard-packed colonies readily adhere to pipes and screens, causing clogs and putting

strain on pumps. The colonies also attach to docks, boats, buoys and even clutter beaches, putting strain on recreational activity as well. Though they flock to hard surfaces, they are also able to attach to soft surfaces as well. The quagga mussel's byssal threads allow it to attach very firmly and they are difficult to remove.

At present, to prevent quagga mussel biofouling there are only a few options available. Applying a preventative wax containing capsaicin to surfaces can decrease the rates of attachment to boats, docks and buoys, but requires constant maintenance and reapplication. Water distribution systems such as those in Arizona, cannot apply a wax throughout, and instead use a chemical pesticide, often derived from chlorine or copper (Takeguchi, Liang, & Yates, 2012). These pesticides can be harmful to local fish and wildlife. Since the mussels are also able to close their shells when they sense harmful chemicals, an otherwise lethal dose must be applied for a long time to ensure eradication. While more effective, better targeted substances are being developed, tested, and marketed, any solution available will still place an economic burden on utilities, industries and communities. A biopesticide using *Pseudomonas fluorescens* strain CL145A has shown promising results as a substance specifically targeted toward dreissenid mussels through intoxication (Molly, et al., 2013). *Pseudomonas fluorescens* CL145A is a common organism in soil which contains a compound that is toxic to dreissenid mussels. Unlike chlorine or copper pesticides, the *Pseudomonas fluorescens* is less likely to be detected as a toxin by the mussels and are more likely to be absorbed, killing the mussels by breaking down their stomach lining. Currently marketed as Zequanox, it is not yet approved in reservoirs and it is, at this time, too expensive to implement (Meehan, Shannon, Gruber, Rackl, & Lucy, 2014). Predators to quagga mussels also exist, though their overall effects on populations need more study. One such predator is the Redear Sunfish which preys on quagga mussels in Lake Havasu, Arizona (US Department of the Interior Bureau of Reclamation, 2015).

Detection. The presence of dreissenid mussels can be difficult to detect. The mussels themselves can be very small, reside in low light areas and are overall difficult for divers to spot. To detect if quagga mussels have contaminated a reservoir, the water is usually tested for quagga mussel veligers. The Bureau of Reclamation Detection Laboratory for Exotic Species (RDLES) in Denver, CO plays a primary role in the detection of invasive dreissenid populations in the western United States. The method they use involves microscopy, followed by DNA detection using Polymerase Chain Reaction (PCR), with the inclusion of scanning electron microscopy (SEM) and flow cell cytometry to confirm results (Carmon & Hosler, 2015). A 64µm plankton tow net with a weighted cup is used to collect water samples which are then preserved using buffer and alcohol. The sample is then allowed to settle overnight. The lab estimates a 98% veliger recovery rate using an optimized method for settling the veligers. They then use Cross Polarizing Light Microscopy (CPLM) to detect the veligers by their shell with 98% identification if the shell is not degraded. SEM is then used to clearly identify dreissenid veligers from other organisms with detectable shells. A taxonomist is consulted to confirm the identification of a quagga veliger and flow cytometry can also be used to determine the zooplankton communities as well as enumerate veligers. In quagga infested waters, there is often decreased zooplankton and high concentrations of veligers, which can indicate the intensity of quagga mussel infestation. The lab also conducts PCR using the DNA of positive and suspect samples to establish the organism's identity as a dreissenid. Prior to 2012, DNA extraction for dreissenid mussels was inefficient at breaking apart the calcium carbonate shell or accounting for humic acid and other PCR inhibitors. After 2013, a method was optimized to remove inhibitors and breakdown the shell, increasing the likelihood of positive PCR results. RDLES uses gel electrophoresis to then obtain a visible band which, if confirmed, is then submitted for gene sequencing (Carmon & Hosler, 2015).

Invasion. First discovered in 1890 by Andrusov in the Bug River, the Quagga mussel originates from the Dneiper River in Ukraine and the Ponto-Caspian Sea. Quagga mussels are closely related to another highly invasive species, the zebra mussel, which originates from the same waters. Although similar in appearance and taxonomy, the two mussels have exhibited

different invasive patterns. The zebra mussel had long been established as an aquatic invasive species, studied in Europe since the 18th century. The quagga mussel, however, has exhibited recent, rapid, and steady spread for only a few decades and is expected to overtake the zebra mussel in many places, including the Great Lakes.

In 1989, quagga mussels were first sighted in the United States, starting in Lake Erie. They were believed to have reached the Great Lakes by stowing away in the ballasts of transatlantic ships. Discharge ballast water from these ships only needed to contain a few veligers, juveniles, or adult mussels to infect surrounding waters. It is theorized that the highly mobile and microscopic veligers may be the primary stage of quagga mussel transport. Transport of veligers through overland trailers was studied and veligers immersed in just 31uL of water were found to survive at least seven days at temperatures below 25°C. For veligers not immersed but stored in humid conditions below 25°C, next day conveyance from one body of water to another was still possible (Snider, Moore, Volkoff, & Byron, 2014). In addition to boat ballasts, they can also spread as adults by attaching to boat hulls and drift along rivers. Adult quagga mussels can release byssal threads and use a foot to drift downstream to new locations.

By 1995, quagga mussels were sighted outside of the Great Lakes in the Mississippi River and in January of 2007, they had made their way across the country to Lake Mead in Nevada, as well as Lake Havasu and Lake Mohave near the border between Arizona and California. By late 2008, quagga mussels were discovered in 15 Southern California reservoirs and 6 Colorado River reservoirs. In 2011, a reservoir in New Mexico also tested positive for quagga mussel veliger DNA.

History in Arizona. In 2007, quagga mussels were positively detected multiple times in several Arizona locations including Lake Mohave, Lake Mead, Lake Pleasant and other locations along the Colorado River. All three lakes are confirmed to host established colonies of this invasive species and all of them are connected by the Colorado River, with the Mohave lake directly downstream of Lake Mead (National Park Service, 2017). Areas along the Colorado river

between Lake Mead and Lake Mohave also tested positive for quagga mussel veligers. Lake Pleasant is fed by a combination of the Agua Fria River and an aqueduct from the Colorado River, downstream of Lake Havasu (Central Arizona Project, 2018). In 2008, the Granite Reef Dam, where water from the Colorado River mixed with the Salt River, also tested positive for quagga mussels. Although just downstream of Lake Mohave, Lake Havasu did not test positive for quagga mussels until 2009, and although it tested positive again in 2010, there has not been an established population confirmed in Lake Havasu. In 2013, Lake Powell, the reservoir which feeds into Lake Mead, tested positive for quagga mussels. Until 2015 in Arizona, only the Colorado River watershed tested positive for quagga mussel veligers. In 2015, the veligers were detected in Canyon Lake, a reservoir of the Salt River system. In 2016, two other lakes in the Salt River system also tested positive for quagga mussels, Apache Lake and Saguaro Lake. (USGS, 2018)

To control the spread of quagga mussels in Arizona, the Arizona Game and Fish Department passed "Directors Orders" laying out new regulations for boaters in Arizona under the Aquatic Invasive Species Interdiction Act, passed July of 2010. The "Don't Move a Mussel" campaign, headed by the Arizona Game and Fish Department, encourages boaters to practice "clean, drain, and dry". The campaign outlines required decontamination protocols and serves to increase boater awareness. Waters officially designated as containing quagga mussels in Arizona include Lake Pleasant, Lake Mead, Lake Mohave, Lake Havasu, and the Colorado River area south of Lake Havasu up until the international boundary with Mexico. The regulations require boaters to follow 4 steps upon leaving the designated waters. These include (1) cleaning off any material off the anchor, boat, motor and trailer, (2) removing the plug and draining all water, (3) allowing the craft, vehicle and equipment to completely dry and (4) waiting at least 5 days before launching the watercraft in another location. In step 4, if the craft is needed in less than 5 days, they must replace the bilge drain plug and disinfect the bilge with a gallon of vinegar (Arizona Game and Fish Department, 2010). Regulations also outline more strict requirements for any boats moored for 5 days or longer in quagga infested waters. To farther prevent the spread of

mussels by overland transport, some states also require boat inspections for boats crossing the borders from Arizona.

For Lake Mead to test positive in 2007, it is hypothesized that reproducing quagga mussels must have been established by 2003 or 2004 to generate enough veliger larvae for detection (Moore, Holdren, Gerstenberger, Turner, & Wong, 2015). After detection, most areas only take 3-5 years before populations become an established infestation (Carmon & Hosler, 2015).

Between 2008 and 2015 quagga mussels were not detected in the nearby Salt River or Verde River systems. The Colorado River, Salt River, and Verde River water systems are in close proximity, and recreational boaters frequently travel between them. A study looking specifically at quagga mussel veligers traveling in the summer and autumn from Lake Mead, exhibited that residual water carried in trailered recreation boats could harbor surviving veligers for approximately 5 days in the summer and 27 days in the autumn (Choi, Gerstenberger, McMahon, & Wong, 2013). Considering a road trip from Lake Mead to the Salt River System would take less than 7 hours, and a trip from the infested Lake Pleasant would take less than 2 hours, it is very likely that despite efforts for raised awareness, that quagga mussel veligers have been frequently introduced to the Salt River and Verde river systems during that time.

An investigation into quagga mussel spread in Arizona reservoirs was conducted and published as a M.S. thesis in 2015 by Matt Sokolowski. The study sought to determine why quagga mussels did not infect the Salt or Verde river systems in Arizona. Lakes resistant to quagga mussel invasion often contain predators or exhibit water quality parameters that are inhospitable to the mussels. Water quality parameters which have been shown to affect quagga mussel vitality include temperature, dissolved oxygen, pH, salinity, turbidity and calcium concentration.

The investigation by Matt Sokolowski compared conditions in Lake Pleasant, to those in Bartlett Lake and Saguaro Lake. Lake Pleasant is part of the Colorado River system and was already

infested at the time of the study. Bartlett Lake is fed by the Verde River, while Saguaro Lake resides in the Salt River system. The study found that, in the laboratory, quagga mussels could survive in extracted Saguaro Lake and Bartlett Lake water. There are fewer predators (calanoid copepods) which prey on quagga mussel veligers, in Saguaro and Bartlett Lake than Lake Pleasant, and the only water quality parameters that the experiment did not account for were temperature and dissolved oxygen. Temperature and dissolved oxygen profiles sourced from field sampling conducted by the Regional Water Quality Sampling Project at Arizona State University revealed that that Saguaro Lake and Bartlett Lake had extended periods of low dissolved oxygen (Sokolowski, 2015). During the summer, each lake becomes heavily stratified. The layer closest to the surface, the epilimnion, of the water is subject to solar heating. In the hypolimnion, where the heat from the sun does not reach, the temperature of the water is lower. Very little mixing occurs between the epilimnion and the hypolimnion due to their temperature differences. During the summer, primary producers, mostly algae, bloom in the euphotic surface layers of the lakes, creating an epilimnion zone that is rich in oxygen. However, in the hypolimnion, there is very little light and decaying algae sink down toward the bottom of the lake. During the summer, it was hypothesized that the dissolved oxygen levels in the hypolimnion of these lakes declines to values below the quagga mussel's minimum tolerance for dissolved oxygen. Meanwhile, the water temperature of in the epilimnion reaches the mussel's upper threshold for temperature tolerance. In 2015, this hypothesis was put into question when quagga mussels were detected in Canyon Lake and in 2016, they were found in the neighboring Apache and Saguaro Lakes, all of which lay in the Salt River Watershed.

CANYON LAKE RESERVOIR

Canyon Lake Reservoir (Figure 1) is situated in the Tonto National Forest and is part of the Salt River Watershed. It lies downstream of Lake Roosevelt and Apache Lake. Canyon Lake is a triangular, boot-shaped lake with toes pointing southeast. Near the top of the boot, the source water and exiting waterways are surrounded by tall canyons. Mormon Flat Dam is to the

northwest, leading out to Saguaro Lake. In the same corner but to the northeast, water from Apache Lake flows into the lake via the Salt River. In the southeast corner, near the toe of the boot lies the marina. Along the bottom of the boot is a sandy beach, while cliffs surround the top of the boot on all sides. The lake is approximately 10 miles long with a shoreline of 28 miles. The reservoir has a capacity of 57,852 acre-feet with a surface area of around 950 acres when full. The maximum depth is recorded at 131.5 feet (40.08m). Mormon Flat Dam was built between 1923 to 1925 and contains two hydroelectric generating units rated at 10,000kW and 50,000kW (Salt River Project, n.d.).

The lake is managed by the Salt River Project, which keeps the lake at a constant elevation, usually around 95% full storing around 54692 acre-feet (Salt River Project, 2018). In 2007, Canyon Lake was drawn down by 50 feet for maintenance. Debris was removed, including sunken boats and cars, and replaced by fish habitats that were constructed using wooden pallets and discarded Christmas trees (Branom, 2007). Repairs were conducted on Mormon Flat Dam and the neighboring businesses took this opportunity to remodel. The Lake was low from September 2007 to February 2008 and closed to the public during that time.



Figure 1. Canyon Lake Reservoir from Google Maps

LANDSAT SATELLITE REMOTE SENSING

Landsat satellites have been providing images of the Earth since the launch of Landsat 1 on July 23rd, 1972 (USGS, 2017). Images of the Earth's surface have been used for science and understanding of the Earth in ways that were previously unachievable. The Landsat's extensive collection of Earth images are archived, and publicly available for research and development.

Landsat 7. Much of the information in this section is taken from the Landsat 7 Data Users Handbook, which exists as a living document created and updated by the U.S. Geological Survey (USGS) Landsat Project Science Office at the Earth Resources Observation and Science Center (EROS) with collaboration from the National Aeronautics and Space Administration (NASA) Landsat Project Science Office.

Landsat 7 was successfully launched by NASA on April 15th, 1999 at the Western Test Range Vandenberg Air Force Base in California. Its objective is to "provide timely, high quality visible and infrared images of all landmass and near-coastal areas on the earth" (USGS Landsat

Project Science Office, 2018). The satellite provides consistent archived data to the Landsat database. Landsat 7 was designed to have a lifetime of 5 years but has continued to collect data into 2018. The satellite uses stabilized attitude control, solar panels and an on-board power storage. The primary part of the satellite is its sensors. The sensors are housed in a pointing instrument called the Enhanced Thematic Mapper Plus (ETM+), an upgrade to the first Thematic Mapper (TM), first placed in Landsat 4. The original ETM was lost during the Landsat 6 launch failure. Landsat 7's ETM+ has several improvements from Landsat 5's TM including two gain ranges, a panchromatic band, a solar calibrator, and improved spatial resolution for the thermal band.

The satellite orbits the earth at an altitude of 705km, synchronized with the sun and traveling at 7.5 km/s, orbiting Earth approximately every 99 minutes. With approximately 14 orbits per day, the satellite covers the Earth at 81 degrees north and south latitude every 16 days. Pictures taken by the satellite are geographically calibrated using the Worldwide Reference System 2 (WRS-2), an upgrade from the WRS-1 system used by Landsat 1-3 which followed a different pattern and had a higher orbit. The WRS-2 creates an index of the orbits (paths) and scene centers (rows) into a global grid system composed of 233 paths, by 248 rows. Spacecraft attitude is then controlled to minimize variation from the intended tracks. A scene size for the pictures taken by Landsat 7 is approximately 170km x 185km (106mi x 115mi) and the nominal scene center can vary by 250 meters.

Onboard the Landsat 7 is a device called the Scan Line Corrector (SLC), an electro-optical mechanism which corrects for the satellite's motion to produce rectilinear scan patterns. The mechanism compensates for the satellite's orbital motion, which would otherwise cause the scan to follow a zigzagging pattern. On May 31st, 2003, the SLC failed and could not be recovered. As a result, the ETM+ line of sight now traces a zig-zag pattern along the ground track. While the center of the image along the track is clear, there are wedge shaped gaps and alternating overlap areas which increase in magnitude farther from the center line. When

processed, duplicate areas are removed, and the wedges leave data gaps, causing 22% of every scene to be lost. The maximum width of the data gap is approximately 390 to 450m and the location varies from scene to scene.

The Landsat 7 satellite uses 8 spectral bands. Bands 1, 2 and 3 are in the visible spectrum (1: 0.45-0.52 μm , 2: 0.52-0.60 μm , 3: 0.63-0.69 μm). Band 4 and 5 are in the Near-Infrared (4: 0.77-0.90 μm , 5: 1.55-1.75 μm). Band 6, the band most relevant to this paper, is the thermal band (6: 10.4-12.50 μm) and is taken with both low gain and high gain. High gain allows for increased dynamic range while low gain increases radiometric sensitivity. Arizona is an arid desert and during the summer, has very high reflectance and radiance. High gain is therefore preferred for use due to its higher dynamic range. Band 7 is mid-infrared (7: 2.08-2.35 μm) and band 8 is panchromatic (8: 0.52-0.90 μm). The ground sampling interval, correlating to pixel size, is 60m for the thermal band, 15m for band 8 and 30m for all other bands. Although band 6 is collected at 60m resolution, it is resampled to 30m resolution matching the other reflective bands.

The publicly available data product of the Landsat 7 ETM+ is called its “Level-1 Products” and appears as high quality corrected images packaged in Geographic Tagged Image File Format (GeoTIFF). The GeoTIFF is based on Adobe’s TIFF format which allows image data to be tagged with additional information. Level-1 Metadata is also available in the package as a text file which contains information for the essential characteristics of the product. Band images are delivered as 8-bit images with 256 grey levels. Pixel values are represented as one of the 256 grey levels and are also known as Digital Numbers (DN).

The DNs represent pixel values, which can be converted to radiance values using the following formula:

$$L_{\lambda} = \text{Grescale} * \text{QCAL} + \text{Brescale} \tag{1}$$

$$= \left(\frac{LMAX_{\lambda} - LMIN_{\lambda}}{QCALMAX - QCALMIN} \right) * (QCAL - QCALMIN) + LMIN_{\lambda}$$

$$L_{\lambda} = \text{Spectral Radiance at sensor aperture} \left(\frac{\text{Watts}}{m^2 * sr * \mu m} \right)$$

$$Grescale = \text{Rescaled gain found in data record} \left(\frac{\left(\frac{\text{Watts}}{m^2 * sr * \mu m} \right)}{DN} \right)$$

$$Brescale = \text{Rescaled bias found in data record} \left(\frac{\text{Watts}}{m^2 * sr * \mu m} \right)$$

$QCAL$ = quantized pixel value (DN)

$QCALMIN$ = minimum quantized pixel value (DN) = 0 or 1 found in data record

$QCALMAX$ = maximum quantized pixel value (DN) = 255

$$LMIN_{\lambda} = \text{spectral radiance scaled to } QCALMIN \left(\frac{\text{Watts}}{m^2 * sr * \mu m} \right)$$

$$LMAX_{\lambda} = \text{spectral radiance scaled to } QCALMAX \left(\frac{\text{Watts}}{m^2 * sr * \mu m} \right)$$

The radiance calculated can be farther refined by conversion to an effective at-satellite temperature, which estimates surface temperature based on pre-launch calibration constants and an assumption of unity emissivity.

(2)

$$T = \frac{K2}{\ln \left(\frac{K1}{L_{\lambda}} + 1 \right)}$$

T = Effective at satellite temperature in Kelvin

$K2$ = Calibration Constant 2 = 1282.71 Kelvin for Landsat 7

$$K1 = \text{Calibration Constant 1} = 666.09 \left(\frac{\text{Watts}}{m^2 * sr * \mu m} \right)$$

$$L_{\lambda} = \text{Spectral radiance} \left(\frac{\text{Watts}}{m^2 * sr * \mu m} \right)$$

The above equation is used for both Landsat 7 and Landsat 8 temperature estimations. The at-satellite temperature does not properly account for Earth's atmospheric water and is a rough approximation, using only one band (band 6 and band 10 from Landsat 7 and Landsat 8 respectively). The estimate from the above equations are referred to as the single-channel generalized method (SCGM). Case studies were then conducted to determine how closely the at satellite temperature could predict surface water temperatures. In the lakes and coastal zones near the Baltic Sea, Germany, nine sites found a Root Mean Square Error (RMSE) value of 1.4K compared to on site measurements and 1.6K with respect to bulk measurements (Wloczyk, Borg,

& Neubert, 2006). RMSE is a value estimating the difference between measured and calculated data, in our case representing the standard deviation between on-site measured data and data calculated from Landsat 7. A case study of Embalse del Río Tercero in Córdoba, Argentina, found that the SCGM method yielded an RMSE of 1.2250K and the method was noted to consistently reflect small differences in temperature between sites (Lamaro, Mariñelarena, Torrusio, & Sala, 2013).

Landsat 8. Much of the information in this section is taken from the Landsat 8 Data Users Handbook, which exists as a living document created and updated by the U.S. Geological Survey (USGS) Landsat Project Science Office at the Earth Resources Observation and Science Center (EROS) with collaboration from the National Aeronautics and Space Administration (NASA) Landsat Project Science Office.

Landsat 8 was launched on February 11th, 2013 by NASA at the same site as Landsat 7. The satellite is designed to last 5 years with 10 years' worth of fuel. With the use of solar panels, thermal control, radio frequency, attitude control and data handling, there are high hopes that the spacecraft will far exceed its design life. The purpose of its launch was to continue to provide data supplementing Landsat 4, 5 and 7 (USGS, 2018). Similarly to Landsat 7, Landsat 8 covers 16-day repetitive Earth coverage, offset from Landsat 7 by 8 days. The images from Landsat 8 help create a periodically refreshed archive of sun-lit, cloud free images. Compared to previous Landsat 7 average collections of 400 scenes per day, the Landsat 8 collects approximately 650 scenes. Landsat 8 has a 2-sensor payload, carrying the Operation Land Imager (OLI) and the Thermal Infrared Sensor (TIRS). Together, these integrated sensors are referred to as the Landsat 8 observatory.

The satellite uses 11 bands total, taken from a 705km altitude. It orbits Earth every 98.9 minutes, following the same WRS-2 ground path as Landsat 7. Each scene covers about a 190 by 180 km surface area. Whereas Landsat 7 had 3 visible bands, Landsat 8 uses 4 visible bands (1: 0.43-0.45 μm , 2: 0.45-0.51 μm , 3: 0.53-0.59 μm , 4: 0.64-0.67 μm). The first band, an ultra-

blue is used for coastal and aerosol studies. Band 5 is the near-Infrared band on board (5 0.85-0.88 μm). Band 6 and Band 7 are the Shortwave Infrared (SWIR) bands (6: 1.566-1.651 μm , 7: 2.107-2.294 μm). Band 8 is panchromatic (0.503-0.676 μm). Band 9 is the cirrus band (9:1.363-1.384 μm), used for cloud detection. Band 10 and band 11 are the two, refined thermal bands (10: 10.60-11.19 μm , 11: 11.5-12.51 μm). The thermal bands (10 and 11) are sampled at 100m resolution but are resampled to 30m. Band 8, the panchromatic band, has a resolution of 15m and all other bands have a 30m resolution.

Unlike the Landsat 7 ETM+, which relied heavily on oscillating mirrors for the satellite's field of view, the OLI and TIRS use linear arrays of photosensitive detectors. The machine is much more sensitive with fewer moving parts and it also outputs 12-bit data rather than 8-bit data. The 12-bit range translates to 4096 grey levels, compared to only 256 from Landsat 7. The OLI is required to produce data calibrated to an uncertainty under 5% for absolute, at-aperture spectral radiance and less than 3% of uncertainty for top-of-atmosphere reflectance, comparable to ETM+ calibration. The TIRS uses Quantum Well Infrared Photodetectors (QWIPs) sensitive to two thermal infrared wavelength bands. The TIRS sensor has a 100m spatial resolution, meaning less resolution than the 60m resolution of the ETM+ band 6. With the two thermal bands, surface temperature should have been easier to separate from atmospheric temperature, however issues with stray light in bands have prevented the data from being used in this way. Band 10 of the TIRS is used for alignment and as a reference for calibration.

Although the TIRS has reduced noise and has greater stability, comparisons between Landsat 8 calibrated data to surface predictions shows that the TIRS results overestimated radiance and had high variability. Differences between TIRS results and ground-based estimates were as high as 5 degrees Kelvin in band 10 and 10 degrees K in band 11. Temperature differences were higher in the summer. Banding was seen in some images, indicating that stray light entering the optical path introduced additional, non-uniform energy on the detectors. It was confirmed during lunar scans that stray light created radiance outside the instrument's field of

view and added non-uniform signal across the detectors. Landsat 8's calibration and validation team adjusted the radiometric bias in order to improve the error for typical growth season Earth scenes to an uncertainty of 1 K from band 10 data and 2K from band 11 data. The stray light error is estimated to be 0.29 W/m²/sr/mm for band 10 and 0.51 W/m²/sr/mm for band 11. The correction adjusts for bias but cannot correct for stray light and in cold scenes, the bias tends to overcorrect.

Temperature at the satellite was also calculated, using the single channel generalized method, for Landsat 8 data and case studies compared the calculated data to on-site data, as well as data from other map sources. In a case study in Poteran Island, Indonesia, 45 data points were assessed for on-site data and estimated brightness temperature with a coefficient of determination of 0.912 and an RMSE of 0.028 (Syariz, et al., 2015). Other studies using Landsat 8 were conducted using both band 10 and band 11 data, however those studies used separate methods and not the USGS recommended single channel generalized method. This study focused only on use of the SCGM, but future studies using multiple bands will likely yield more accurate findings.

DATA COLLECTION

Data was acquired from 3 different sources. The first source of data was the Regional Water Quality Sampling Project. A previous study by Matt Sokolowski used Regional Water Quality data from Saguaro Lake to hypothesize that surface warming and low dissolved oxygen from stratification of the Salt River Reservoirs, including Canyon Lake, created inhospitable water quality parameters for quagga mussels. For Canyon Lake, however, the Regional Water Quality Sampling Project did not have sufficient data. I then turned to the availability of surface temperature data from the USGS Landsat project. Landsat 7 and Landsat 8 provide overhead temperature data from before quagga mussels were detected in Canyon Lake. Surface temperature readings could indicate whether temperature changing events, such as El Niño or climate change, may have affected the stratification of Canyon Lake. Finally, I took on-site data, collected from 21 locations on Canyon Lake, during the lake's stratification period from late May to mid-October. On-site measurements explored if certain areas of the lake were more susceptible to quagga mussel infestation due to physical conditions.

REGIONAL WATER QUALITY DATA

Data was acquired from the Regional Water Quality Sampling Project by ASU. The Regional Water Quality Center at ASU has been collecting data on watersheds around Arizona since 2000 and sought to investigate algal impacts on water quality. The 2015 investigation by Sokolowski used detailed regional water quality data acquired between 2001-2002 from Saguaro Lake, Bartlett Lake and Lake Pleasant to determine that the Salt and Verde river systems were inhospitable to quagga mussels for period of 2-3 months. During that time surface temperatures at the Saguaro and Bartlett Lakes exceeded 28 degrees Celsius in the epilimnion and in the hypolimnion, dissolved oxygen concentrations dipped below 2mg/L.

Upon reviewing the data from Saguaro Lake, the lake just downstream of Canyon Lake in the Salt River system, I found that stratification of the lake during the summer could have significant impacts on the dissolved oxygen levels and the overall survivability of quagga mussels

within the reservoir. In Figure 2 and Figure 3 temperature and dissolved oxygen profiles were analyzed and compared with relative depth. The orange line in Figure 2 indicates a temperature of 28°C and in Figure 3, it highlights a dissolved oxygen concentration of 2mg/L. Temperatures above 28°C and dissolved oxygen levels below 2mg/L are both factors which make Saguaro lake inhospitable to quagga mussels (Sokolowski, 2015).

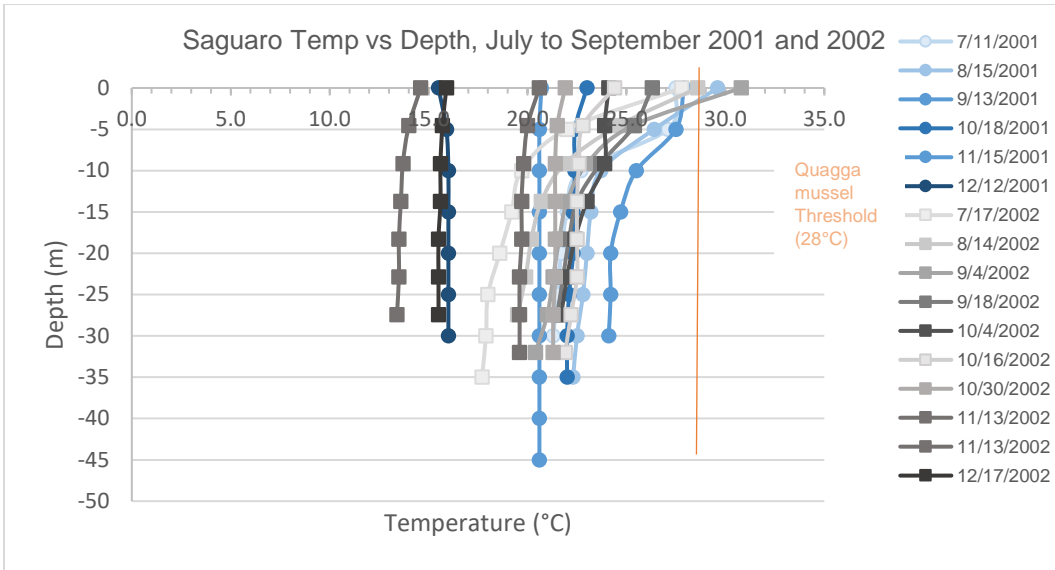


Figure 2. Regional Water Quality Data at Saguaro Lake, Temperature vs Depth

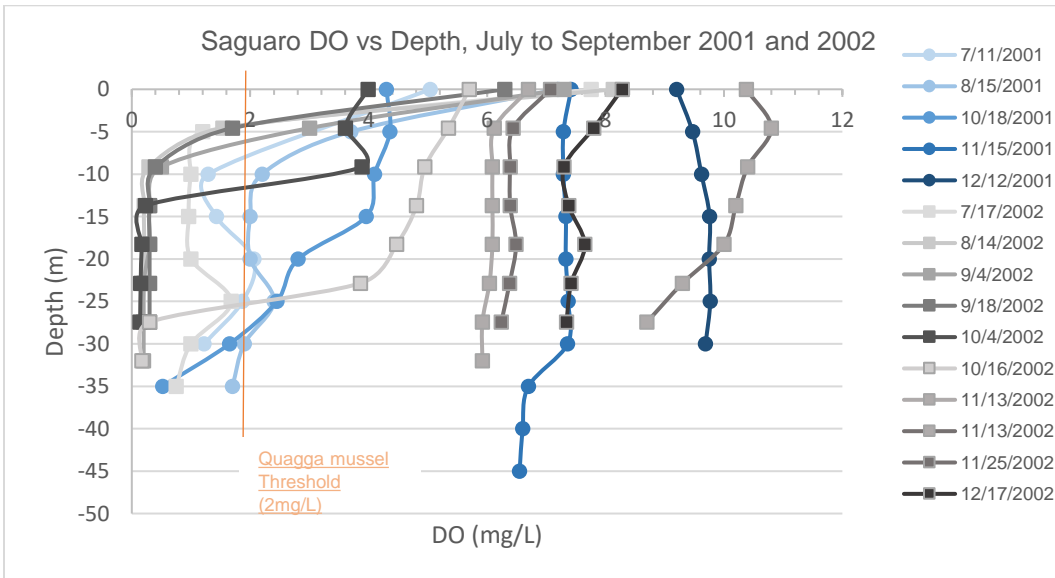


Figure 3. Regional Water Quality Data at Saguaro Lake, Dissolved Oxygen vs Depth

Water quality data for Canyon Lake was sparser, as seen in Figure 4, with dissolved oxygen and temperature measurements only taken about twice a year since 2014. In 2017, a water quality sample was taken in August, finally yielding a sample within the time of lake stratification. Dissolved oxygen was also included in the measurement. Dissolved oxygen levels from August of 2017 follow a stratified trend seen in Figure 5.

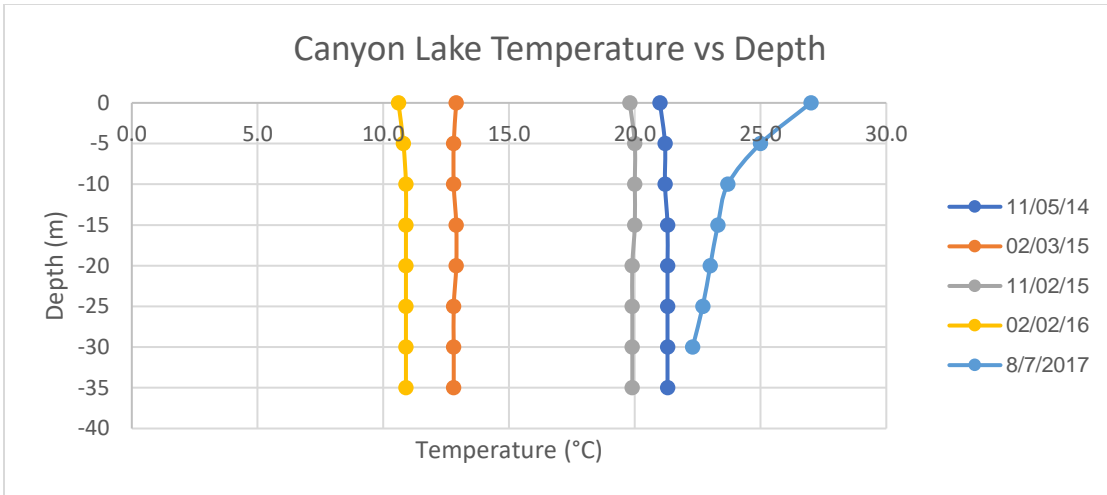


Figure 4. Regional Water Quality Data at Canyon Lake, Temperature vs Depth

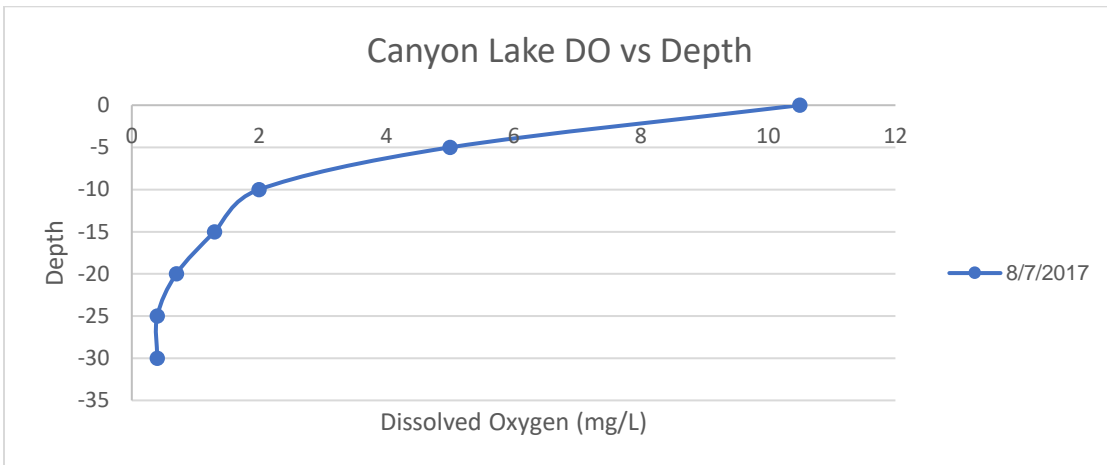


Figure 5. Regional Water Quality Data at Canyon Lake, Dissolved Oxygen vs Depth

Regional Water Quality data confirms that Canyon Lake experienced stratification during the summer, but the data was too sparse to note any significant differences between before quagga mussels were detected at Canyon Lake, and after. At the time of this experiment, water quality data during the time frame of interest was unavailable and so other means were pursued to understand conditions surrounding Canyon Lake around the time of quagga mussel contamination.

LANDSAT 7 SATELLITE DATA COLLECTION

Landsat data was acquired from the USGS GloVis Next website. On the website, Canyon Lake was identified and corresponding images containing Canyon Lake were selected. There were 2 possible configurations for image selection and the configuration wherein Canyon Lake was closest to the center of the image was prioritized. Due to the breaking of the SLC device on the Landsat 7 satellite, bands lacking data can be seen in the images of Canyon Lake. The farther Canyon Lake was in proportion to the center of the image, the wider these bands of missing information would be. I therefore chose images in which Canyon Lake was as close to the center of the image as possible. The WRS-2 path allows the Landsat Satellites to take images in roughly the same location. Figure 6 below indicates the location of Canyon Lake with a yellow circle. Landsat data corresponding to the path of the right-side image were prioritized because Canyon Lake is located closer to the center of those scenes. Scenes in the figure below are from August of 2017, taken from the GloVis Website.

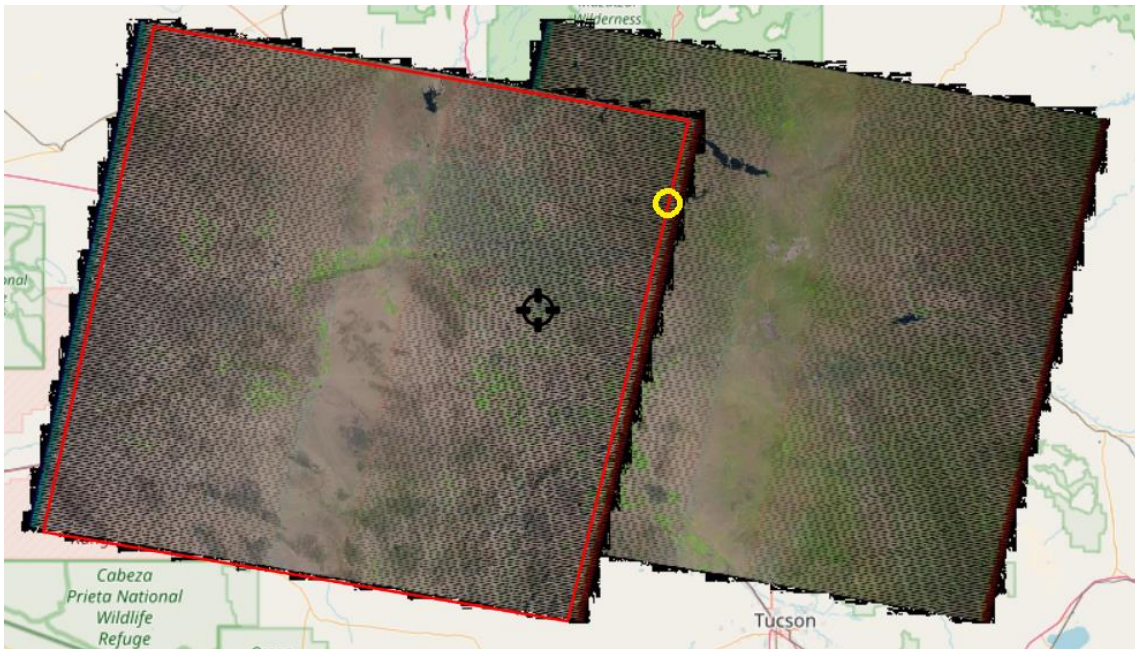


Figure 6. GloVis Available scenes containing Canyon Lake for August 2017 (Lake in yellow circle)

USGS software for downloading from GloVis, known as Bulk Download Application, was used to download selected Landsat products from the website. Although the Landsat Look Thermal Image was considered as a usable product for this research, the thermal image had lower resolution compared to a GeoTIFF image. GeoTIFF images were downloaded in GZip file format and the program, ZipReader was used to unpack GZip files into readable folders. Among the image data unpacked from the Landsat GeoTIFF files, this research primarily focused on using the available Metadata text file and, for Landsat 7, the band 6, high gain data image was used. The high gain image is less sensitive than low gain but has a higher dynamic range and can better measure the high temperatures found around Arizona's arid landscape.

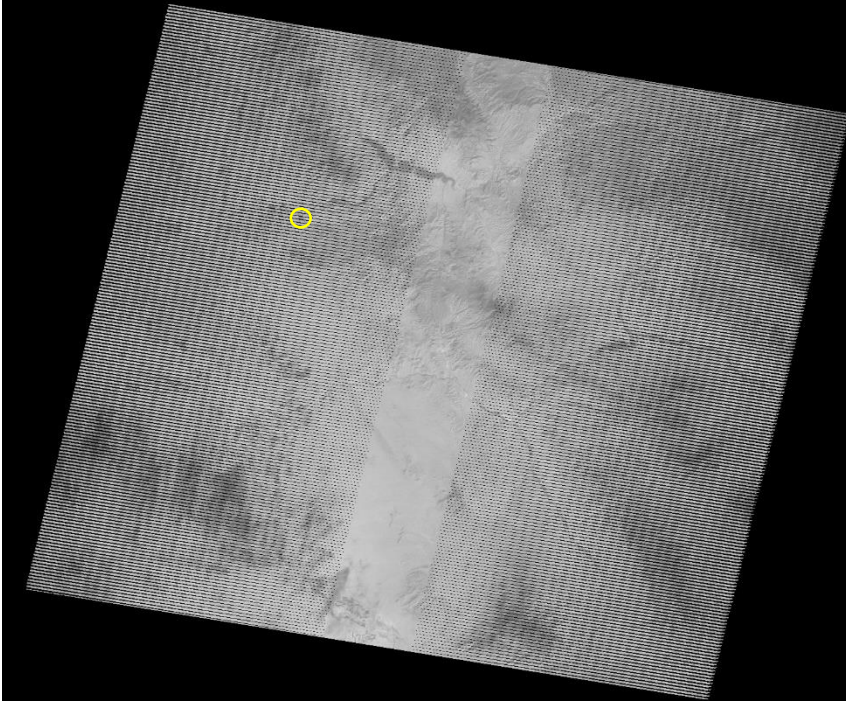


Figure 7. Landsat 7, Band 6, High Gain Product for October 20, 2017

Figure 7 is a sample of the Landsat 7, band 6, high gain image. The greyscale on the image corresponds to a digital number. The digital number, as found in the equation for at satellite radiance (equation 1), can be used to find approximate surface temperatures of the Lake (see equation 2). Canyon Lake is indicated in yellow, with the large Roosevelt Lake to the northeast and Saguaro Lake to the west. Dark areas in the lower corners of the image are indications of clouds, which can also cause issues in measuring temperature. Cloud cover lowers the digital number reading and can impact temperatures read. Cloud cover often causes much lower temperatures to be read. Because Arizona experienced constant heat during the summer with temperatures never dropping below 17°C , water temperatures that were read below 10°C were assumed to be caused by cloud cover.

Using MATLAB's image processing suite and location data from the metadata files, the thermal image data was cropped to focus on Canyon Lake. An affine transformation equation was used to correlate an input longitude and latitude to an output pixel coordinate. To make the initial crop, the upper left, upper right and lower left corners were used as reference longitude and

latitudes, along with their corresponding pixel coordinates to determine the constants in the equation. Once all the constants were found, inputting the desired longitudes and latitudes would output corresponding column and row values through solving the system of equations.

(3)

$$X_0 = A + BX_i + CY_i$$

$$Y_0 = D + EX_i + FY_i$$

X_0 = Latitude

Y_0 = Longitude

Y_i = Column Pixel Value

X_i = Row Pixel Value

A, B, C, D, E, F = Constants



Figure 8. Landsat 7, Cropped image of Canyon Lake for August 2017, August 2016, and August 2015

The resulting images are about 102x132 pixels, (Figure 8). Lines lacking data can be observed due to the failure of the SLC. The lines are random and change from scene to scene. Although the results of cropping showed good consistency, using the same constants to map specific locations on the lake were not as accurate. To achieve higher levels of accuracy to correspond specific points on the lake to on-site measurements, I ran a second affine transformation, using landmarks on each image to farther correct the constants of the equation. Landmarks used included the southeast river branching from the lower tip of the lake, the southern cove near the sole of the boot-shape, and the western cove, near the heel of the boot. With these three locations added to the equation, subsequent latitude and longitude points inputted to the map showed higher location consistency.

Just as in the larger image, the cropped image resolution is 60m, resampled to 30m, meaning that each pixel represents roughly a 30m x 30m square. The accuracy of each square is less than the other bands sampled at higher resolutions. One result of this is that at locations near to the land, intrusion may occur wherein heat data from the land is projected as part of the thermal data farther inland. Although I attempted to choose areas of interest that had sufficient distance from the land, points that were closer to the center of the lake were the most closely relatable to on-site data. In addition, the digital number value of the Landsat 7 data ranged from 0 to 255. This represents a limit to the accuracy of each degree kelvin, with one DN point roughly calculating to a change of about 0.3°C in the relevant range of temperatures (about 10°C-30°C). Since the satellite would have to approximate a DN value for the measured radiance, the resulting temperature is a rough estimate, comparable to on-site data but in this research, used mostly to determine long-term trends.

LANDSAT 8 SATELLITE DATA COLLECTION

The two thermal bands, band 10 and band 11 for Landsat 8 were designed to correct for the atmosphere so that surface temperature would be more accurate to measure. A set method to do so, however, has not been established and the Landsat 8 handbook does not currently list any official ways to process the data for exact surface temperature. Due to issues with stray light, the readings from the thermal bands vary significantly and although individual algorithms have been put forward in the literature, there is not yet a common consensus to correct readings globally for stray light.

In this study, Landsat 8 data was processed in the same way as Landsat 7 data. GeoTIFF files were downloaded from GloVis. The metadata file and the file for band 10 was obtained. Band 10 was favored over band 11 because stray light had a higher impact on band 11, causing band 11 readings to be farther off than those of band 10. Landsat 8 satellite sensors did not require as many moving parts as Landsat 7 and the more robust design protects against

issues such as Landsat 7's SLC failure. The images from Landsat 8 are more complete and lack lines of missing data.

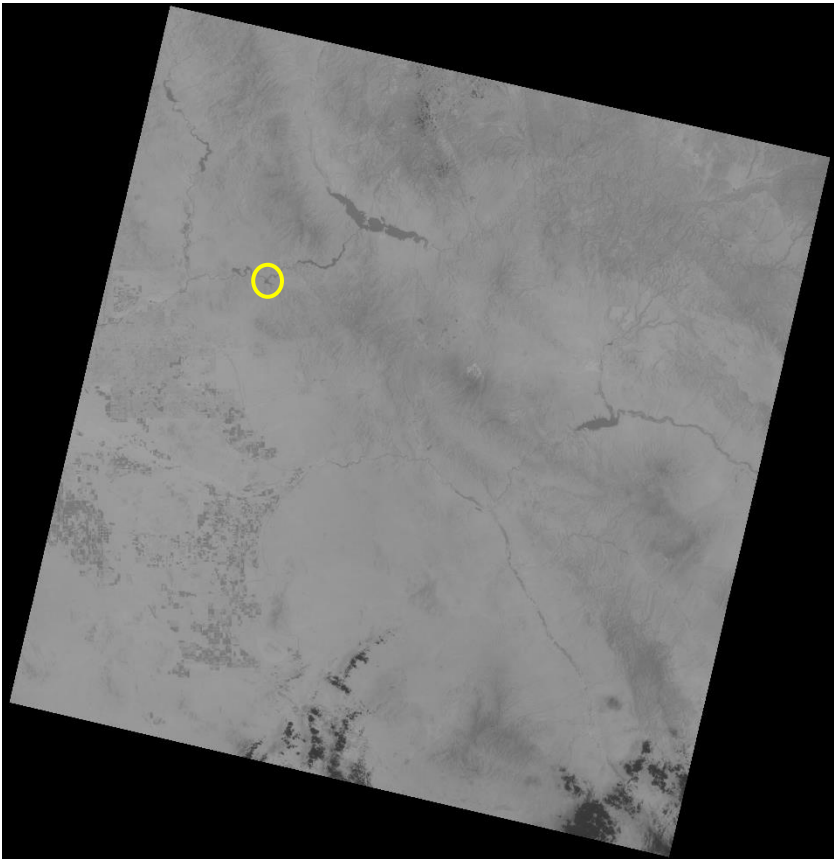


Figure 9. Landsat 8, Band 10, Product for June 22, 2017

Figure 9 is an example of Landsat 8 band 10 image data. The greyscale corresponds to a digital number (DN). The DN from Landsat 8 ranged from 0 to 4095, in contrast to Landsat 7's 0 to 255. Higher accuracy of the digital number allows Landsat 8 much higher precision in temperature measuring and recording. One major drawback, however, is that the Landsat 8 TIRS had a lower resolution than Landsat 7's thermal band. Whereas the Landsat 7 band 6 had a 60m resolution resampled to 30m, Landsat 8 has a 100m resolution resampled to 30m. As a result, pixels from band 8 have higher precision but possibly lower accuracy as land intrusion has a more significant impact on data close to the shore. Images in Figure 10, although displaying a higher variety of greyscale, shows less clearly defined edges between the shore and the lake surface.



Figure 10. Landsat 8, Cropped image of Canyon Lake for August 2017, August 2016, and August 2015

Landsat 8 was processed using the same equations and code as Landsat 7, with adjustments for Landsat 8's higher volume of data due to its higher range of DN values. Although Landsat 8 data is more precise, a combination of issues from stray light and a lower resolution make the data less reliable than that of Landsat 7. Landsat 8 data was obtained offset from Landsat 7 data by 8 days and contains more complete data. The images do not have any missing data in them. As research confirms more accurate methods to compensate for the stray light, Landsat 8 data can become much more precise than the data from Landsat 7, however development of such an algorithm was not the focus of this research and Landsat 8 data was analyzed for overall trends.

ON-SITE DATA COLLECTION

The YSI ProDSS is a multiparameter water quality meter that I used to measure and record depth, dissolved oxygen, conductivity and temperature along with GPS coordinates for several locations around Canyon Lake, in Arizona. The sampling schedule was coordinated with days that the Landsat 7 and Landsat 8 satellites would be overhead. In accordance, the time of sampling was between 10am and 3pm to coordinate with the satellite's daytime measurements. 21 different locations were sampled throughout the lake (Figure 11). Locations were found on-site using landmarks, then confirmed using the YSI ProDSS GPS. A Venterior Portable Fish Finder was used to approximate depth to the bottom of the lake to avoid hitting the probe on the bottom or catching the probe on sunken debris. The probe was lowered to approximately 3m from the detected "bottom" of the lake.

The calibrated and prepped probe was initially held above the surface of the water, and the auto-logging feature was initiated. The auto-logger would record and save measured water quality parameters for later download. It was set to record measurements every 3 seconds. The first temperatures taken by the multimeter were actually air temperatures, comparable to Landsat which measures just above the Lake's surface temperature. Temperatures were then automatically taken until 1m in depth. The 1m depth measurement is the epilimnion measurement and the probe was held at 1.0m in depth for 3 seconds to ensure logging. The probe was then lowered to 5m, suspected to be near the thermocline, and held at 5.0m until logged. If deep enough, the probe continued to be lowered to 10.0m, 15.0m, 20.0m, 25.0m, 30.0m and 35.0m. The deepest part of the lake I recorded was 35.0m near the Dam, but I was not able to measure this depth very often due to changes in flow and presence of nearby debris.

The multimeter was capable of continuous data logging and saved data to an on-board SD card. On August 22nd, it was found that an issue occurred in the software of the onboard SD card that prevented data from being saved and therefore could not be automatically logged. The measuring probe continued to function normally, however data after the SD card malfunction is considerably sparser in comparison to before. After the SD card malfunction, data had to be recorded by hand and due to time constraints, fewer data points could be taken.

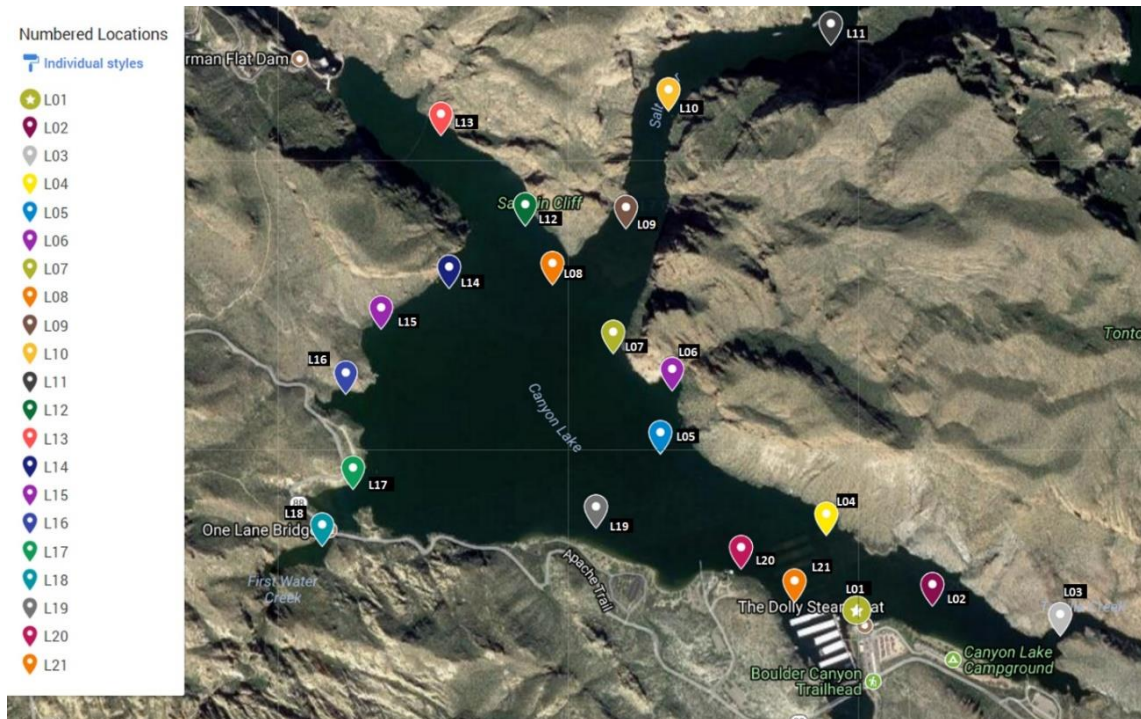


Figure 11. Sampling Points

Sampling points for Canyon Lake were numbered L01 to L21 and are indicated in Figure 11. Boating rules specified counterclockwise travel around the lake. The first sample for the day was taken at L01, just east of the marina. Samples were then taken around the lake and up the rivers, finally leading back to location L21 on the west side of the marina. The marina is a significant location because the Canyon Lake sample that was positive for quagga mussel veligers was taken at a site near the marina. Location L08, near top of the lake, is the approximate location of the Regional Water Quality sampling. Location L13 is one of the deepest locations, and the nearest location to Morman Flat Dam, which exhibited quagga mussel sightings. Location L20 is a boat dock for boating law enforcement, who regularly travel to the marina to get gasoline.

Near some locations, the multimeter GPS would designate a location that was a significant distance from landmarks. At these times, I prioritized landmarks over GPS because this often occurred in locations with high cliffs nearby and it was possible the cliffs caused delays in GPS updating.

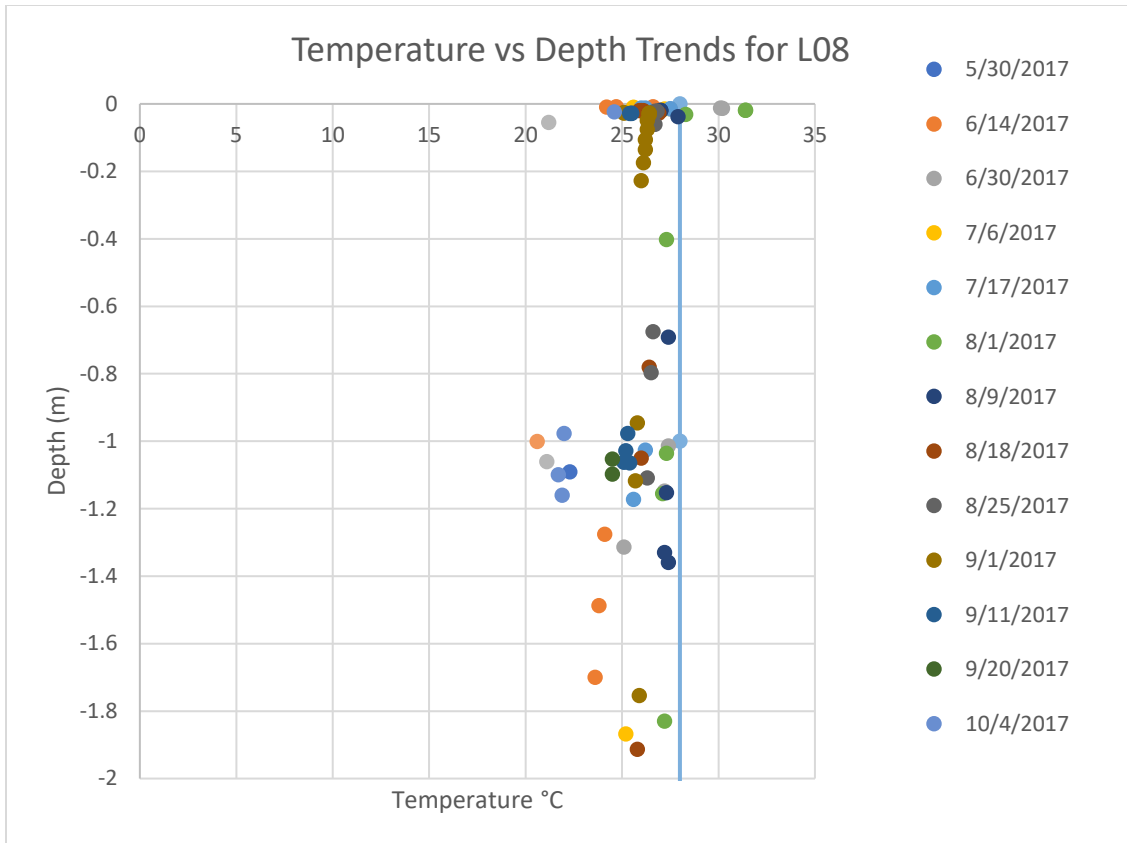


Figure 12. Close up Air Temperature and Water Temperature from 0 to 2m Depths

In Figure 12, we see a close up of readings from the multimeter. Surface temperatures are begun above the surface of the water, measuring the air temperature. The air temperature measured by the probe is directly compared to Landsat satellite temperature. The probe is then slowly lowered into the water and allowed to log continuously until it reaches a depth of 1m. At 1m, I stop lowering the probe and allow it to log for 3 seconds, sometimes taking multiple readings. The probe is then lowered to 5m and, if applicable, it is continued to be lowered until 3m before the 'bottom' as read by the fish finder. From Figure 12, we see that there may be a slight difference in temperature between the 'air' surface temperature and the 0m water temperature but they follow similar trends.

RESULTS

SURFACE TEMPERATURE: SATELLITE DATA COMPARED TO ON-SITE DATA

Before I could analyze the temperature trends measured by satellite over Canyon Lake, I must first compare the accuracy of the satellite data to on-site sampled data.

Table 1
SRP Daily Water Report Data

Date	Mormon Flat Elevation (ft)	%Full	Rain	Boat Ramp Depth @ Canyon Marina (m)
5/30/2017	1656.89	94	0	22
6/6/2017	1658.89	97	0	24
6/14/2017	1657.25	95	0	22
6/22/2017	1657.61	95	0	23
6/30/2017	1657.37	95	0	22
7/6/2017	1657.18	95	0	22
7/17/2017	1657.56	95	0.5	23
8/1/2017	1657.7	95	0.12	23
8/9/2017	1657.06	94	0	22
8/18/2017	1657.22	95	0	22
8/25/2017	1657.32	95	0	22
9/1/2017	1657.16	95	0	22
9/11/2017	1657.78	96	0	23
9/20/2017	1658.08	96	0	23
9/22/2017	1657.15	95	0	22
9/27/2017	1657.58	95	0	23
9/28/2017	1657.13	95	0	22
10/4/2017	1657.04	94	0	22
10/16/2017	1656.95	94	0	22
10/20/2017	1657.52	95	0	23

A factor potentially impacting the level of land intrusion is the water level of the lake itself (Table 1). If the water level of the lake is lower, there is a higher likelihood of land intrusion in the satellite data due to receding edges in the lake. The overall elevation of Canyon Lake, however, was kept relatively the same, though areas which this may have created the most impact are also locations with the least accuracy, including the surrounding rivers. During days of low flowrate through the Salt river, the size of the areas read by the satellite would be smaller and land intrusion may have greater effects on the data. The SRP daily water report is taken at Mormon Flat Dam, near location L13. The overall elevation of Canyon Lake is kept relatively the same. Boat ramp depth at the marina is seen to change from day to day and similarly, water levels in areas of the lake could have varied. Precipitation was detected for July 17th, and August 1st. The precipitation did affect Landsat data on July 17th due to higher water vapor changing the atmospheric emissivity and data from that date was excluded from calculations.

Temperature data from Landsat 7 and Landsat 8 was compared to on-site data averages at each of the 21 locations. Due to land intrusion, many of the near-shore sample points exhibited higher temperatures than those measured on-site. In addition, since Landsat 8 had a lower resolution, Landsat 8 data was found to be less accurate than Landsat 7 data due to land intrusion. If true, the most accurate data would be from location L08, due to its position nearer the center of the lake. Meanwhile, areas with the least accuracy would be areas that were nearly surrounded by land, such as points along the river and coves. The RMSE was found for each location and are included in Table 2 below.

Table 2
 Root Mean Squared Test for Each Location, All Landsat vs Landsat 7 vs Landsat 8

L01: All LS	4.37	L01: LS7	4.02	L01: LS8	4.85
L02: All LS	2.17	L02: LS7	1.54	L02: LS8	2.66
L03: All LS	11.63	L03: LS7	12.74	L03: LS8	8.79
L04: All LS	3.60	L04: LS7	3.49	L04: LS8	3.40
L05: All LS	1.53	L05: LS7	0.79	L05: LS8	1.87
L06: All LS	6.89	L06: LS7	8.07	L06 LS8	5.72
L07: All LS	2.06	L07: LS7	2.40	L07 LS8	1.74
L08: All LS	0.80	L08: LS7	0.55	L08 LS8	1.02
L09: All LS	4.07	L09: LS7	2.24	L09 LS8	5.31
L10: All LS	6.82	L10: LS7	7.98	L10 LS8	5.43
L11: All LS	10.64	L11: LS7	9.39	L11 LS8	11.97
L12: All LS	5.37	L12: LS7	3.10	L12 LS8	6.70
L13: All LS	4.29	L13: LS7	2.13	L13 LS8	5.79
L14: All LS	3.01	L14: LS7	3.08	L14 LS8	2.95
L15: All LS	13.08	L15: LS7	14.33	L15 LS8	11.94
L16: All LS	13.67	L16: LS7	16.14	L16 LS8	11.73
L17: All LS	11.69	L17: LS7	15.60	L17 LS8	6.91
L18: All LS	14.64	L18: LS7	18.56	L18 LS8	7.60
L19: All LS	2.81	L19: LS7	1.30	L19 LS8	3.62
L20: All LS	5.80	L20: LS7	4.41	L20 LS8	6.56
L21: All LS	5.08	L21: LS7	3.07	L21: LS8	6.75

The RMSE for location L08 was found to be the lowest with an RMSE of 0.80K, while the highest degrees of land intrusion were seen in areas with a high amount of surrounding land (Table 2). The next lowest RMSE, 1.53K, is at location L05. Locations L07 and L02 also had relatively low RMSE, 2.06K and 2.17K. We found that location L08 is the most ideal location to analyze. To compare, I determined the coefficient of correlation (R^2) for L02, L05, L07 and L08.

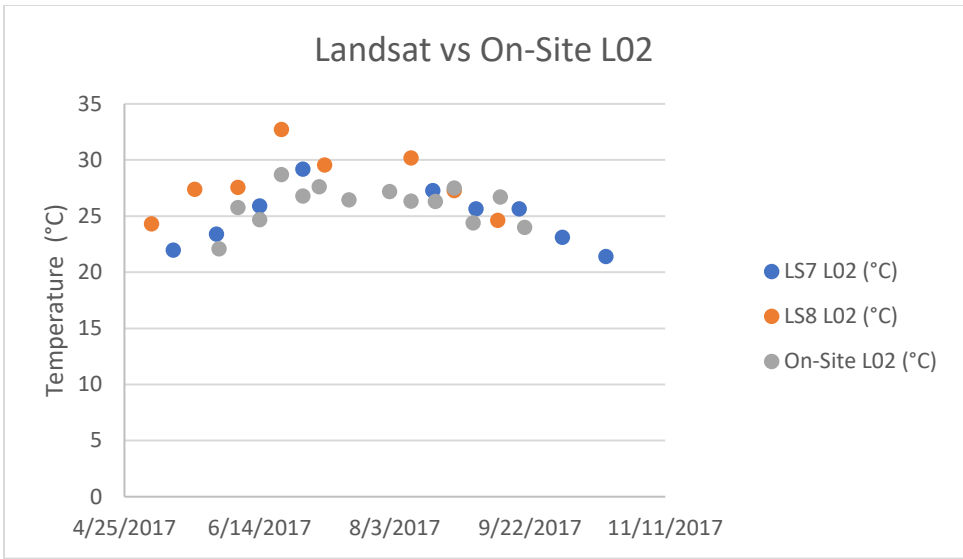


Figure 13. Landsat Temperature vs On-Site Temperature Over Time at L02

Landsat 8 (LS8) overestimates values for location L02, and Landsat 7 (LS7) slightly overestimates values (Figure 13) when compared to on-site data at L02. L02 is located towards the center of a narrow section in the south eastern portion of the lake.

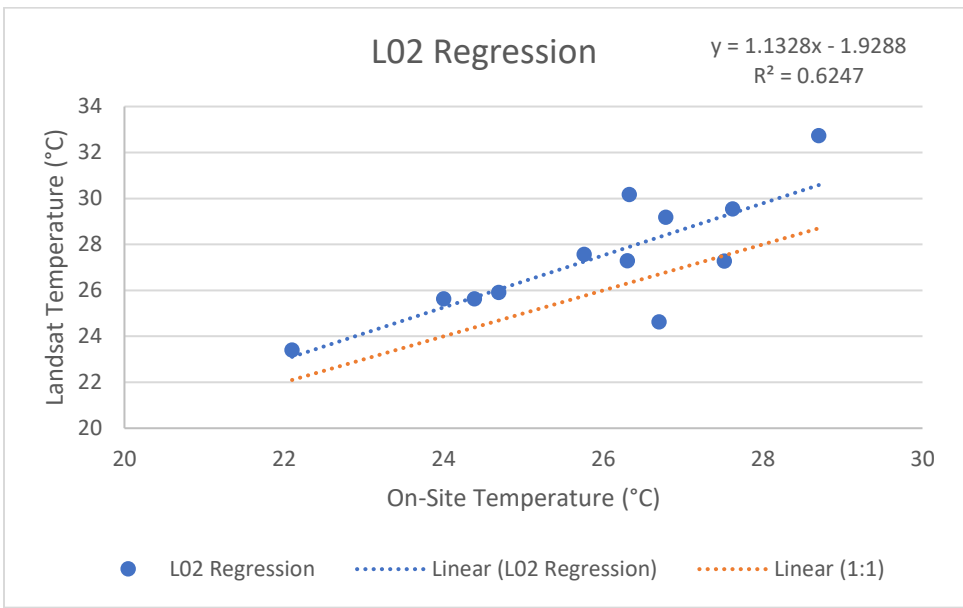


Figure 14. Landsat Temperature vs On-Site Temperature at L02 Regression

In a linear regression (Figure 14), comparing the combined Landsat Temperatures to on-site temperatures, we see the effects of Landsat 8's overestimation impacting the accuracy of data from location L02. Although L02 is not close to a land point, stray light can still interfere with readings from Landsat 8. Overall, L02 had a linear regression coefficient of 0.62.

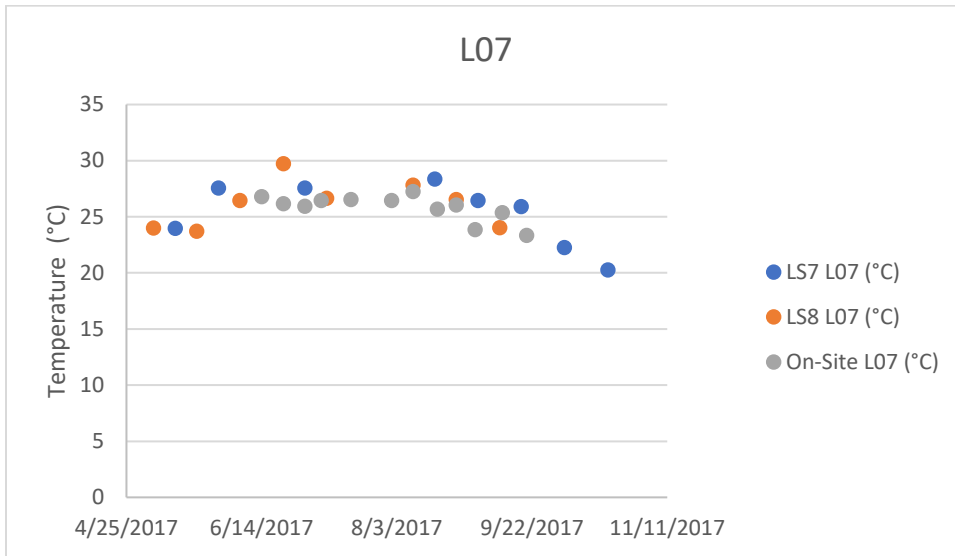


Figure 15. Landsat Temperature vs On-Site Temperature Over Time at L07

Location L07 is not far from L08, though closer to the shore. Compared to L02, Landsat 8 did not overestimate temperatures for the location as much, but for Landsat 7, there were more overestimations (Figure 15). Although not precise, both satellites still follow the overall temperature trends at location L07.

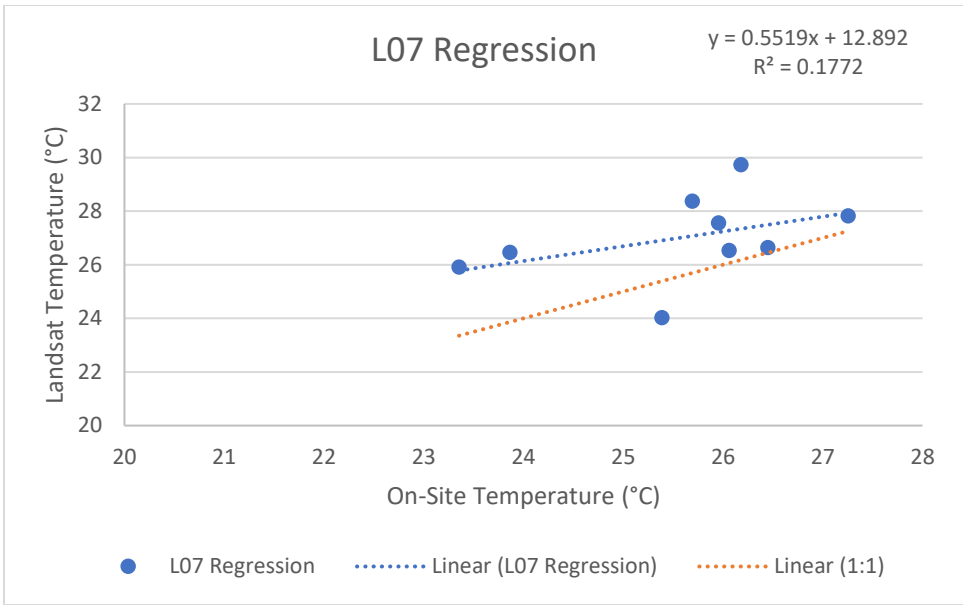


Figure 16. Landsat Temperature vs On-Site Temperature at L07 Regression

A linear regression reveals that the satellite data performs uneven over estimates as well as too few underestimates of the on-site data (Figure 16), evening out to a good RMSE, but a low R^2 value of only 0.2.

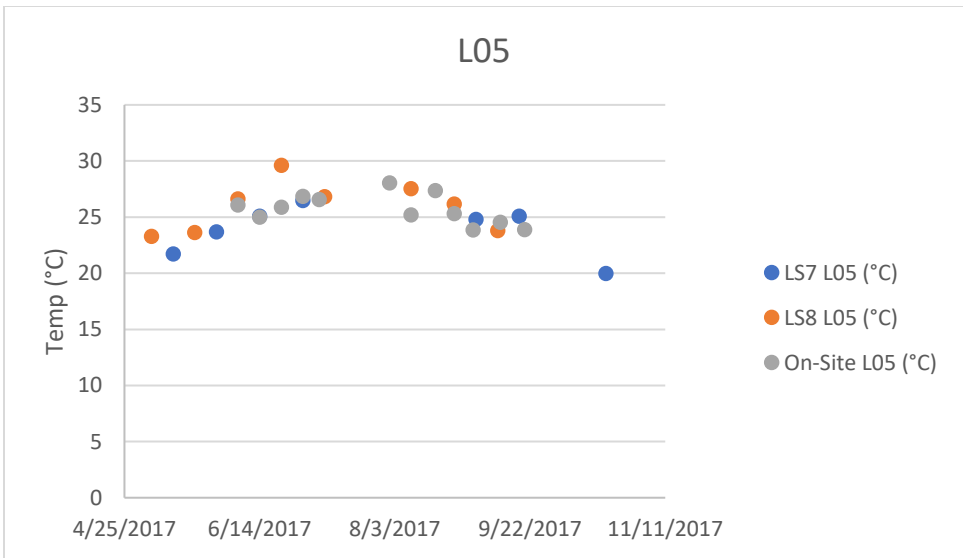


Figure 17. Landsat Temperature vs On-Site Temperature Over Time at L05

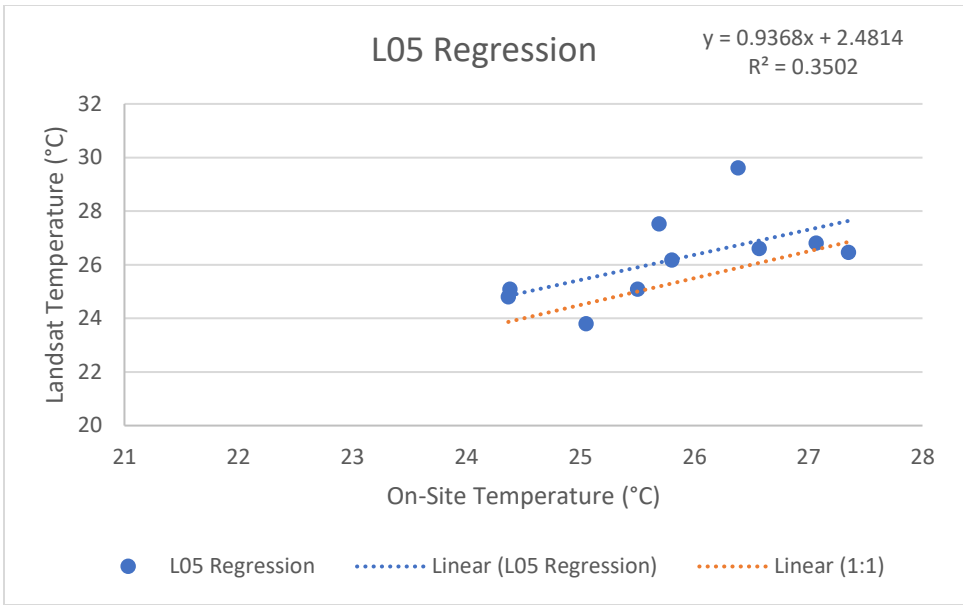


Figure 18. Landsat Temperature vs On-Site Temperature at L05 Regression

Location L05 shared similar characteristics with L02 and L07 in that it looked to follow similar trends as on-site data (Figure 17), however failed to produce a well correlated R^2 value (Figure 18).

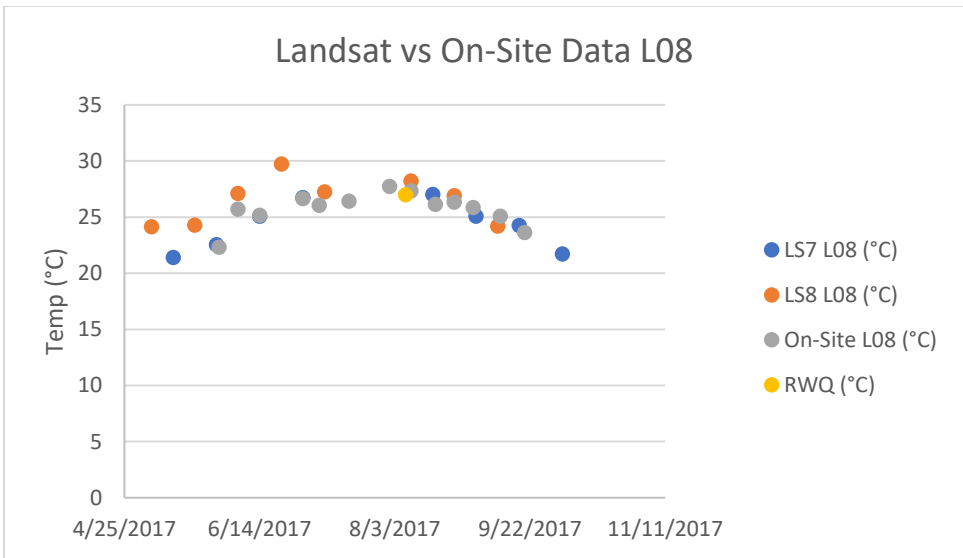


Figure 19. Landsat Temperature vs On-site Temperature vs RWQ data Over Time for L08

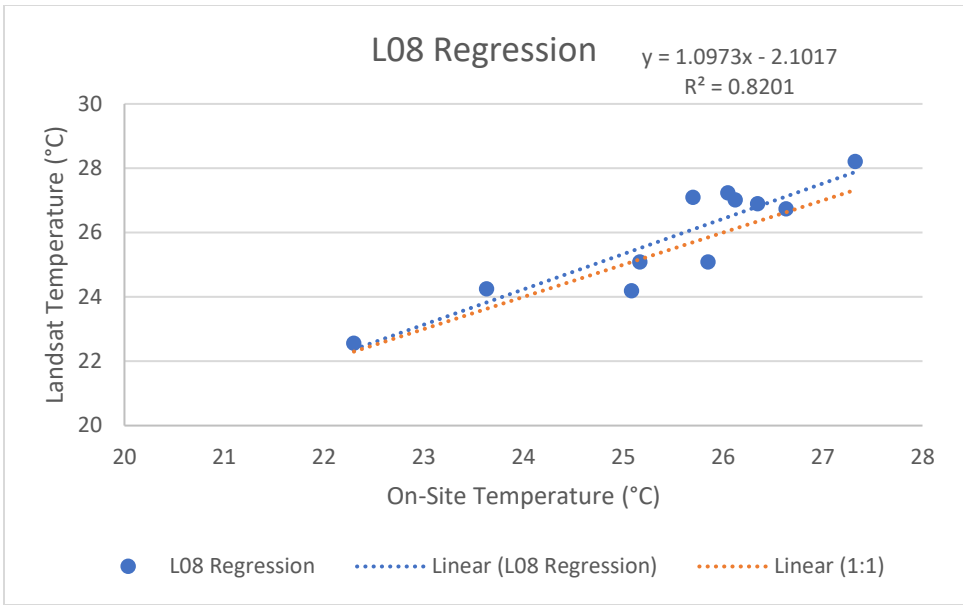


Figure 20. Landsat Temperature vs On-Site Temperature for L08 Regression

At location L08, the sampling location shared by the Regional Water Quality Project, satellite data and on-site data can be compared (Figure 20). The RMSE for L08 is 0.80K and the coefficient of determination (R^2) 0.82. Location L08 was therefore used to analyze long term trends at Canyon Lake.

Since many of the other locations could not be accurately analyzed, I must also consider whether analysis of L08 is representative enough of other locations on Canyon lake. The Regional Water Quality Project shared use of location L08 as a representative point on Canyon Lake, however regarding quagga mussel infestation, other areas of the lake may be more susceptible to infestation.

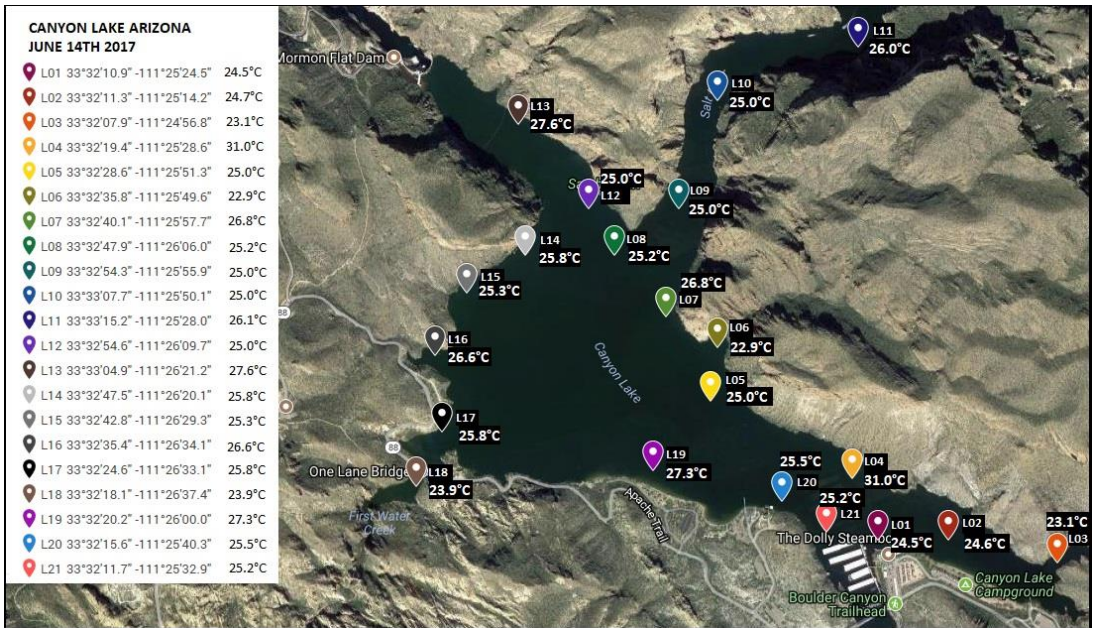


Figure 21. Canyon Lake On-Site Surface Temperatures for June 14th, 2017



Figure 22. Canyon Lake On-Site surface temperatures for August 9th, 2017

A comparison of Figure 21 and Figure 22 show that in June, different areas of the lake have significantly different surface temperatures. In August, some of those surface temperatures become more uniform. Regarding quagga mussels, the peak of the heat in August is of more concern than the surface temperatures in June. Quagga mussels have an upper threshold of 28 °C before high mortality and the primary interest of the Landsat research is to determine how often, and for how long, Canyon Lake approaches this threshold each year.

SURFACE TEMPERATURE TRENDS

Stratified lakes have different layers. The surface of the water is exposed to the air and sun. The epilimnion is the area of the lake nearest the surface. It is the layer in which algae grow. Farther down you reach the thermocline, a layer of declining temperature that acts as a barrier between the epilimnion and the mixed lower layer, the hypolimnion. Compared to the epilimnion, which can source oxygen from the surrounding air and algae, the hypolimnion mostly contains oxygen consuming processes such as decay. The hypolimnion is also colder than the epilimnion, with no sun to heat it up. Stratification in lakes is temperature dependent. The sun-heated warm water rises above cold water. Therefore, the warm water in the epilimnion and the cold water of the hypolimnion are separated and do not mix. During the fall, the air begins to cool, also cooling the surface of the lake. If the surface of the lake cools to a temperature near to, or lower than the hypolimnion of the lake, the lake will turnover. Cold water sinks and warmer water rises, leading to mixing which distributes oxygen throughout the lake.

Data from Landsat 7 and Landsat 8 were combined, and I looked at the surface temperatures from location L08 during the time of interest, May through October. One deterrent for Quagga mussels is high temperatures. The quagga mussels struggle to survive when temperatures reach near 28°C. In Saguaro Lake, these temperatures were regularly reached, and prevented quagga mussels from surviving in the oxygen-rich epilimnion of the lake. I took average summer surface temperatures from the year quagga mussels were first detected in

Arizona (2007), to present. If the average surface temperature fell, it would explain why quagga mussels were recently able to invade Canyon Lake.

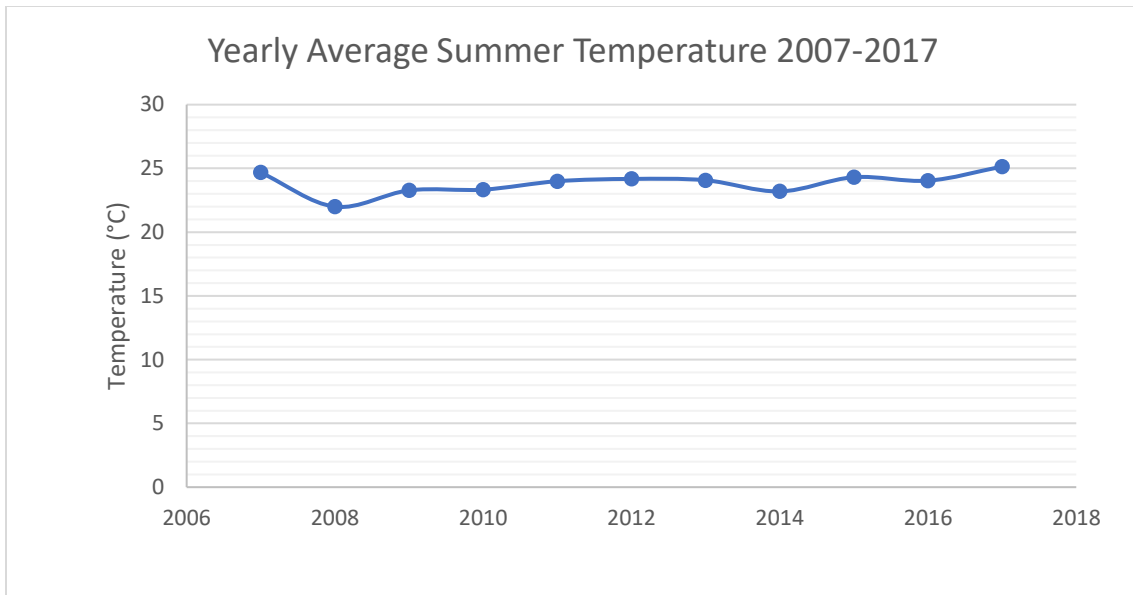


Figure 23. Yearly Average Temperature from May to October for Canyon Lake 2007-2017

The overall average summer temperature was near 24°C with an RMSE of 1°C, the variation in the data is not significant enough to assume that the overall temperature of the lake changed significantly, and the trend has been relatively steady since 2007 (Figure 23).

Comparing summer temperatures from the satellites to onsite data, I found that the summers followed a general trend reflected by the satellite data. Temperatures would rise between May and June and fall September to October. Late June, July, August, and early September stayed relatively warm. It should be noted that during the monsoon season in July, both on-site temperature and Landsat temperatures could not be acquired with the same frequency as other months due to severe weather and high cloud cover.

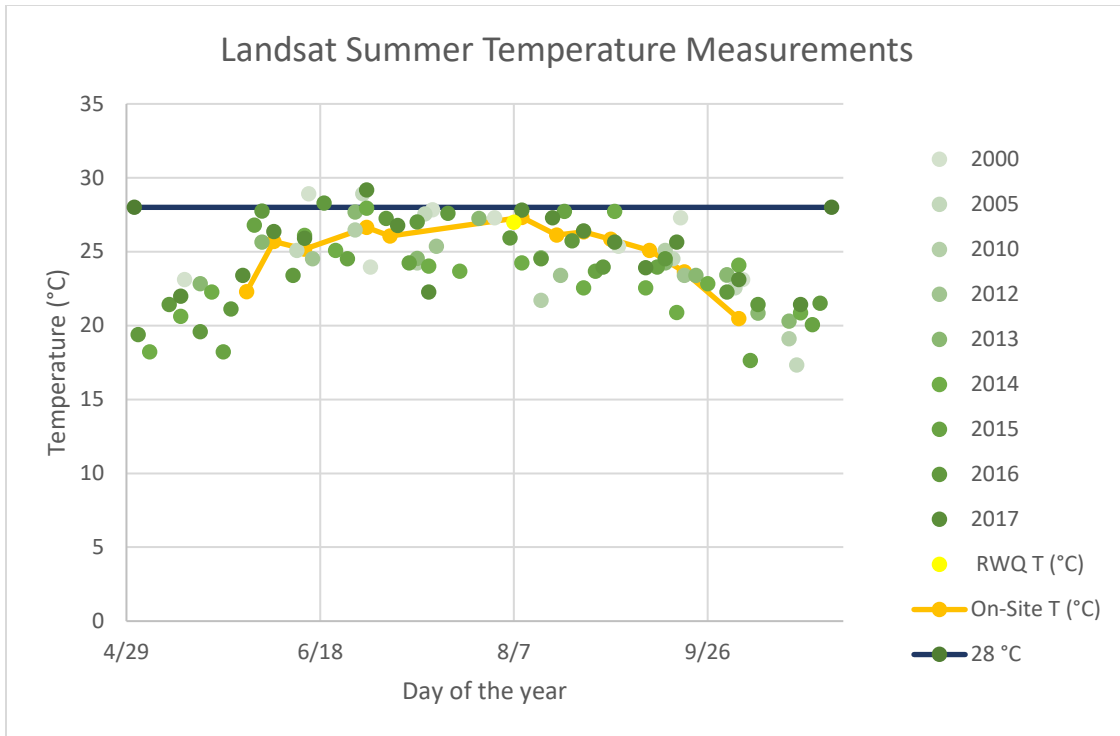


Figure 24. Long Term Summer Temperature Trends using Landsat and On-Site Data

Overall, with an RMSE of 0.80K and an R^2 of 0.82 at location L08, I was not able to determine significant deviations from typical temperature trends from before Canyon Lake became infected and after (Figure 24). Studies with lower RMSE, potentially using standardized algorithms to determine accurate surface temperatures from Landsat 8, may provide more clarity to the data in the future. Higher accuracy in other locations may yield more results, especially with respect to the exact time in which turnover occurs, and whether, in the past, turnover occurred uniformly throughout the lake. Landsat satellite imaging is an important tool for retrieving otherwise inaccessible data such as the historic data displayed in this section. The accuracy of the data, however, must be carefully accessed and with the level this study was able to achieve, there were no significant temperature impacts to the lake which caused it to become more susceptible to quagga mussel infection.

ON-SITE TEMPERATURE AND DISSOLVED OXYGEN DATA

During the summer of 2017, the Salt River area had large algal blooms that led to very low levels of dissolved oxygen just below the thermocline. Canyon Lake exhibited very low levels of dissolved oxygen in many locations throughout the lake and deep regions of Canyon Lake remained anoxic for an extended period. Temperature and dissolved oxygen (DO) levels for each location can be found in Appendix B. In this section, I will focus on the representative location, L08 (Figure 25).

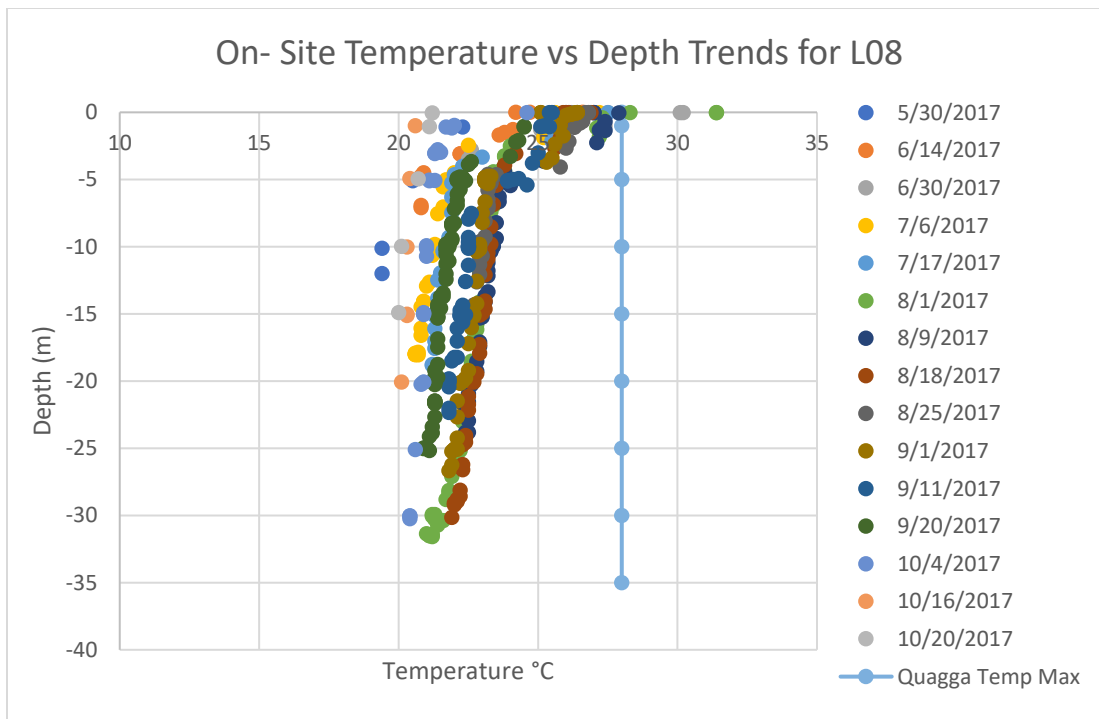


Figure 25. On-Site Temperature Trends for L08

On-Site temperature trends mapped against depth in Figure 25 shows that below approximately 5m, the water temperature stabilizes, indicating that the water below that depth freely mixes. During this period, the position of the end of the mixed layer, is approximately near 5m during the summer of 2017, (the depth of the mixed layer is subject to change seasonally). Above 5m, the temperature is frequently above 25°C, sometimes moving into the region of 28°C, the upper threshold for quagga mussels. Below 5m, temperatures approach 20°C in the deepest

portions of the lake, though I see a lot of measurements of about 22-23°C. As surface temperatures lower, such as seen in data from October 20th, the change in temperature with depth becomes smaller. When the surface temperature lowered to near the temperature of the hypolimnion, (near 22-23°C), the lake experienced turnover after which there is no more stratification.

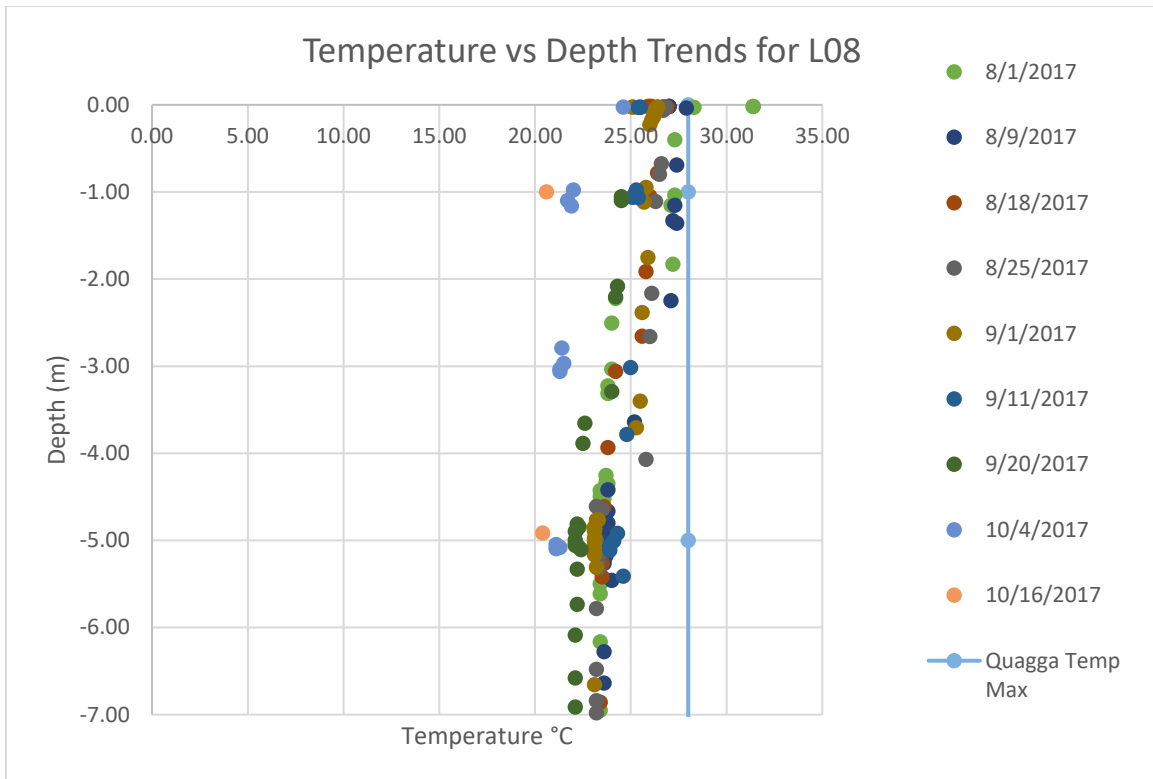


Figure 26 Close up Stratified Temperature vs Depth Trends for L08

Figure 26 shows a detailed image of the temperature vs depth trends for location L08 between 0m and 7m in depth during the time the lake is most stratified. During the peak of stratification in August, the epilimnion is from 0m to 2m in the graph. The thermocline layer is 2m in depth to 5m, where we observe a temperature gradient. After 5m, the temperature evens out to the next mixed layer, the hypolimnion.

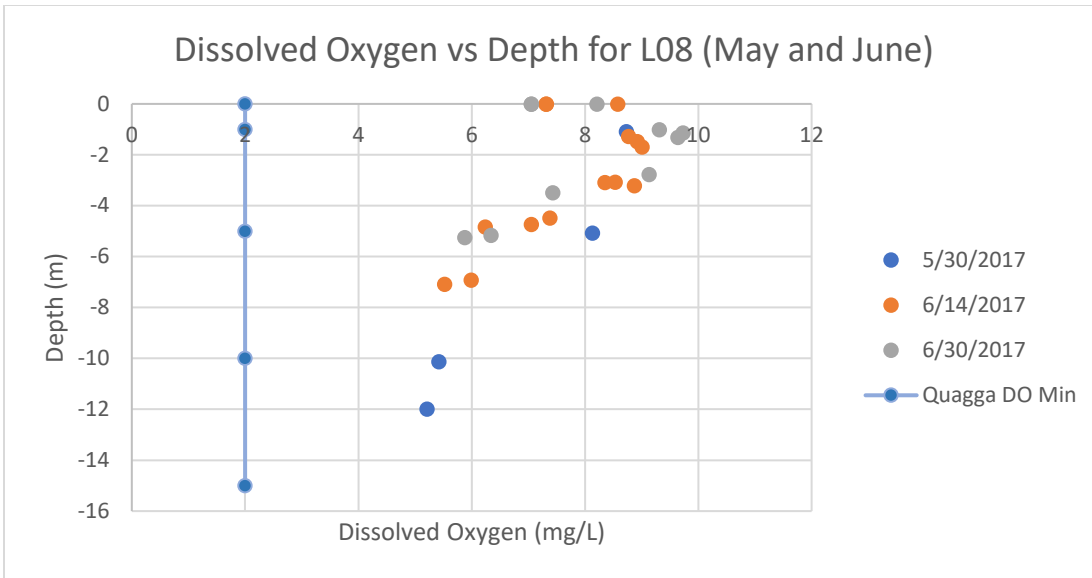


Figure 27. Dissolved Oxygen vs Depth for L08 May and June

Sampling began May 30. In late May and June, there was some stratification in the lake, but dissolved oxygen levels did not dip below levels stressful to quagga mussels (Figure 27). Some algae growth caused increased dissolved oxygen in the epilimnion and a slight drop in dissolved oxygen can be observed below 5m, dropping the dissolved oxygen from about 9mg/L to 5mg/L.

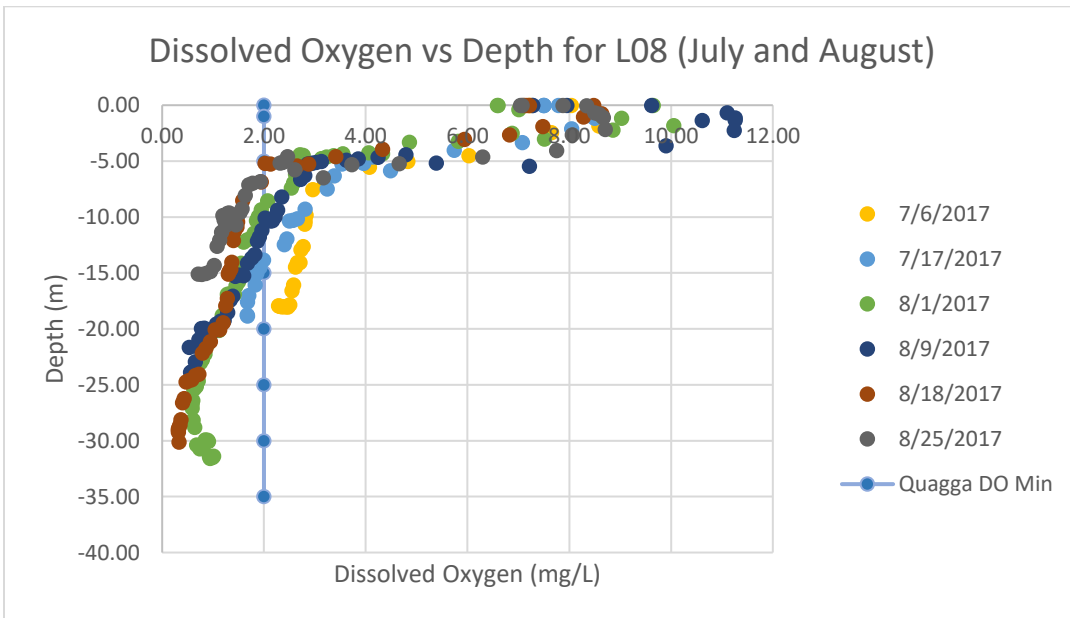


Figure 28. Dissolved Oxygen vs Depth for L08 July and August

In July and August (Figure 28), the lake becomes fully stratified and significant changes can be observed. Algal blooms cause the dissolved oxygen in the epilimnion to jump as high as 11mg/L while dissolved oxygen levels below 5m begin to drop to levels well below where quagga mussels are capable of surviving, dropping to nearly 0 in the deepest parts of the lake.

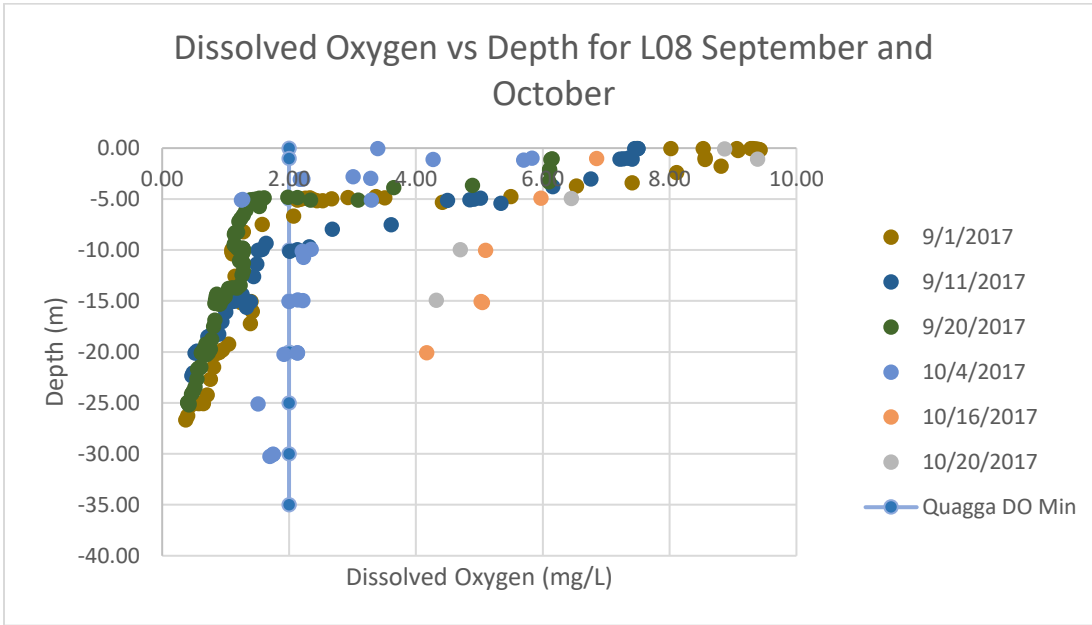


Figure 29. Dissolved Oxygen vs Depth for L08 September and October

By late September (Figure 29), anywhere in the hypolimnion the dissolved oxygen has dropped to below 2mg/L and stayed near 1mg/L until turnover in the beginning of October. After the surface temperatures began to drop, increased mixing between the epilimnion and hypolimnion promote increases in dissolved oxygen in the hypolimnion.

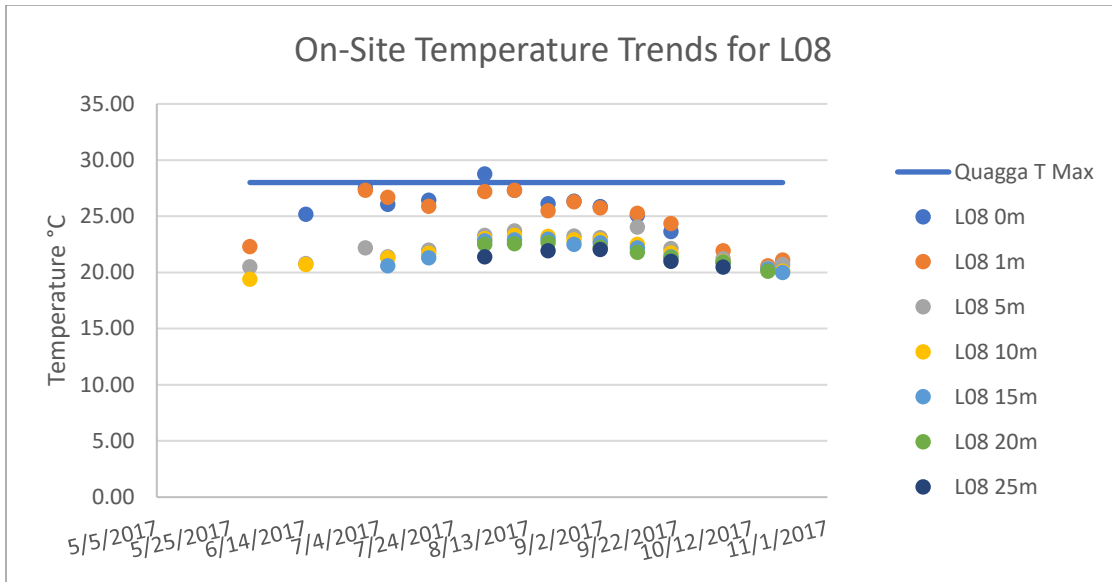


Figure 30. On-Site Temperature Trends for L08

The automatic nature of the data logger meant that I often had multiple readings for each location near certain depths in a single day, for example a reading at 0.9m in depth and another at 1.1m. In Figure 30, these readings were averaged into a single point per day. Readings more than 0.2m from the target depth were excluded and all readings within $\pm 0.2m$ were averaged and graphed as a time series. Using this time series, I can see the temperature effects on stratification and observe how long surface temperatures remained near the max threshold of 28°C. At L08, the surface temperature, (an averaged air and 0m depth water temperature), did pass 28°C, but only for one recorded day. The subsequent day of measuring, the average temperature only reached 27.3°C. The wider the vertical gap between temperature readings at each subsequent depth, the more dramatic the drop in temperature was after passing the thermocline.

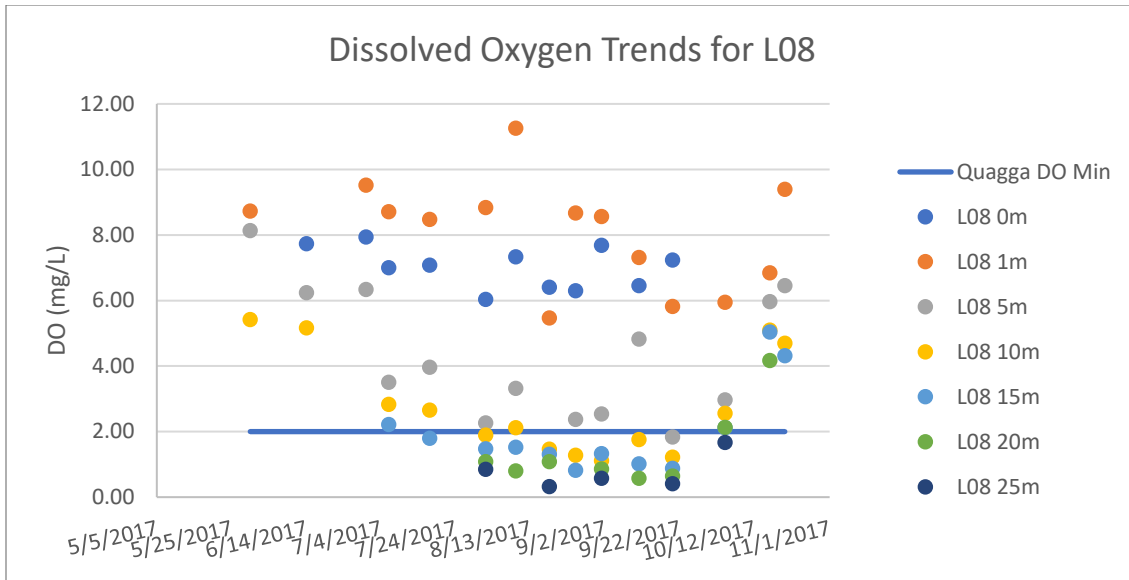


Figure 31. Dissolved Oxygen Trends for L08

We see stratification mirrored in the dissolved oxygen trends (Figure 31). Readings from the epilimnion at 1m depth contained high amounts of dissolved oxygen from the oxygen producing organisms in the epilimnion. Near 5m, the reading closest to the end of the mixed layer, the dissolved oxygen began to drop. Very near 5m, the dissolved oxygen concentrations would vary significantly in just a short distance. Readings near the thermocline layer can be expected to vary drastically depending on if the reading was above, below or within the thermocline layer (Figure 32). In some locations, such as location L08, this led to readings near 5m staying relatively above the dissolved oxygen threshold for quagga mussels.

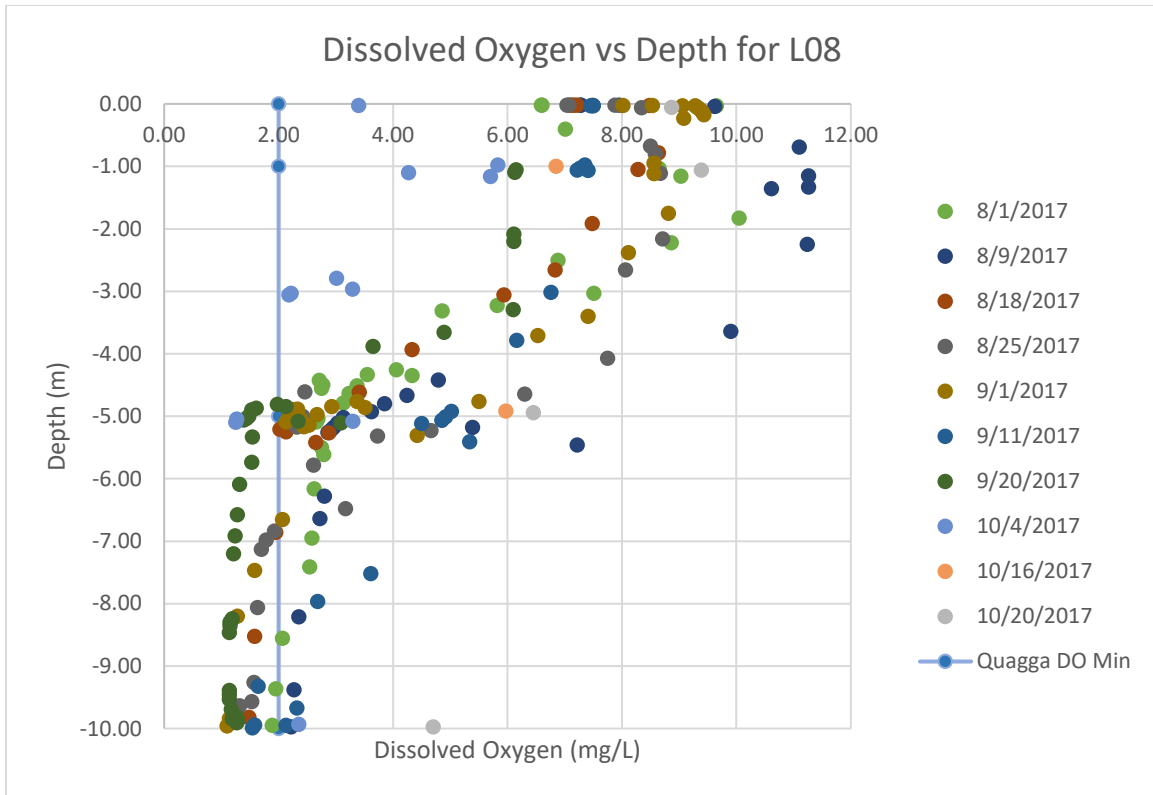


Figure 32 Close up Stratified Dissolved Oxygen vs Depth for Location L08

Additional evidence can be found in Figure 32 that just before the end of the mixed layer around 5m in depth, the thermocline shows a rapid decline in dissolved oxygen between depths of 2m and 5m. Below the thermocline, in the mixed layer, dissolved oxygen dropped, and the lower limit of quagga mussel tolerance was passed for an extended period. In Figure 31 and Figure 32 dissolved oxygen above the hypolimnion stayed well above 2mg/L. Combined with knowledge that the temperature in the regions above 5m in depth rarely passed 28°C for an extended period of time, the region above the hypolimnion mixed layer may be the location that quagga mussels are most likely to reside if they populate Canyon lake.

QUAGGA MUSSEL SURVIVABILITY IN CANYON LAKE

The dissolved oxygen above 5m of depth at all locations did not drop below 2mg/L. The driving force preventing quagga mussels from populating the epilimnion and thermocline layers would be a temperature above 28°C. Meanwhile, below 5m, a dissolved oxygen above 2mg/L allows quagga mussels to survive. Depletion of dissolved oxygen is often due to decay, a process that is concentrated in the hypolimnion, especially near the bottom of the lake.

Table 3
Days of Inhospitable Conditions at Canyon Lake by Location and Depth

Days of Inhospitable Conditions at Canyon Lake by Location and Depth (days)							
d: Depth, T: Temperature, DO: Dissolved Oxygen							
Sampling Location	d=0m T >28°C (days)	d=1m T >28°C (days)	d=5m DO<2m g/L (days)	5<d≤10m DO <2mg/L (days)	10<d≤15m DO<2mg/L (days)	15<d≤20m DO<2mg/L (days)	d= (20+) m DO<2mg /L (days)
L01	16	0	47	96	X	x	x
L02	0	0	64	96	X	x	x
L03	0	0	64	104	X	x	x
L04	0	0	64	90	104	x	x
L05	0	0	23	56	X	x	x
L06	0	0	14	64	79	96	x
L07	0	0	0	23	90	90	90
L08	0	0	0	33	65	65	x
L09	0	0	0	24	79	79	x
L10	0	0	0	56	79	90	x
L11	0	0	0	73	79	90	x
L12	0	0	0	19	50	50	x
L13	8	8	0	9	26	50	90
L14	17	9	7	50	65	79	x
L15	0	0	0	79	X	x	x
L16	24	17	0	14	X	x	x
L17	7	0	9	64	X	x	x
L18	8	11	26	79	X	x	x
L19	8	0	0	x	X	x	x
L20	0	0	14	47	X	x	x
L21	0	0	14	90	104	x	x

In Table 3, the epilimnion contains a hospitable zone for quagga mussels to take shelter during the otherwise very inhospitable summer months. At location L08, there were 0 inhospitable days in which the quagga mussels could not survive above 5m, meaning that above the hypolimnion, quagga mussels can survive through the summer. Areas toward the center of the lake and up the river towards Apache lake are most prone to having hospitable zones as deep as 5m. For L08, it isn't until the hypolimnion is reached, that as many as 23 days were estimated to have passed with dissolved oxygen levels too low for quagga mussels to proliferate. The 23 days is calculated from the first day that I recorded low dissolved oxygen levels to the uninterrupted last day I recorded low dissolved oxygen. Data details for each location can be found in Appendix C.

CONCLUSIONS

The epilimnion of many locations around Canyon Lake does not have temperatures high enough to prevent quagga mussel infestation from occurring. This may be due to the high cliffs surrounding Canyon Lake providing shade, wind or flow conditions circulating the water, or the elevation of Canyon Lake, which is 154 ft higher than Saguaro Lake. Canyon Lake is not, however, entirely hospitable to quagga mussels. Quagga mussels need to attach to a surface and, since Canyon Lake was described to have a relatively flat lake bed (Branom, 2007), there are few places to attach above the hypolimnion. To create an established population year after year, the quagga mussels have likely found their way to substrates such as the chains of buoys, which provide a location not too near the surface and not too deep. In areas especially near the center of the lake, quagga mussels are likely to be found attached to substrate that can be found between 1m and 5m depth.

Based on the Landsat data collected in this research, it is unlikely that Canyon Lake's surface temperature varied significantly enough from past years that it would have affected the ability of quagga mussels to start inhabiting Canyon Lake. It is more likely that while populations have tried to establish, most hospitable locations in Canyon Lake lack the substrate for them to

attach. This also plays an essential role in the testing for quagga mussel veligers as well. Depending on the location and depth sampled, quagga mussels may not be in high density in one region of the lake simply due to a lack of places to attach. Recent detection may indicate then, that a colony has either newly established itself near the sampling point, or that an established colony has sent out more veligers which made their way to the sampling point. Most likely, considering estimates that Lake Mead had been infested years before detection, it is quite likely that Canyon Lake has already become infested with quagga mussels. It is likely that without preventative measures, Canyon Lake will steadily see an increase in quagga mussels as more and more quagga mussels populate the hospitable locations they can survive within.

Another location that should be tested for veligers is the shaded boat area of the Canyon Lake Marina. The boats and docks are likely places that the quagga mussels will readily adhere to. A shaded canopy prevents hot temperatures from affecting the quagga mussels, and underwater plants such as seaweed growing near the marina may shelter quagga mussels from some of the low dissolved oxygen levels found in the rest of Canyon lake. Testing the epilimnion of the marina may yield more precise indications of the presence of quagga mussels in the reservoir. In addition, sightings of quagga mussels at Mormon Flat Dam may also be an indication that the dam is providing substrate and a suitable location for quagga mussel colonies to thrive.

Our research was able to meet our first objective of determining a probable cause for the recent detection of quagga mussels in Canyon Lake. I determined that quagga mussels can infect Canyon lake, and I established the hospitable locations that can likely harbor quagga mussel colonies. The objectives of the study were met.

Findings of this study can be expanded to the Salt River watershed, the Verde watershed, and other watersheds that follow a similar pattern of stratification. Although Canyon Lake is a difficult lake for quagga mussels to populate, enough exposure to quagga mussels have likely caused it to become partially infested. Recent detection of quagga mussels in Saguaro Lake and Apache Lake may follow similar trends and it is recommended that surface

temperatures at various locations of each reservoir are tested to ensure that quagga mussels cannot infect the epilimnion of those reservoirs. Further refinement of satellite data and the ability to determine accurate and precise surface temperatures of these watersheds could become an indispensable tool into understanding the spread of quagga mussels to similar reservoirs.

Canyon Lake is an artificially created lake and may therefore have more options than other reservoirs for quagga mussel treatment. Introduction of predator fish species that prey on quagga mussels may help stem the population. Redear sunfish, already present in other Arizona Lakes (US Department of the Interior Bureau of Reclamation, 2015) could potentially help control quagga mussel populations in Canyon Lake. Divers, looking specifically in areas such as docks and buoy chains for quagga mussels may also find ways to apply deterrents to prevent attachment at those locations. Although complete eradication of this invasive species in Canyon Lake may pose a challenge to reservoir managers, the concentration of quagga mussels in specific locations may help focus efforts to control their negative ecological and economic impacts.

REFERENCES

- Arizona Game and Fish Department. (2010, March 24). *Don't Move a Mussel- Now it's the law*. Retrieved from Arizona Game and Fish Department: <http://www.azgfd.net/artman/publish/NewsMedia/Don-t-move-a-mussel-now-it-s-the-law.shtml>
- Benson, A. J., Richerson, M. M., Maynard, E., Larson, J., Fusaro, A., Bogandoff, A. K., & Neilson, M. E. (2017, June 5). *Dreissena rostriformis bugensis*. Retrieved from USGS Nonindigenous Aquatic Species: <https://nas.er.usgs.gov/queries/FactSheet.aspx?speciesID=95>
- Branom, M. (2007, December 25). *On Empty: SRP drains Canyon Lake*. Retrieved from East Valley Tribune: http://www.eastvalleytribune.com/news/on-empty-srp-drains-canyon-lake/article_c56dea5e-e323-50d4-b1e9-588ef0639f9f.html
- Carmon, J., & Hosler, D. M. (2015). Understanding Dreissenid Veliger Detection in the Western United States. In W. H. Wong, *Biology and Management of Invasive Quagga and Zebra Mussels in the Western United States* (pp. 123-140). Boca Raton: CRC Press.
- Central Arizona Project. (2018, February 19). *Lake Pleasant Operations*. Retrieved from CAP-AZ: <http://www.cap-az.com/departments/water-operations/lake-pleasant-operations>
- Choi, W. J., Gerstenberger, S., McMahon, R. F., & Wong, W. H. (2013). Estimating survival rates of quagga mussel (*Dreissena rostriformis bugensis*) veliger larvae under summer and autumn temperature regimes in residual water of trailered watercraft at Lake Mead, USA. *Management of Biological Invasions*, 61-69.
- Davis, C. J., Emma, R. K., Achara, K., Chandra, S., & Jerde, C. L. (2015). Successful survival, growth and reproductive potential of quagga mussels in low calcium lake water: is there uncertainty of establishment risk? *PeerJ*, 1276.
- Lamaro, A. A., Mariñelarena, A., Torrusio, S. E., & Sala, S. E. (2013). Water surface temperature estimation from Landsat 7 ETM+ thermal infrared data using the generalized single-channel method: Case study of Embalse del Río Tercero (Córdoba, Argentina). *Advances in Space Research*, 492-500.
- Meehan, S., Shannon, A., Gruber, B., Rackl, S., & Lucy, F. E. (2014). Ecotoxicological impact of Zequanox, a novel biocide, on selected non-target Irish aquatic species. *Ecotoxicology and Environmental Safety*, 148-153.
- Misamore, M. J., Barnard, S., Couch, E., & Wong, W. H. (2015). Reproductive Biology of Quagga Mussels (*Dreissena rostriformis bugensis*) with an Emphasis on Lake Mead. In W. H. Wong, *Biology and management of invasive quagga and zebra mussels in the western United States* (pp. 53-70). Boca Raton: CRC Press.

- Molly, D. P., Mayer, D. A., Gaylo, M. J., Morse, J. T., Presti, K. T., Sawyko, P. M., . . . Griffin, B. H. (2013). *Pseudomonas fluorescens* strain CL145A-Abiopesticide for the control of zebra and quagga mussels. *Journal of Invertebrate Pathology*, 104-114.
- Moore, B. G., Holdren, C., Gerstenberger, S. L., Turner, K., & Wong, W. H. (2015). Invasion by Quagga Mussels (*Dreissena rostriformis bugensis* Andrusov 1897) into Lake Mead, Nevada-Arizona: The First Occurance of the Dreissenid Species in the Western United States. In W. H. Wong, *Biology and management of invasive quagga and zebra mussels in the United States* (pp. 18-30). Boca Raton: CRC Press.
- National Park Service. (2017, April 4). *Lake Mead Hydrology*. Retrieved from NPS.gov: <https://www.nps.gov/lake/learn/hydrology.htm>
- Nelson, M. S., & Nibling, F. (2013). Monitoring invasive quagga mussels, *Dreissena rostriformis bugensis* (Bivalvia: Dreissenidae) and other benthic organisms in a western US aqueduct. *Management of Biological Invasions*, 51-59.
- Salt River Project. (2018, February 19). *Daily Water Report*. Retrieved from [data.Hydrometdataservice.info](http://data.hydrometdataservice.info): <http://data.hydrometdataservice.info/dwr/report.aspx?dt=2/19/2017>
- Salt River Project. (n.d.). *Mormon Flat Dam*. Retrieved from Salt River Project Dams: <https://www.srpnet.com/water/dams/mormon.aspx>
- Snider, J. P., Moore, J. D., Volkoff, M. C., & Byron, S. N. (2014). Assessment of quagga mussel (*Dreissena bugensis*) veliger survival under thermal, temporal and emersion conditions simulating overland transport. *California Fish and Game*, 640-651.
- Sokolowski, M. (2015). An Investigation of Factors Affecting the Spread of *D. bugensis* in Arizona's Reservoirs. *ASU Electronic Theses and Dissertations*. Arizona, USA: Arizona State University. Retrieved from <https://repository.asu.edu/items/36450>
- Syariz, M. A., Jaelani, L. M., Subehi, L., Pamungkas, A., Koenhardono, E. S., & Sulisetyono, A. (2015). Retrieval of sea surface temperature over Poteran Island water of Indonesia with Landsat 8 TIRS image: A preliminary algorithm. *The International Archives of the Photogrammetry, Remote Sensing and Spacial Information Sciences*, 28-30.
- Takeguchi, W., Liang, S., & Yates, R. (2012). Evaluating Potential Quagga Mussel Control Measures in Colorado River Water. *American Water Works Association*, 49.
- US Department of the Interior Bureau of Reclamation. (2015, Fall). *Do Reddear Sunfish Eat Quagga Mussels?* Retrieved from Reclamation Managing Water in the West: <https://www.usbr.gov/research/docs/updates/2015-15-redear-sunfish.pdf>
- USGS. (2017, June 22). *Landsat Missions*. Retrieved from [Landsat.usgs.gov](https://landsat.usgs.gov): <https://landsat.usgs.gov/landsat-missions-timeline>

- USGS. (2018, 04 25). *Landsat 8 Data Users Handbook*. Retrieved from USGS Landsat Missions: <https://landsat.usgs.gov/landsat-8-l8-data-users-handbook>
- USGS. (2018, Feb 16). *USGS NAS Dreissena rostriformis bugensis records*. Retrieved from USGS NAS: <https://nas.er.usgs.gov/viewer/omap.aspx?SpeciesID=95#>
- USGS Landsat Project Office. (n.d.).
- USGS Landsat Project Science Office. (2018, February 16). *Landsat 7 Science Data Users Handbook*. Retrieved from USGS Landsat Missions: <https://landsat.usgs.gov/landsat-7-data-users-handbook>
- Ventura, L. D., Sarpe, D., Kopp, K., & Jokela, J. (2016). Variability in phenotypic tolerance to low oxygen in invasive populations of quagga and zebra mussels. *Aquatic Invasions*, 267-276.
- Wloczyk, R. R., Borg, E., & Neubert, W. (2006). Sea and lake surface temperature retrieval from Landsat thermal data in Northern Germany. *International Journal of Remote Sensing*, 2489-2502.

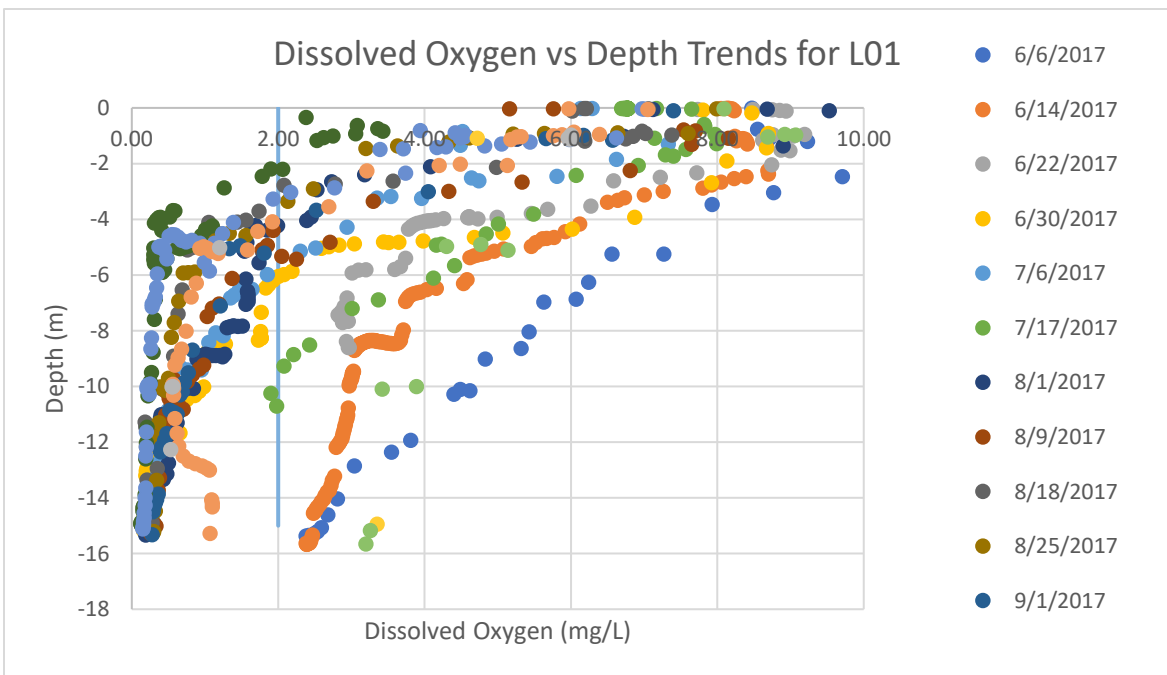
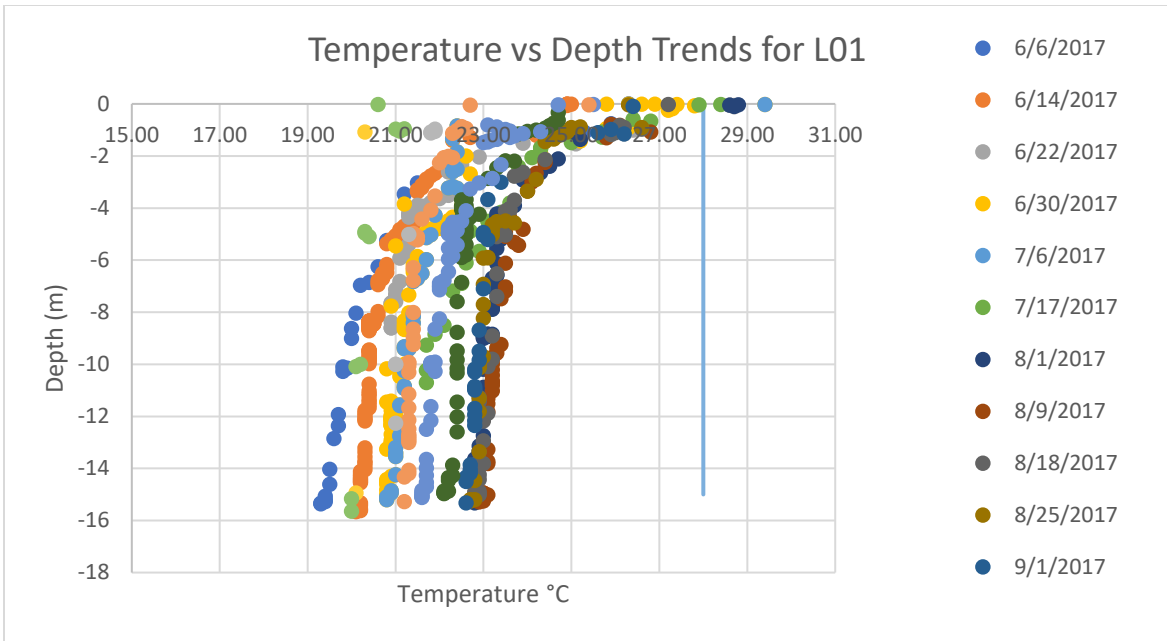
APPENDIX A

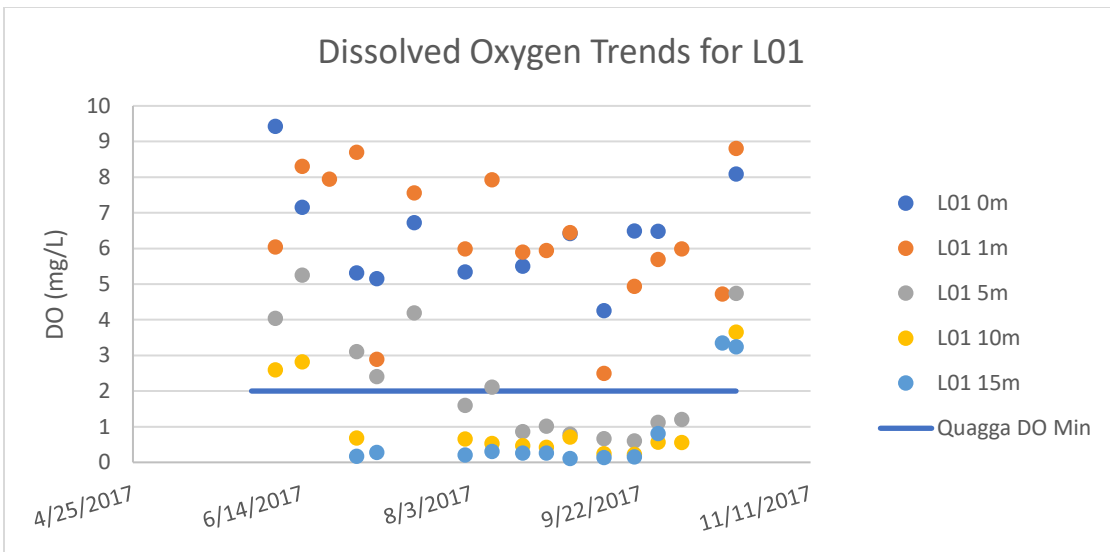
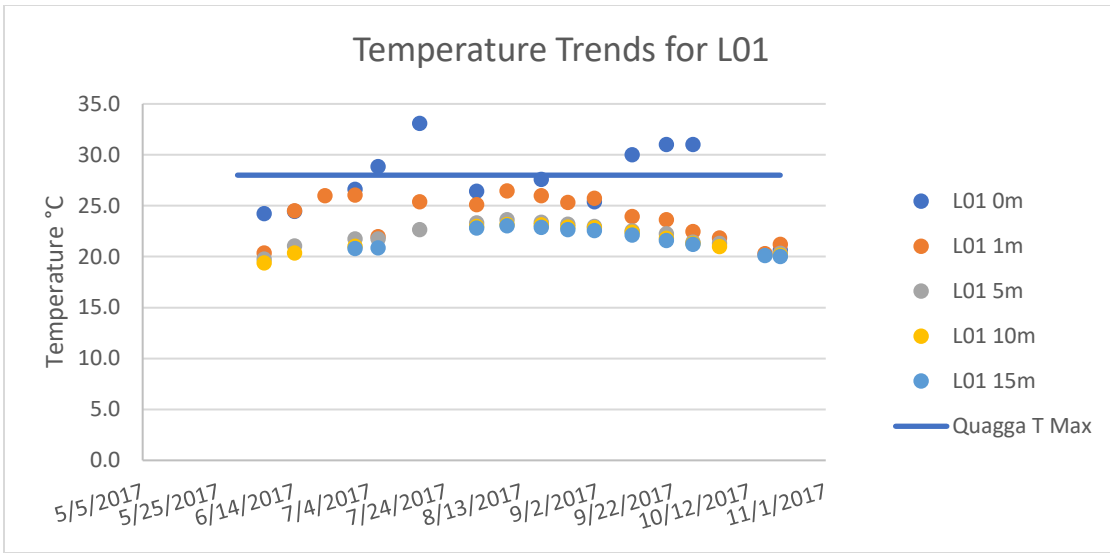
ACRONYMS

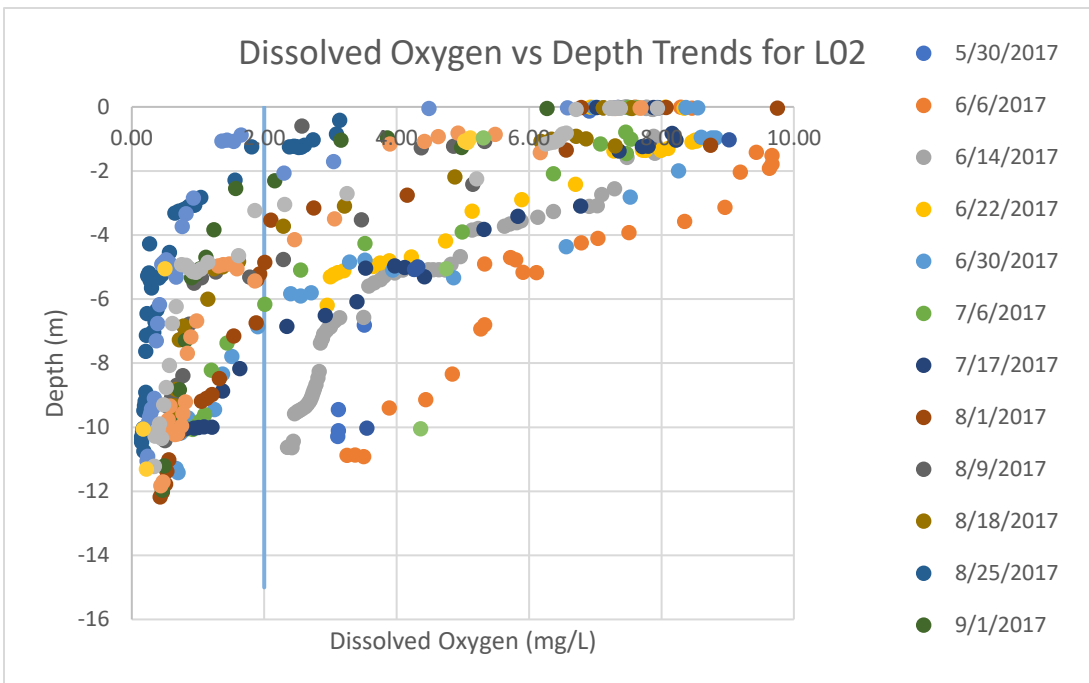
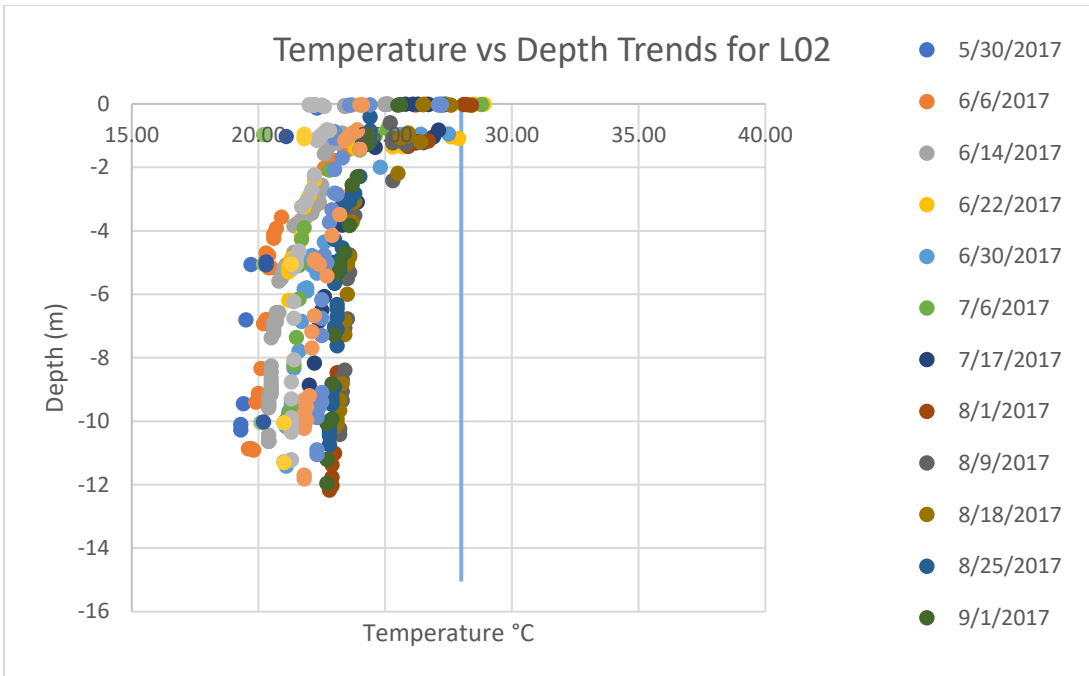
CPLM	Cross Polarizing Light Microscopy
EROS	Earth Resources Observation and Science Center
GeoTIFF	Geographic Tagged Image File Format
L01, L02, ... L21	Location 1, Location 2, ... Location 21
LS7	Landsat 7
LS8	Landsat 8
NASA	National Aeronautics and Space Administration
OLI	Operation Land Imager
PCR	Polymerase Chain Reaction
QWIP	Quantum Well Infrared Photodetectors
RDLES	Reclamation Detection Laboratory for Exotic Species
RMSE	Root Mean Square Error
SCGM	single-channel generalized method
SEM	scanning electron microscopy
SLC	Scan Line Corrector
SRP	Salt River Project
SWIR	Shortwave Infrared
TIRS	Thermal Infrared Sensor
USGS	U.S. Geological Survey
WRS-2	Worldwide Reference System 2

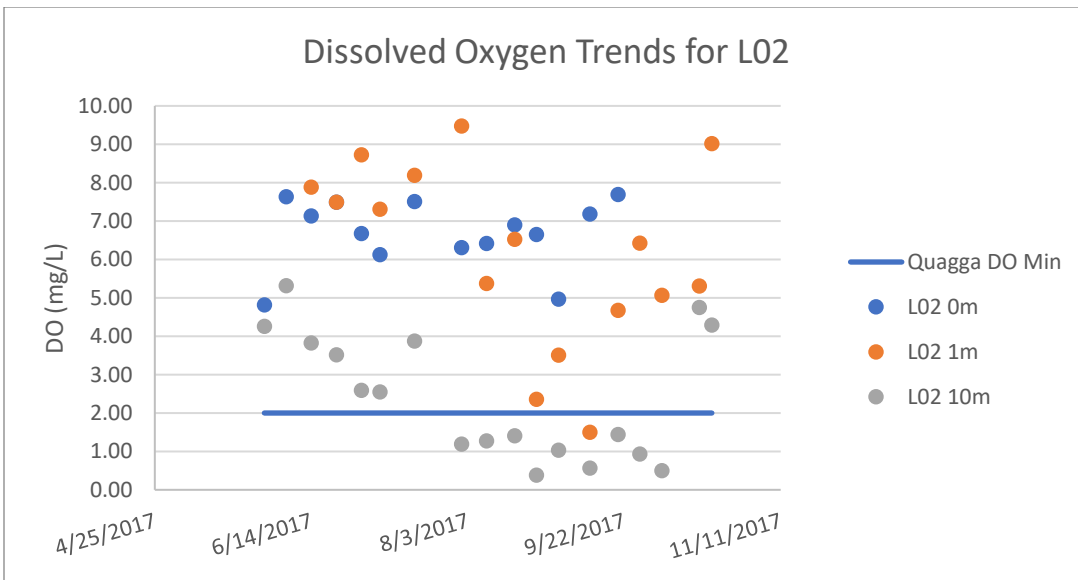
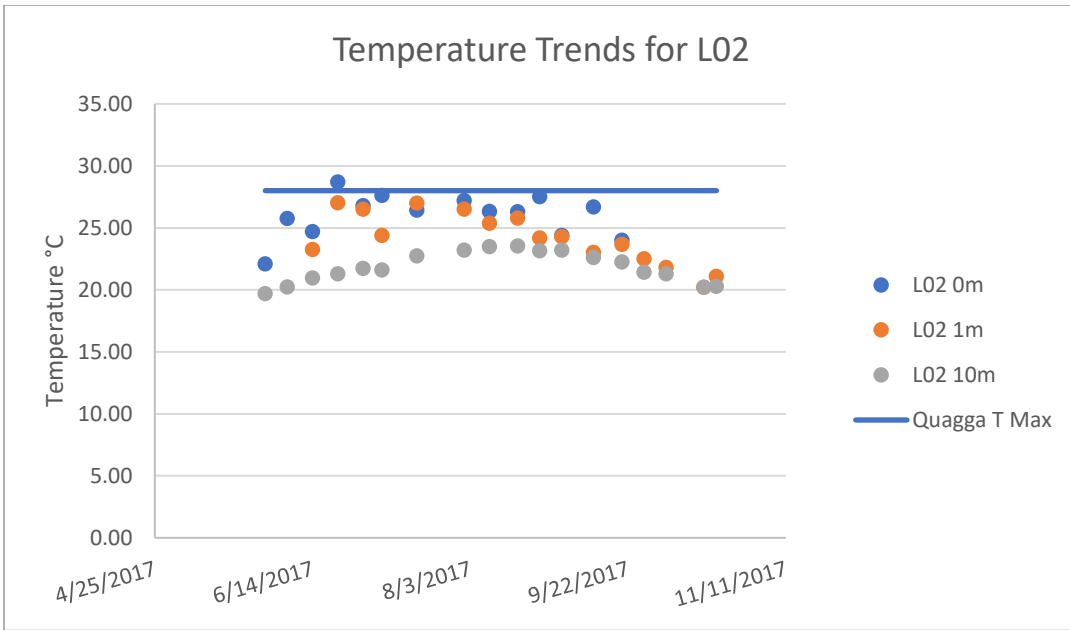
APPENDIX B

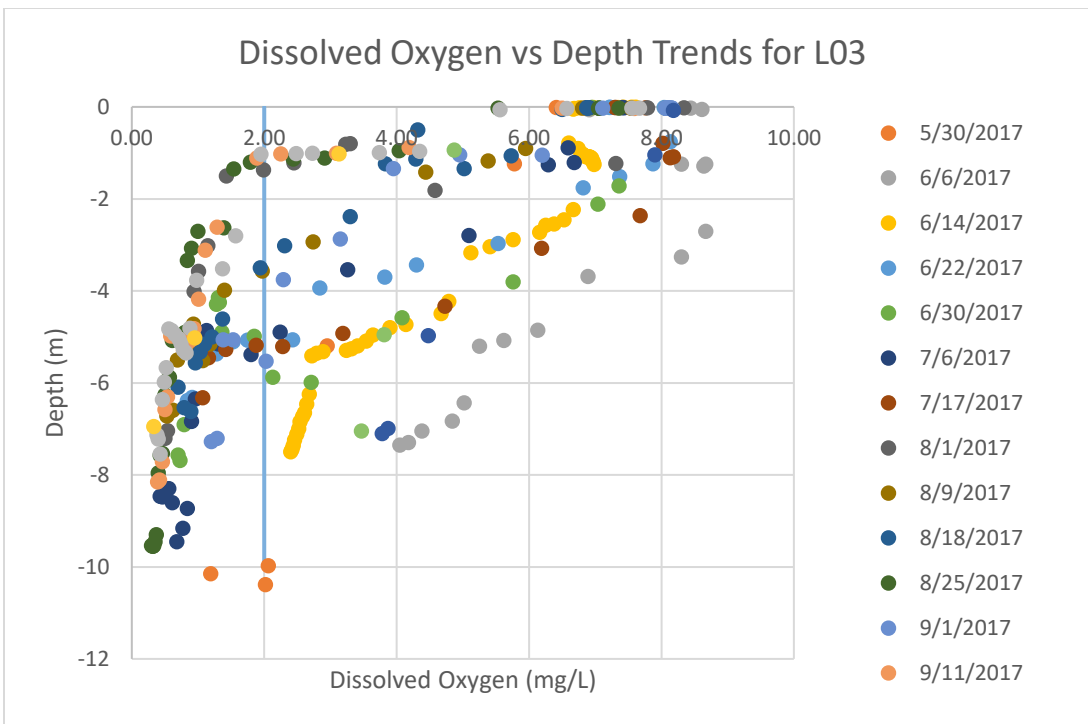
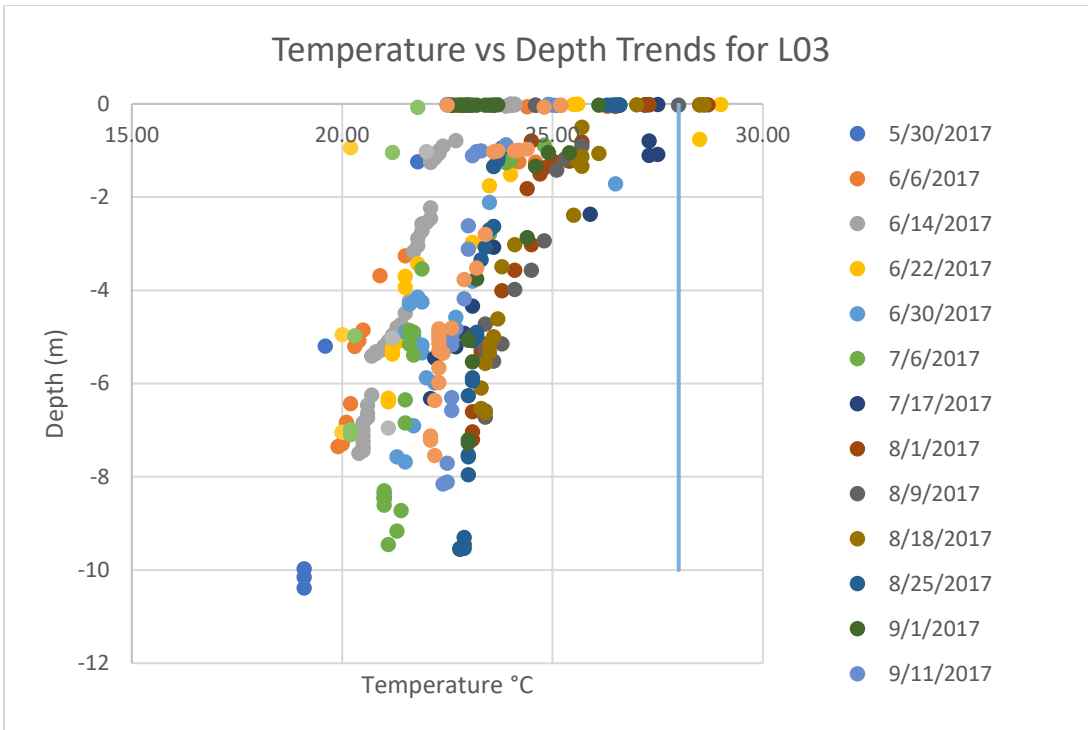
ON-SITE TEMPERATURE AND DISSOLVED OXYGEN TRENDS FOR ALL LOCATIONS

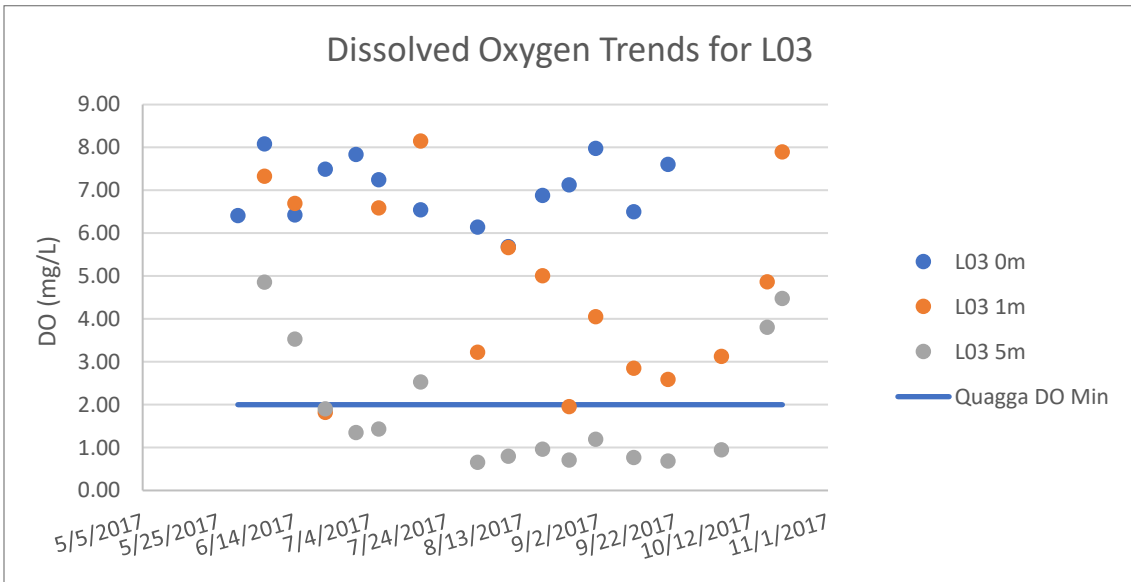
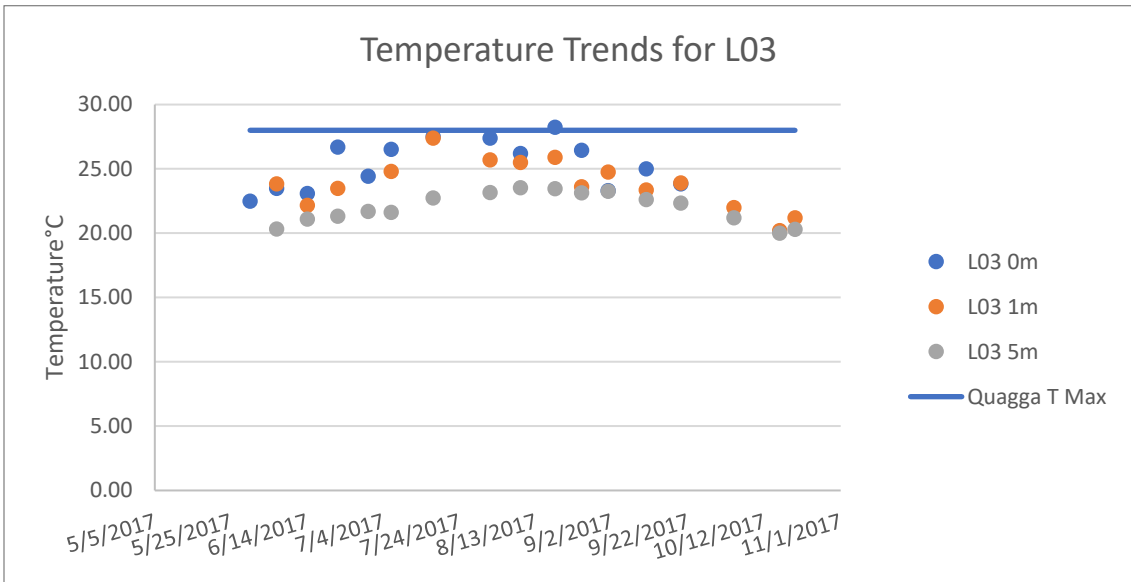


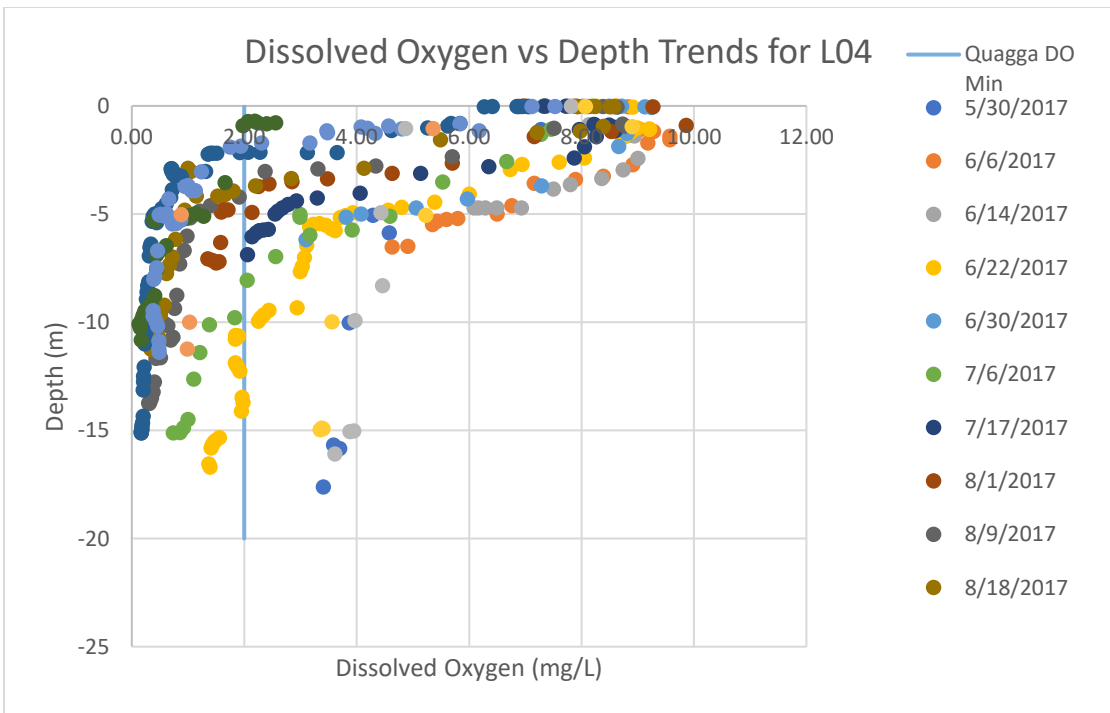
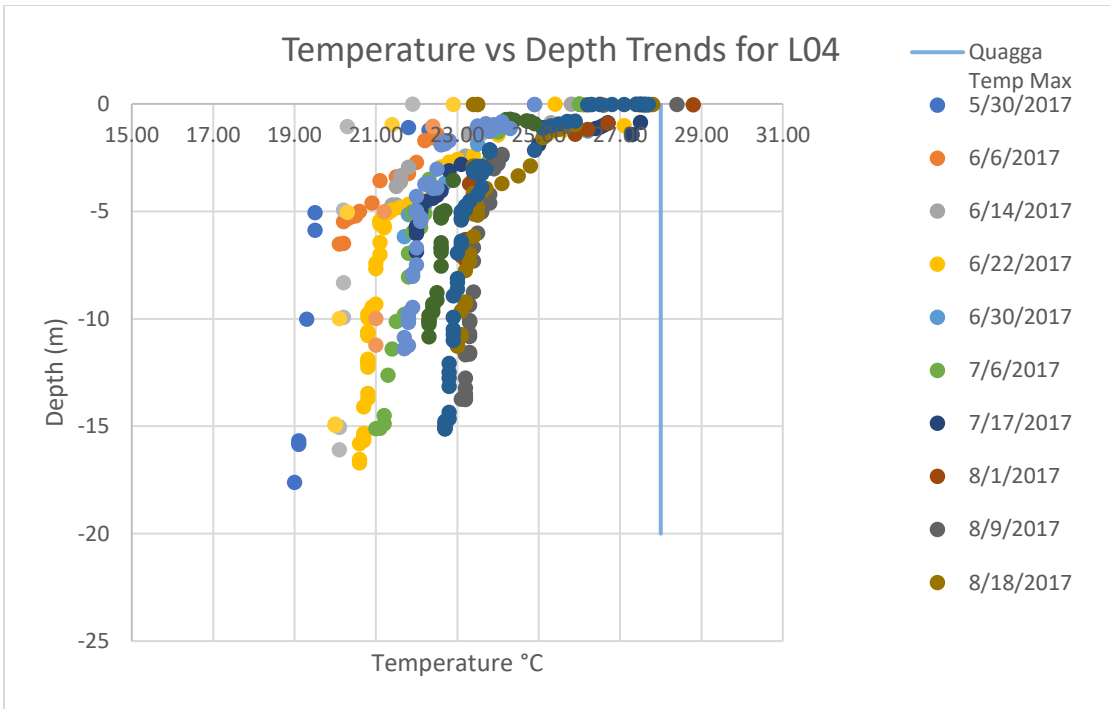


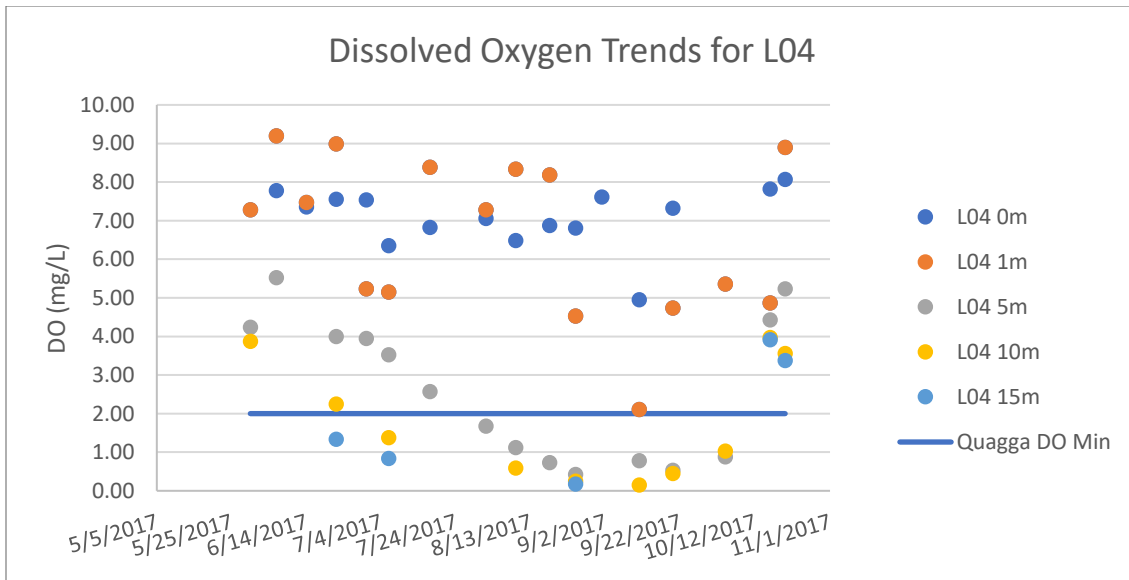
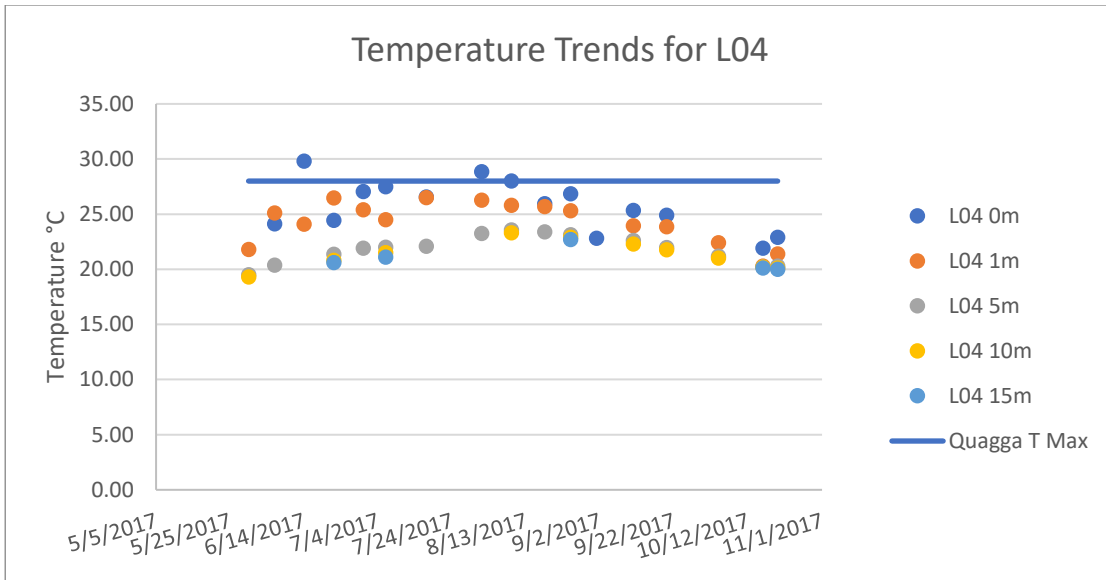


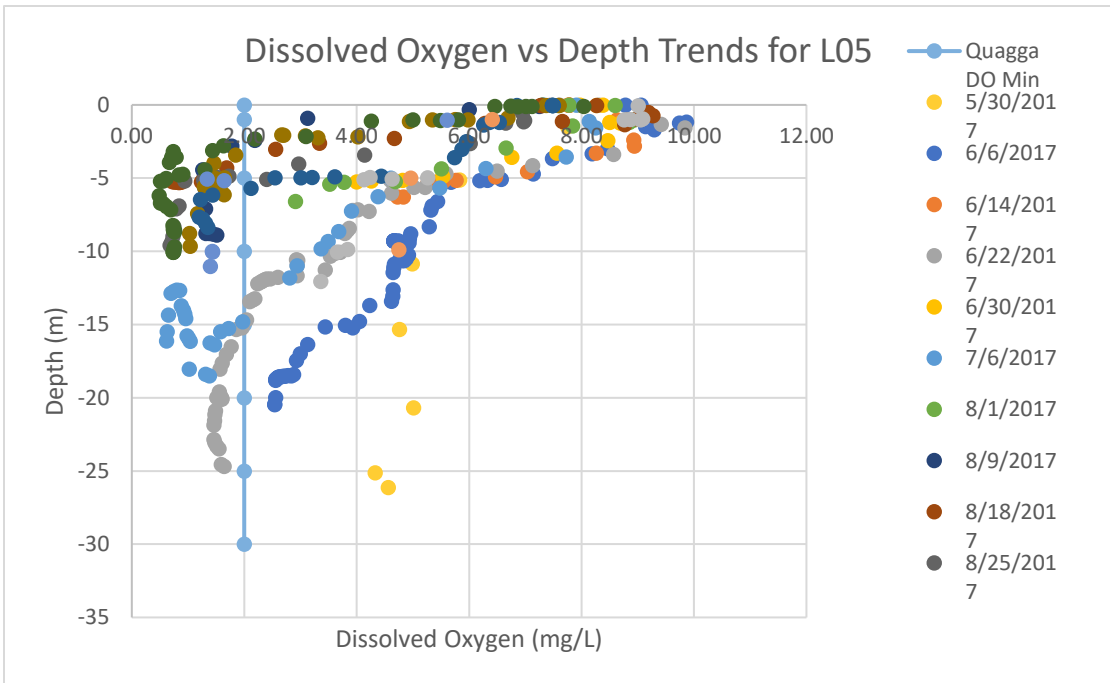
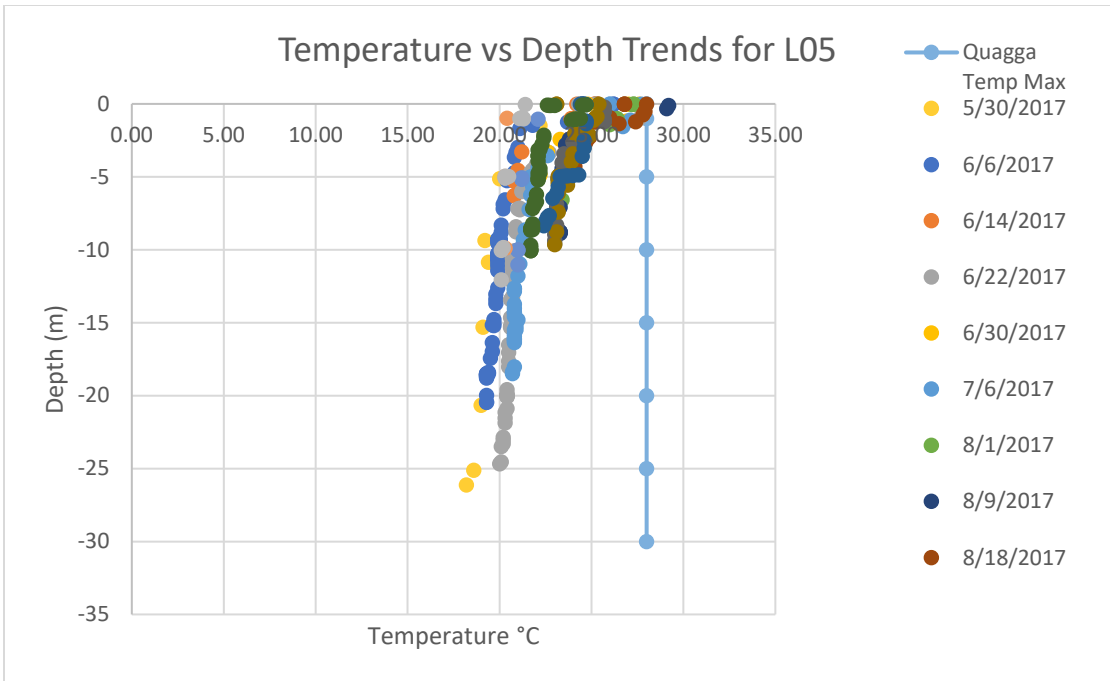


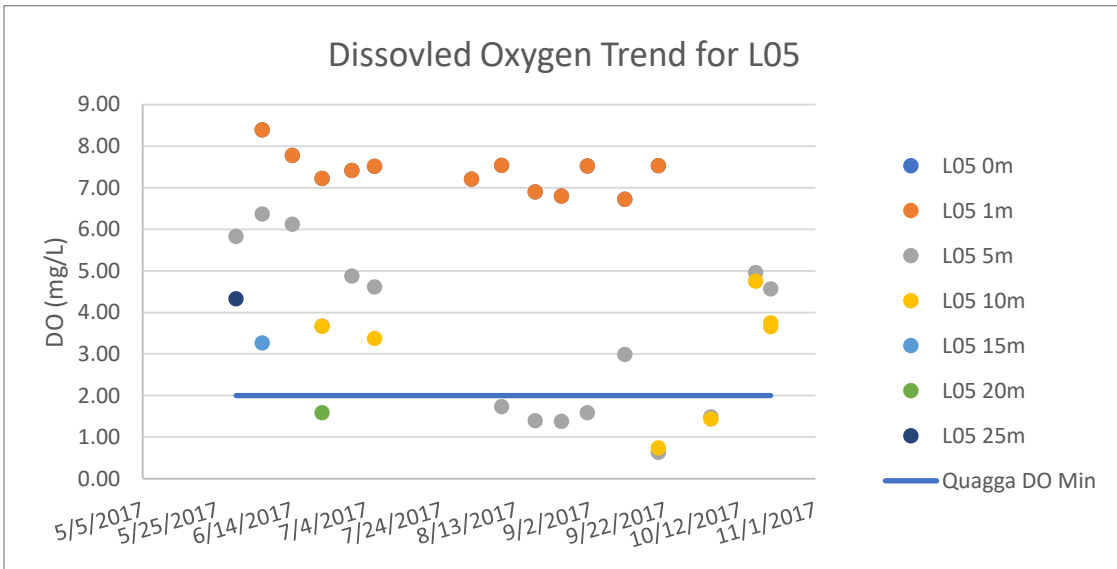
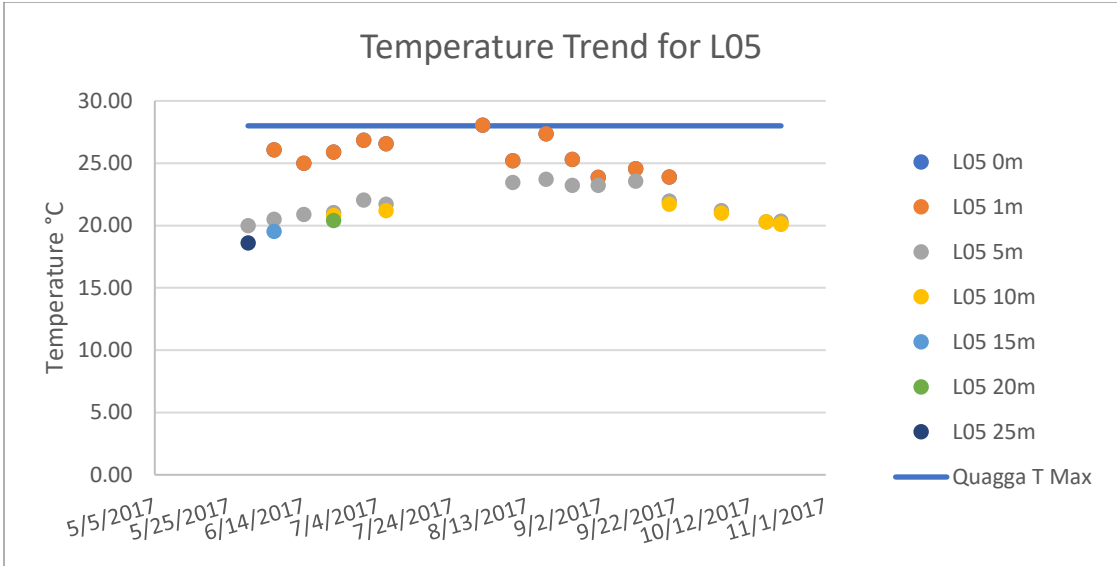


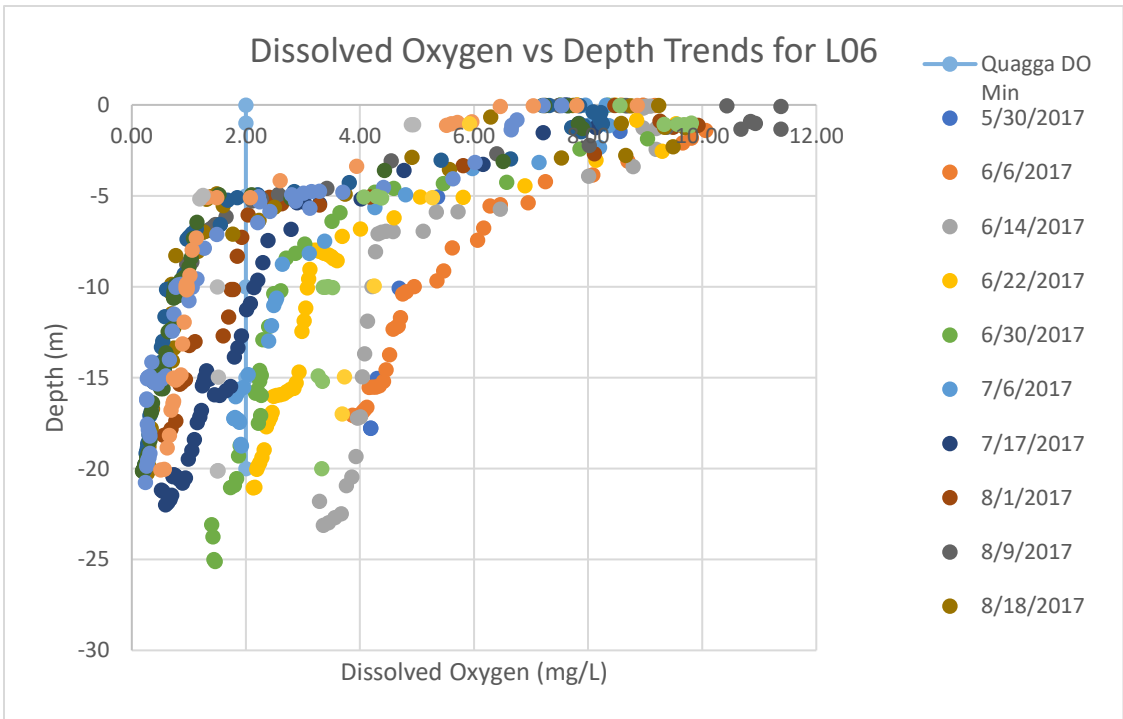
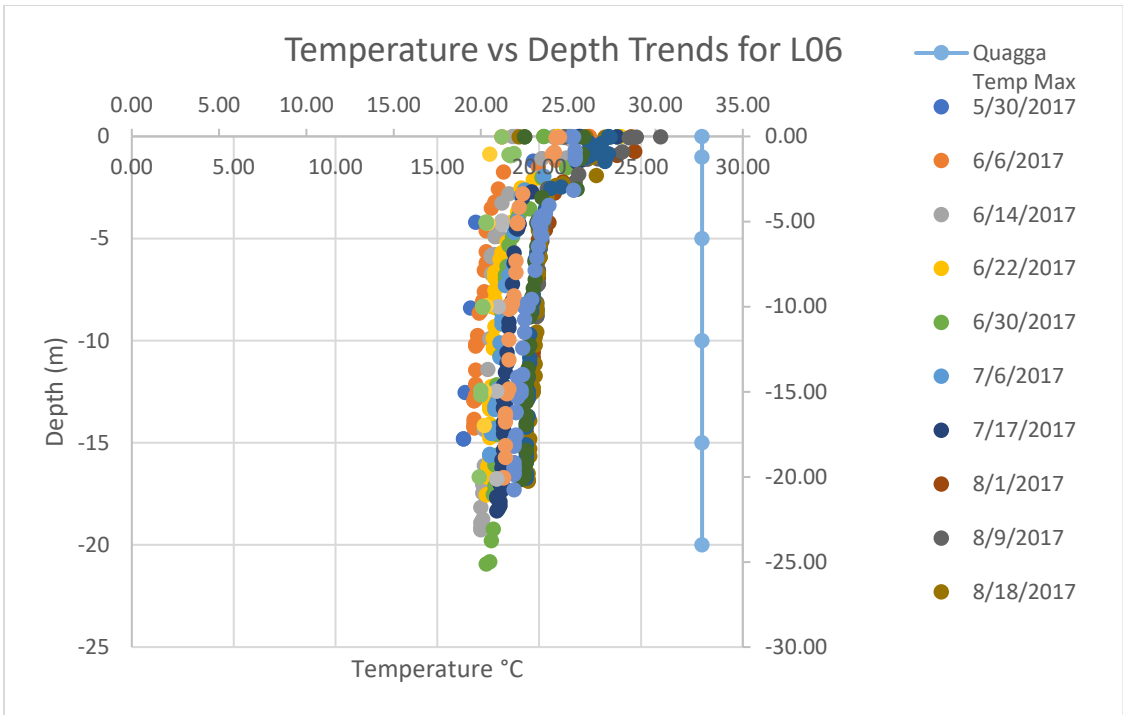


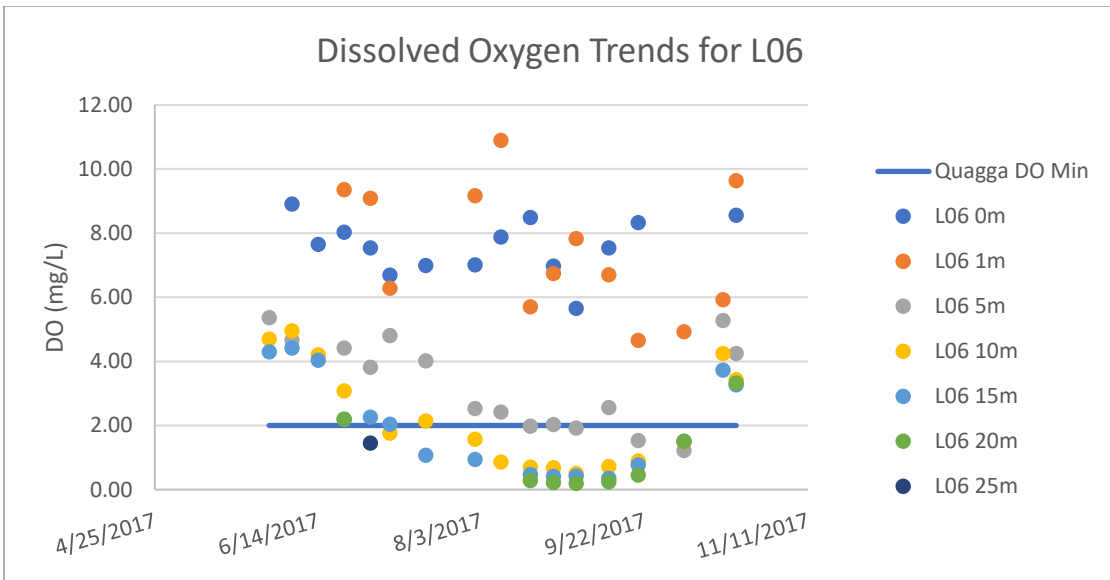
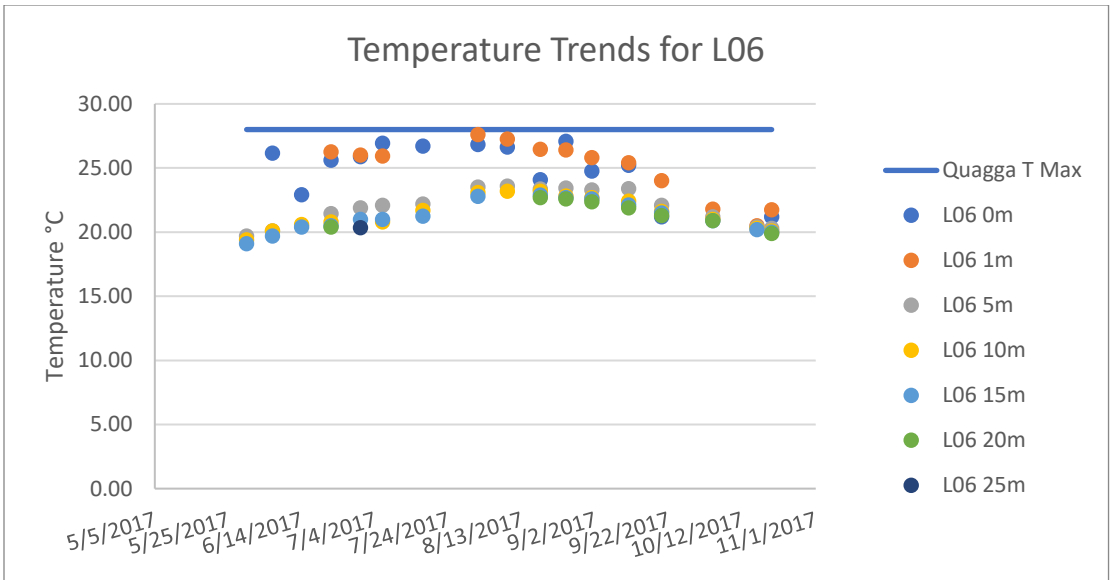


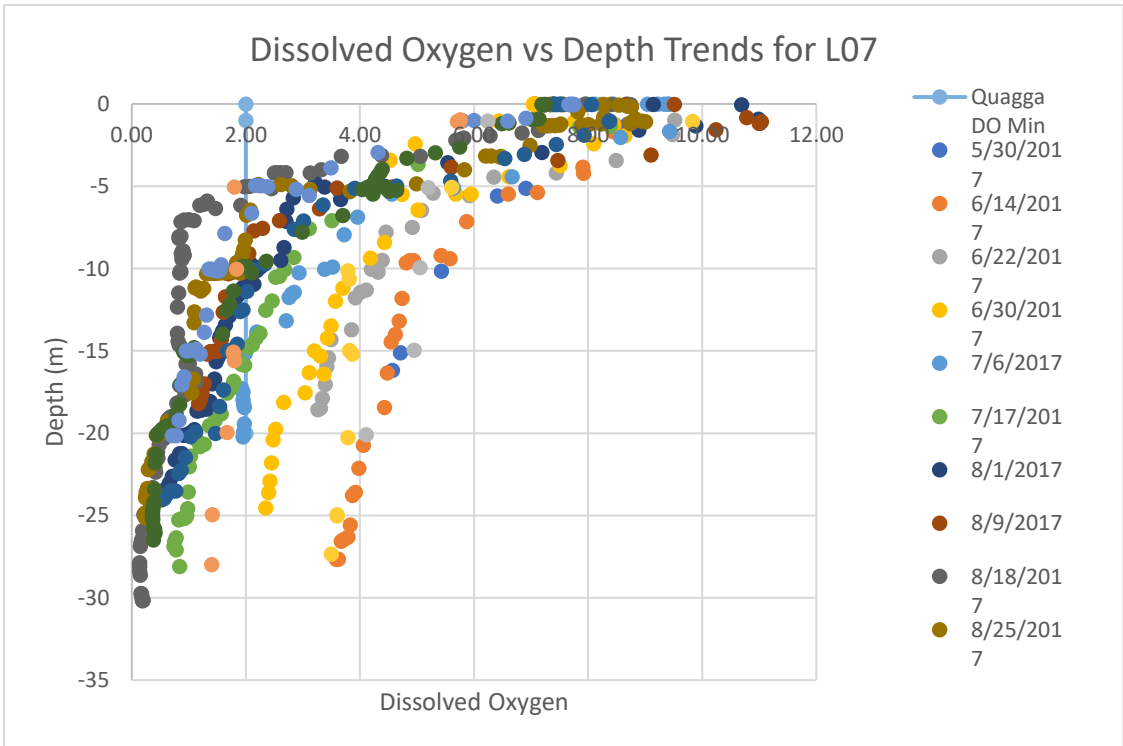
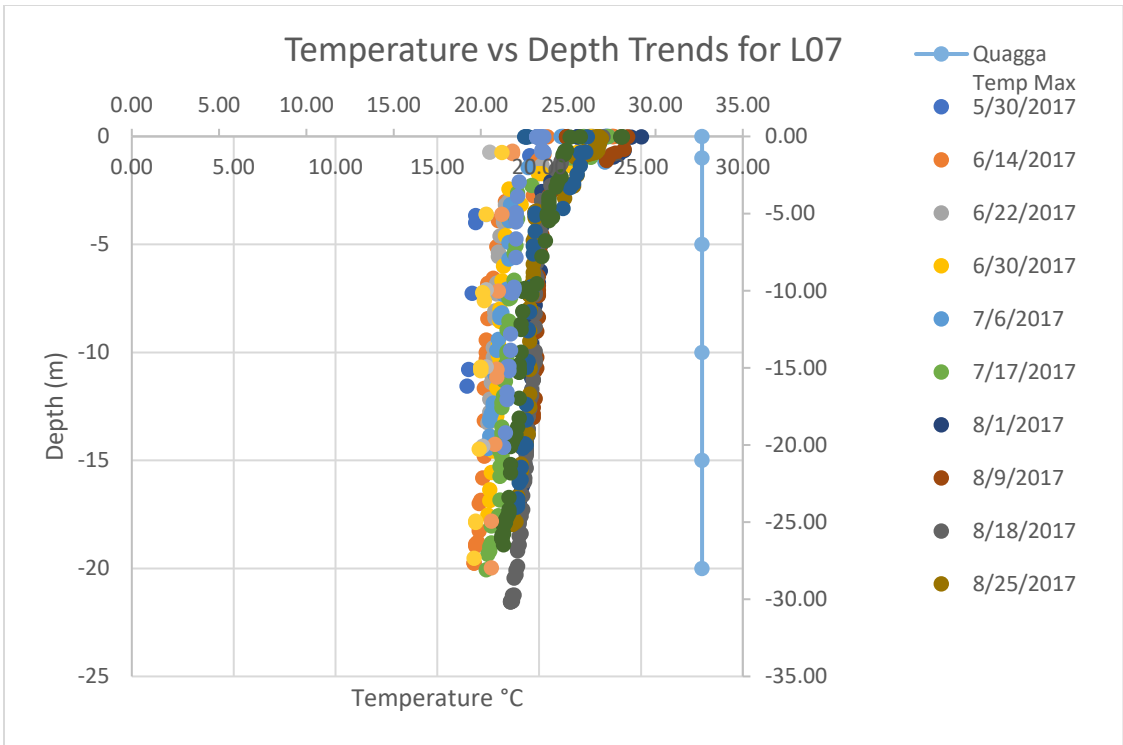


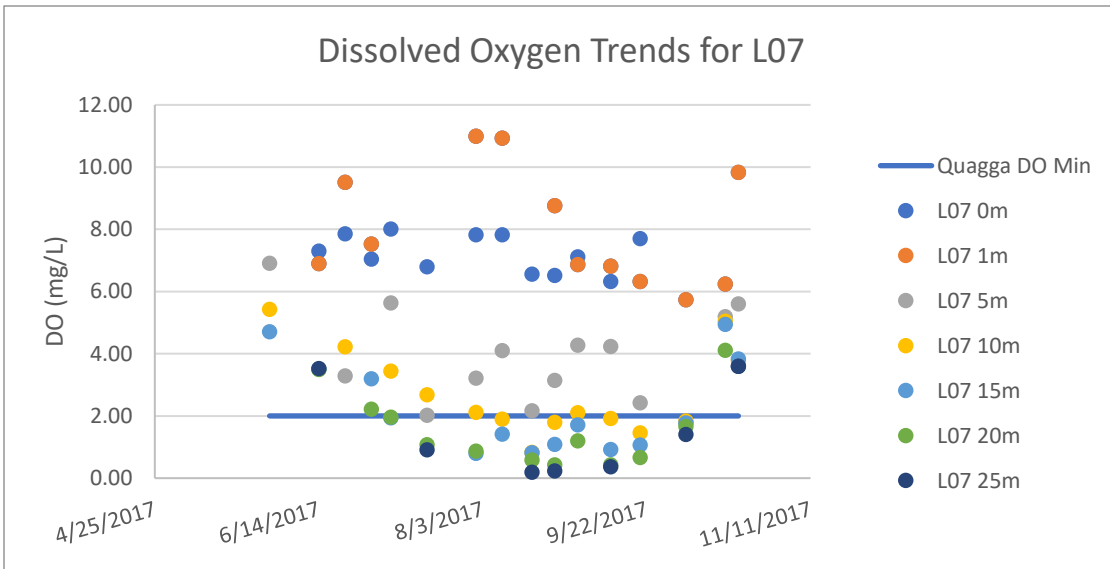
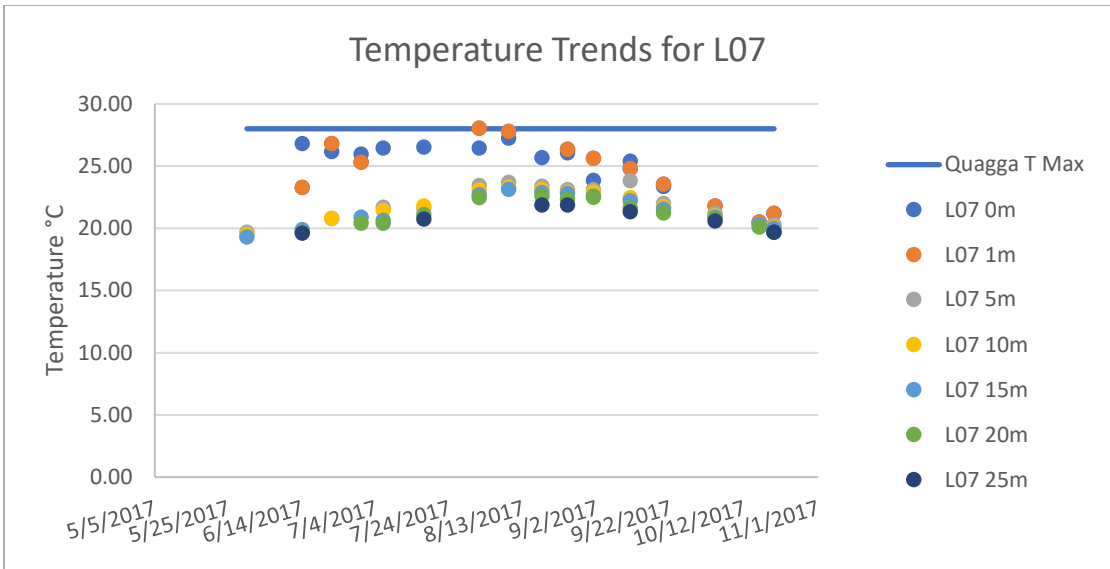


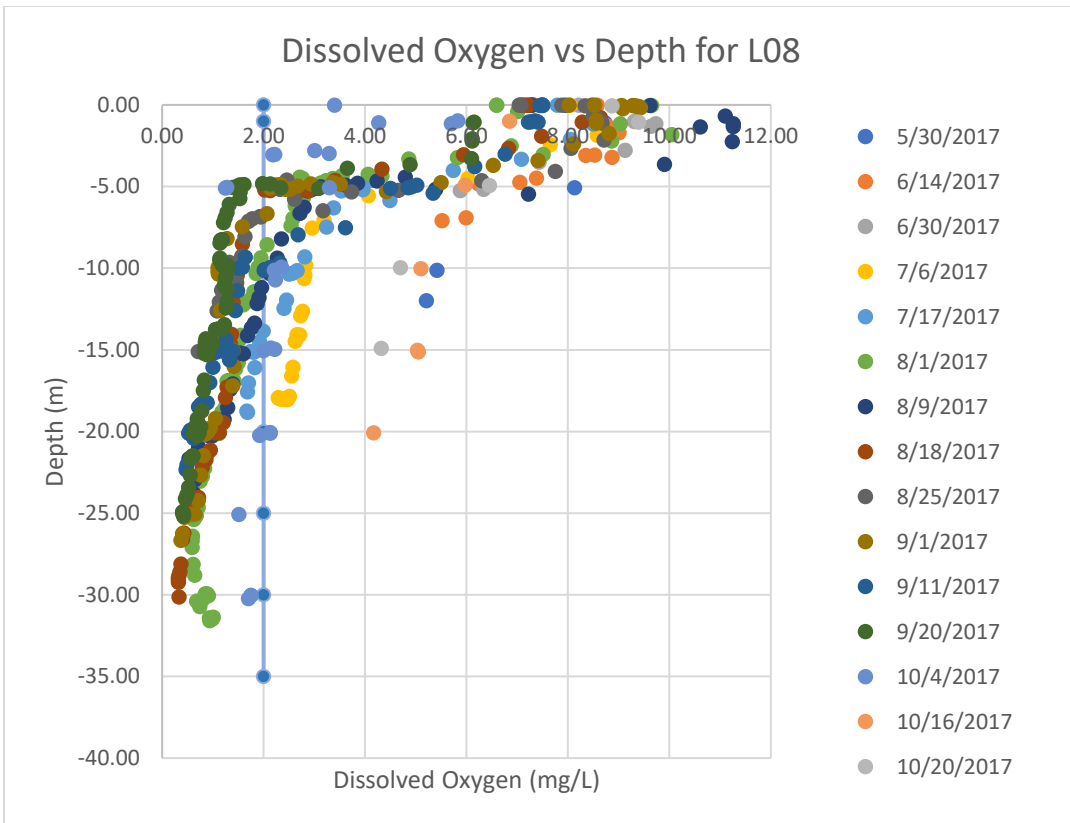
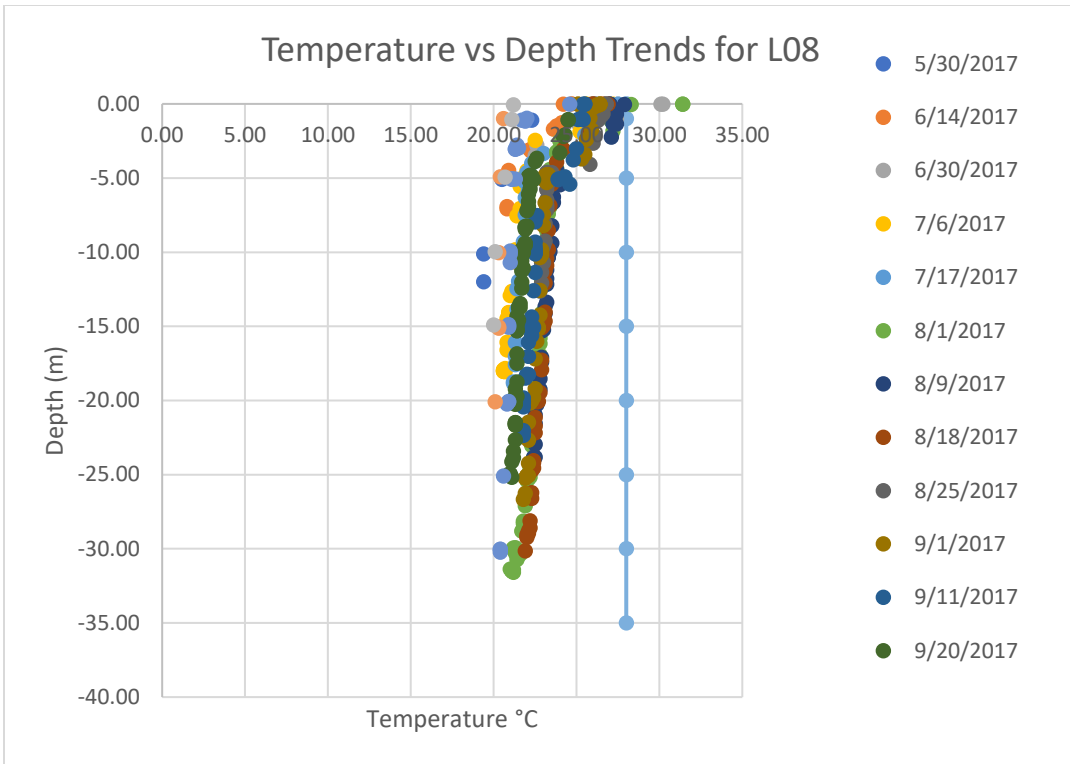


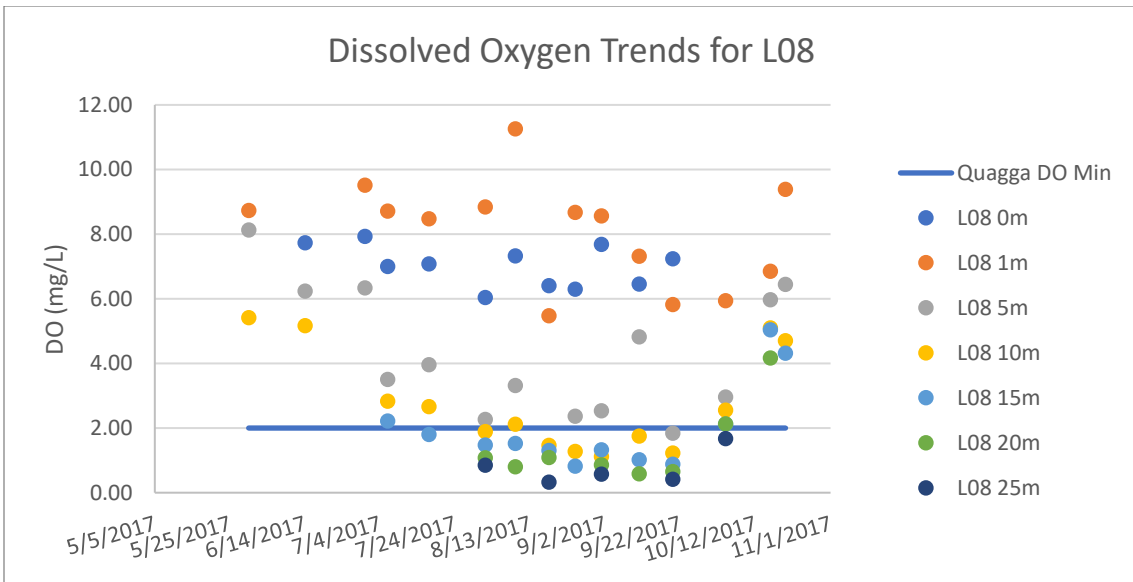
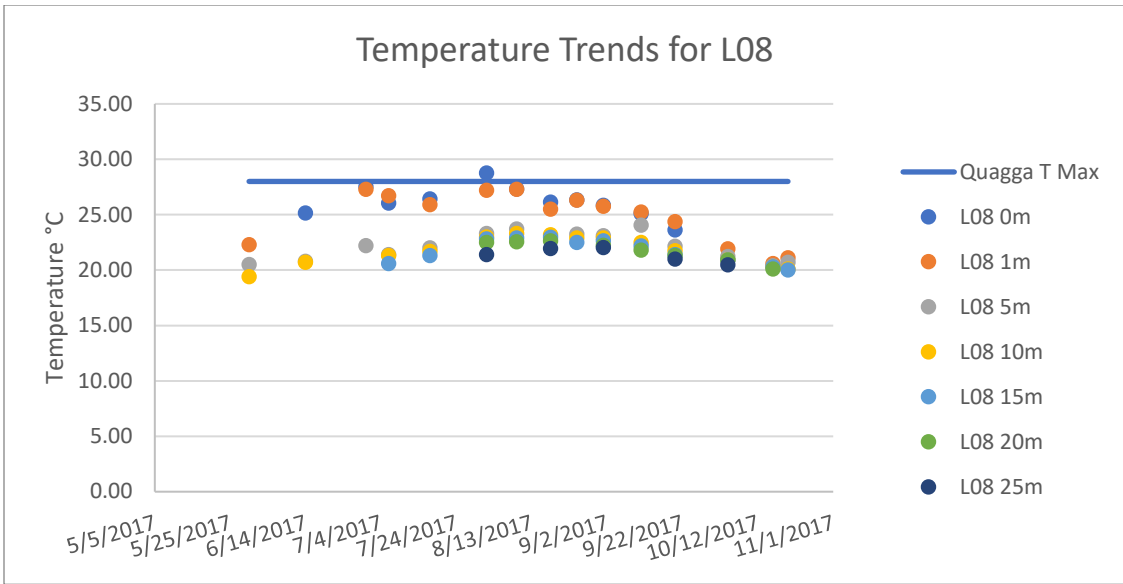


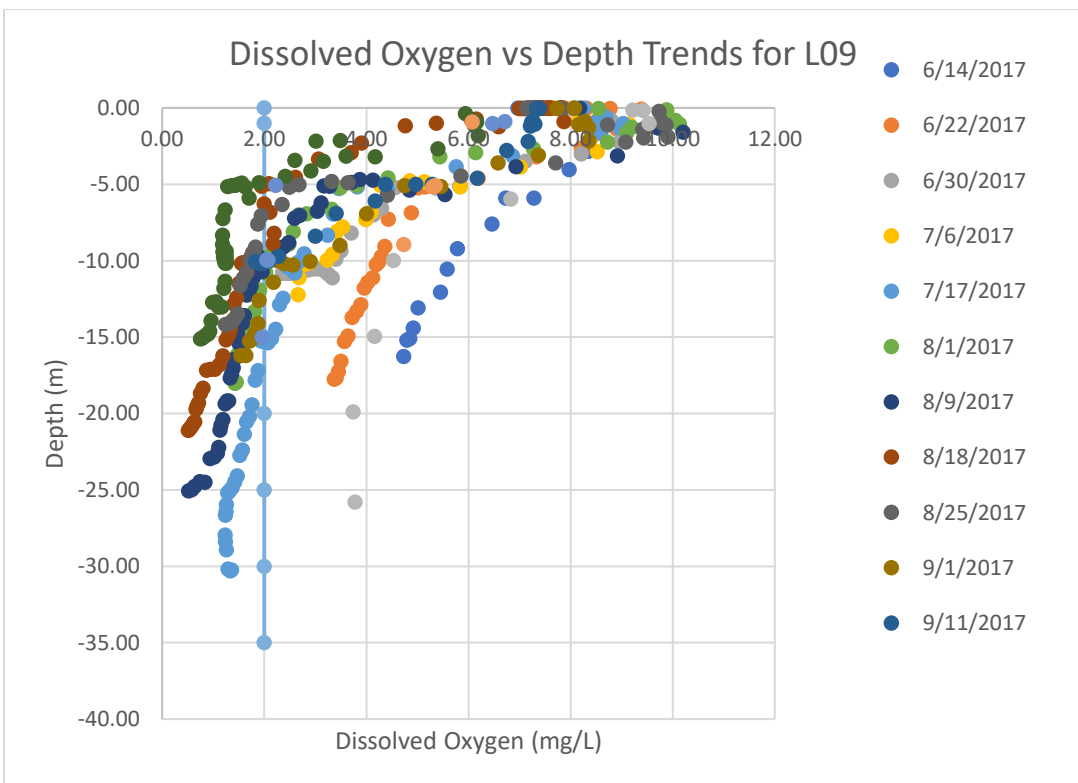
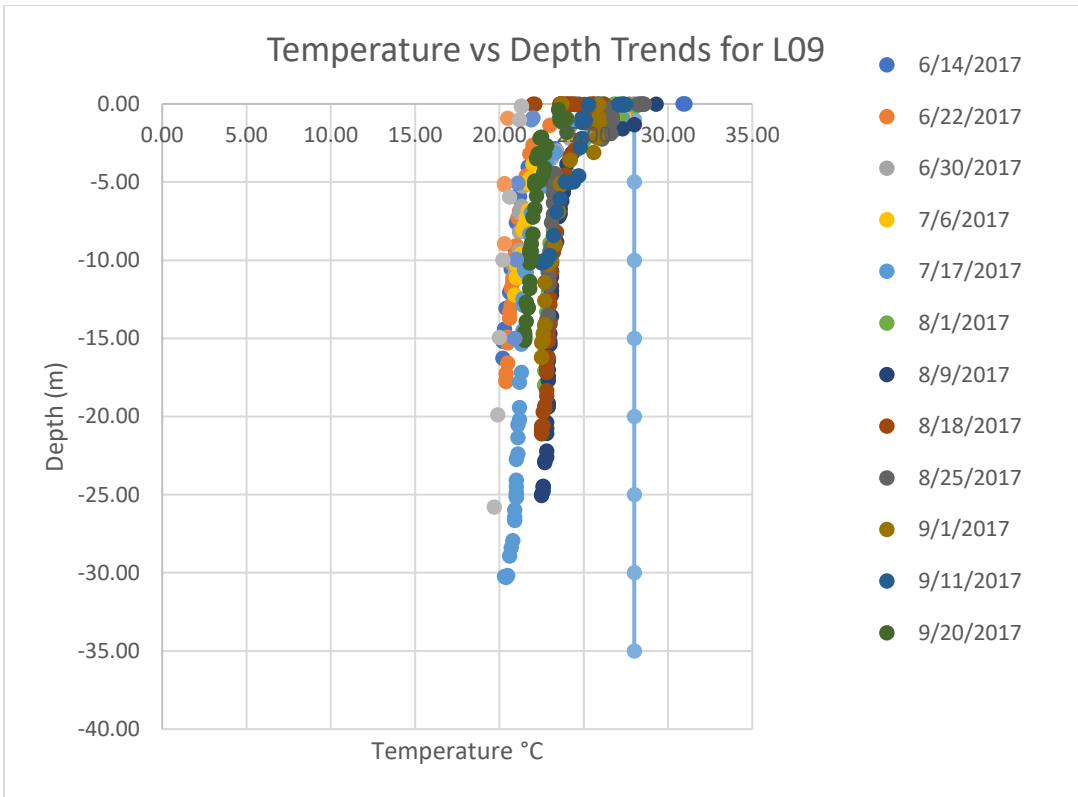


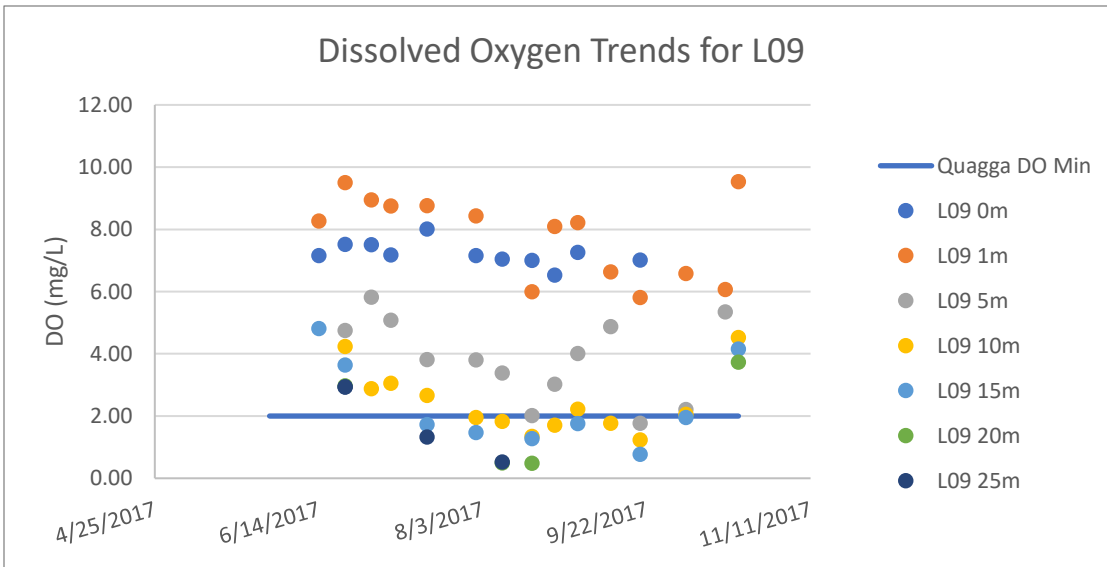
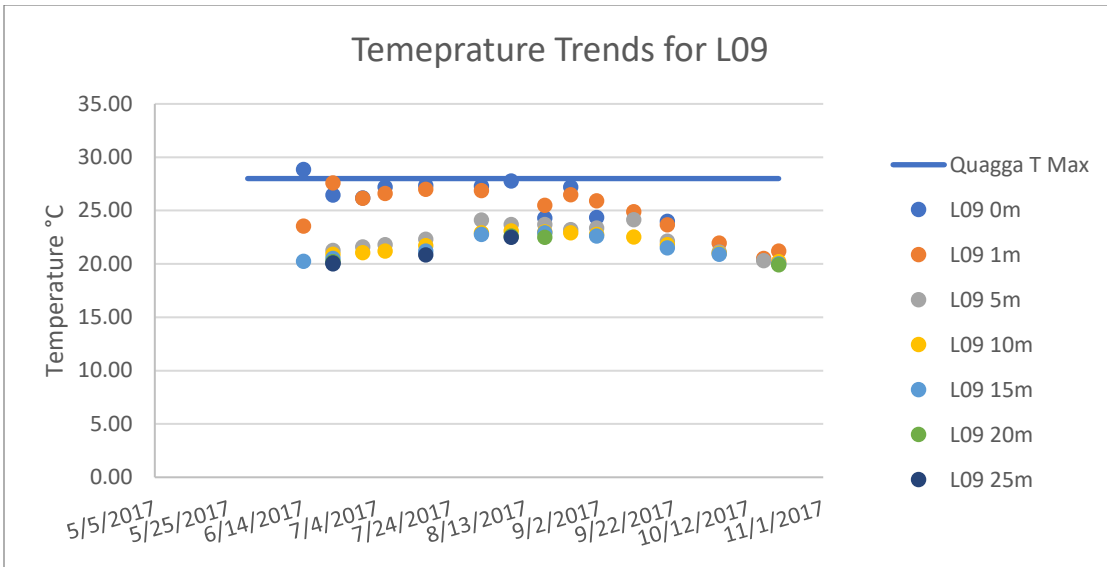


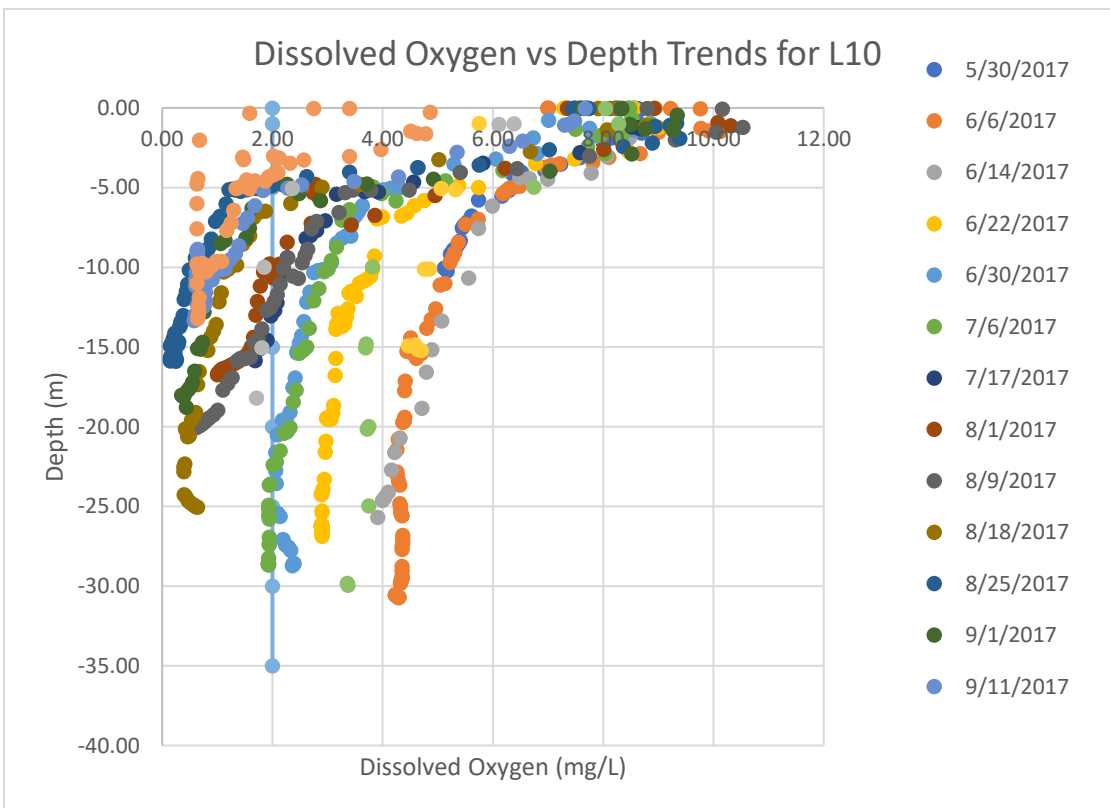
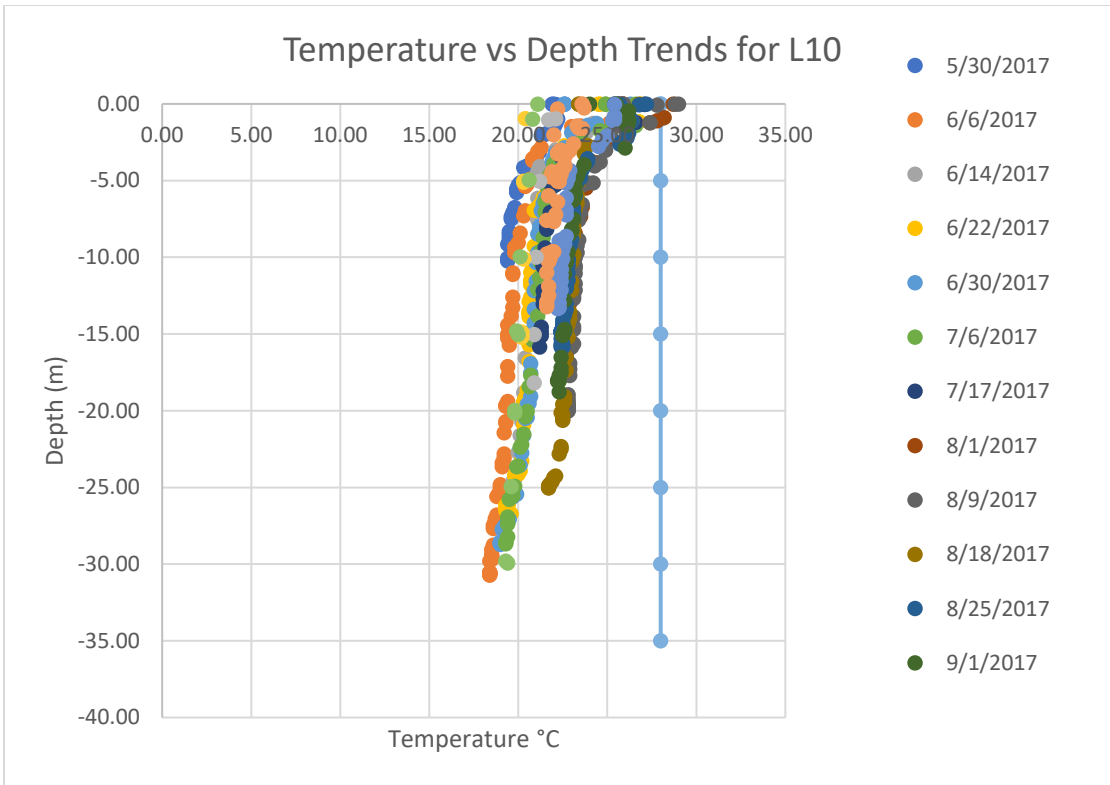


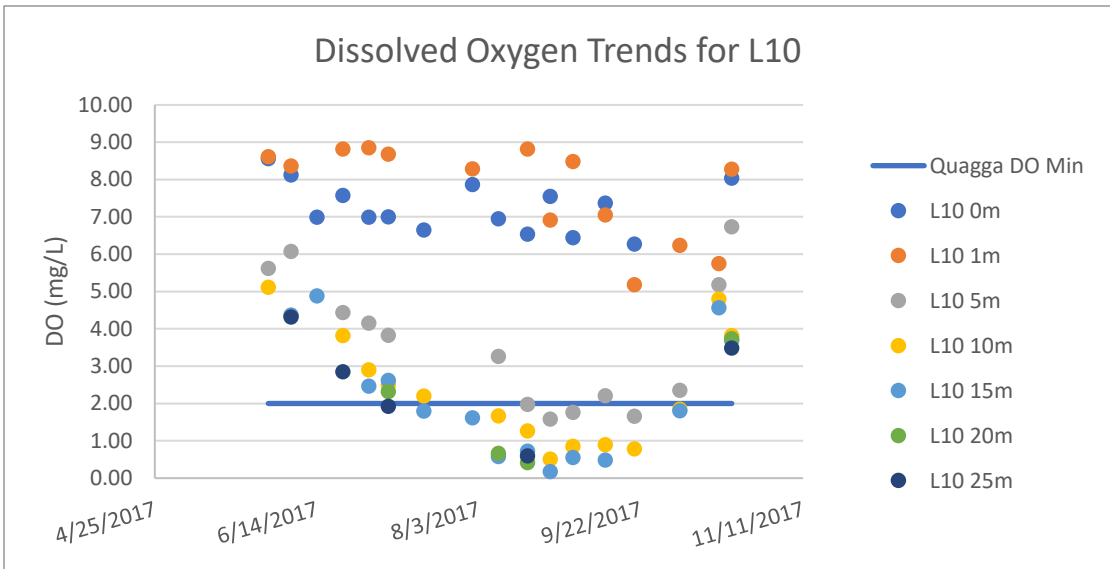
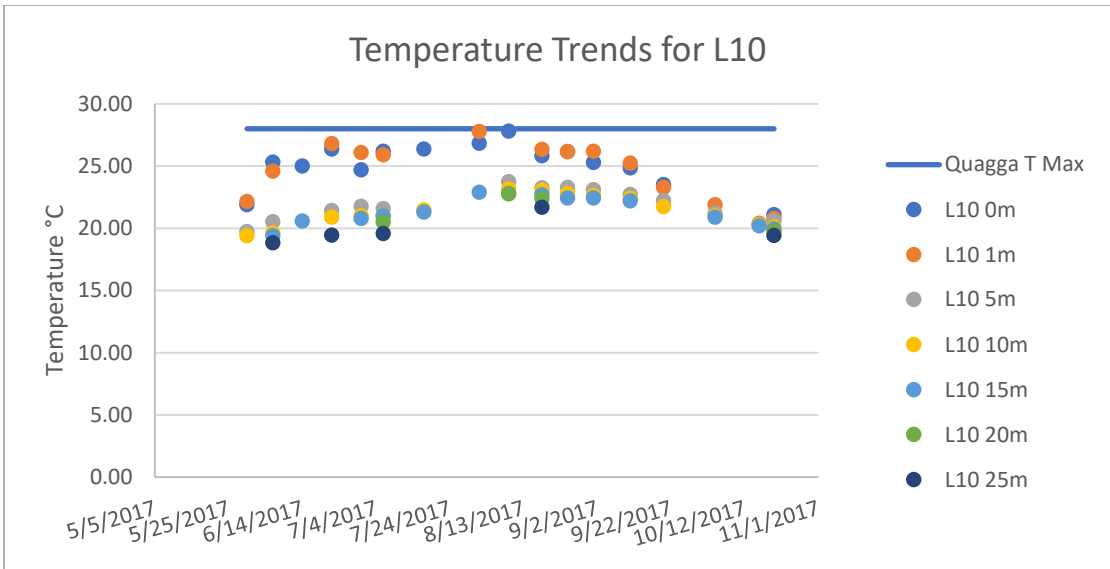


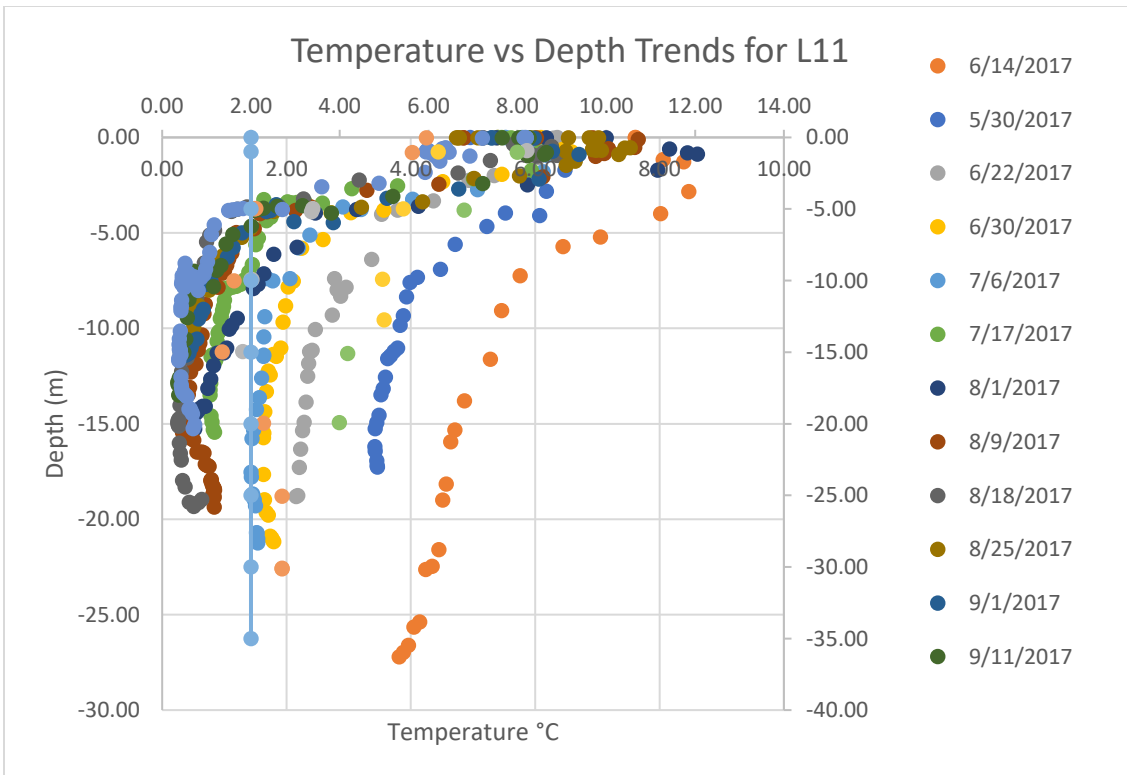
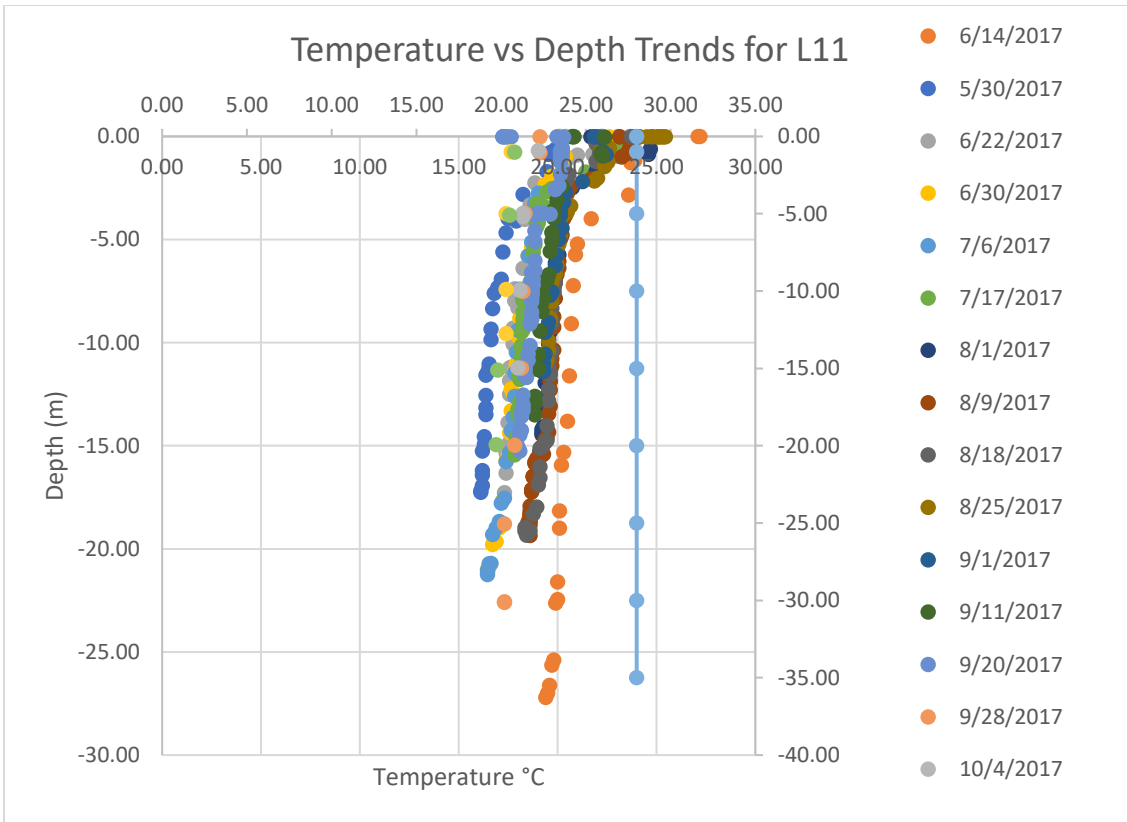


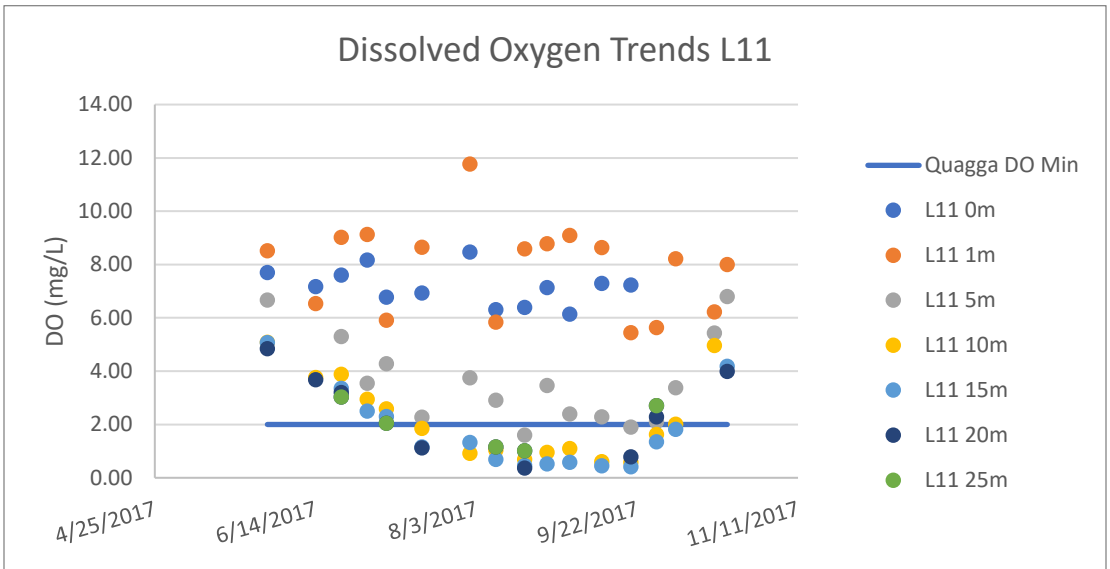
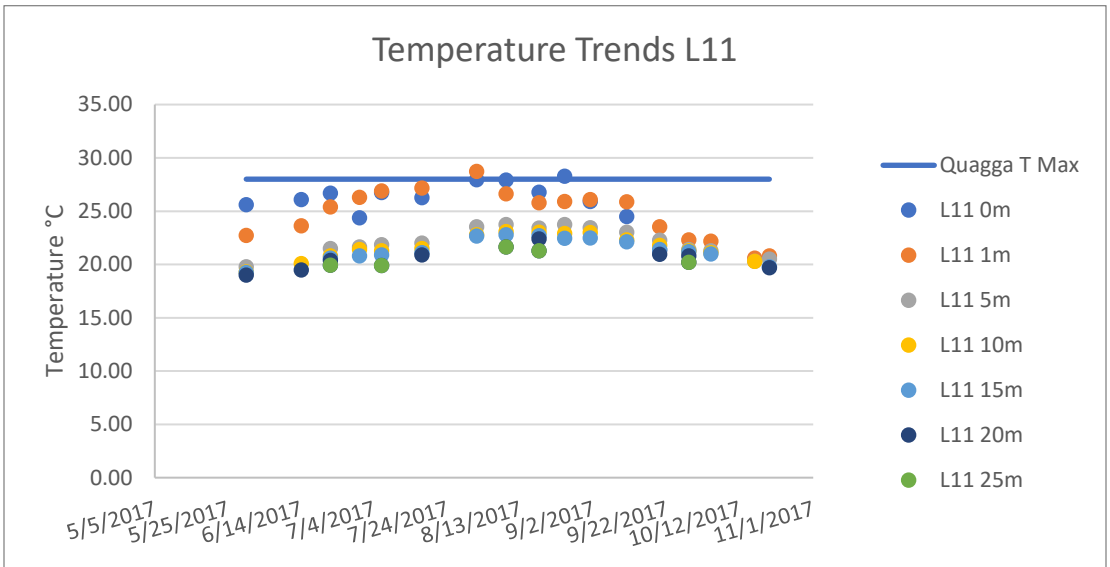


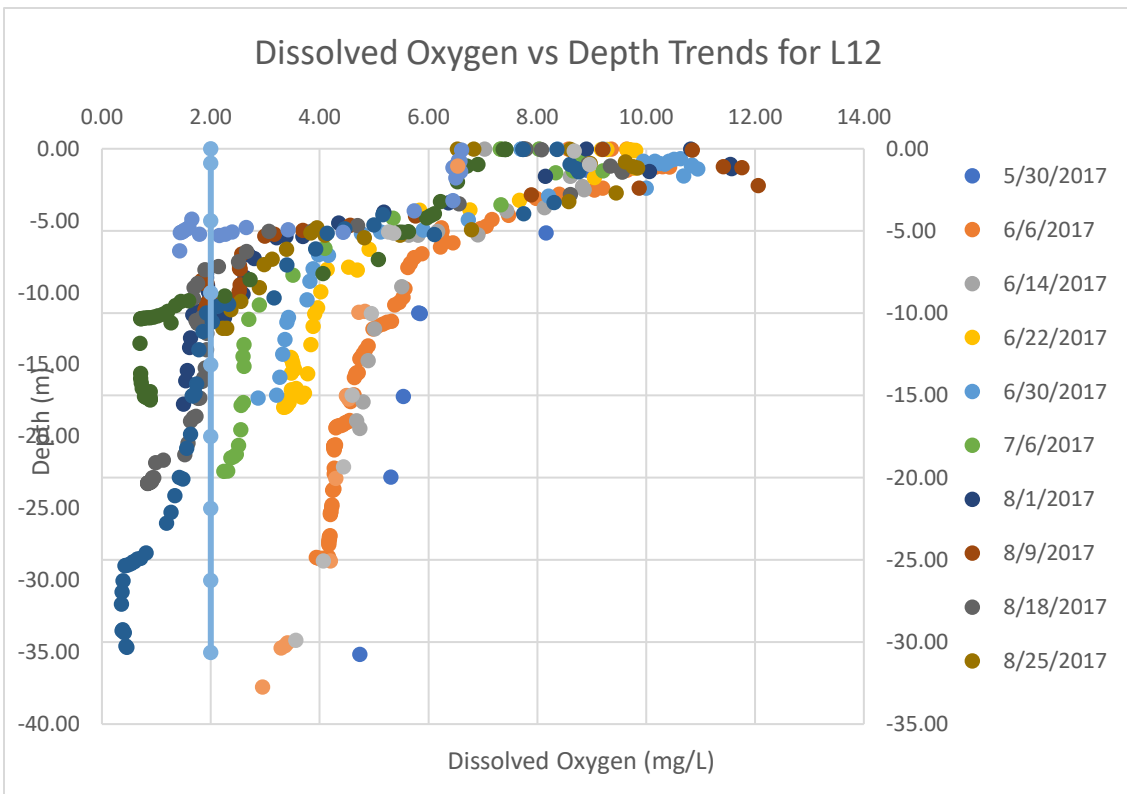
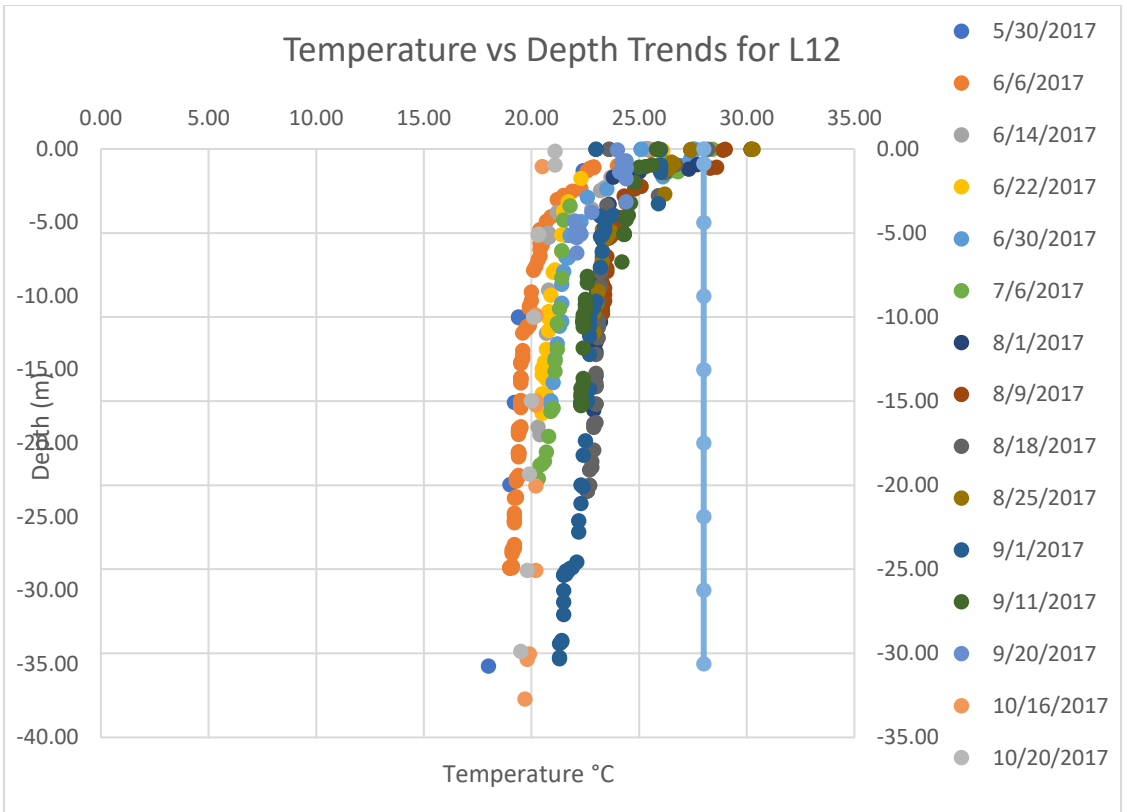


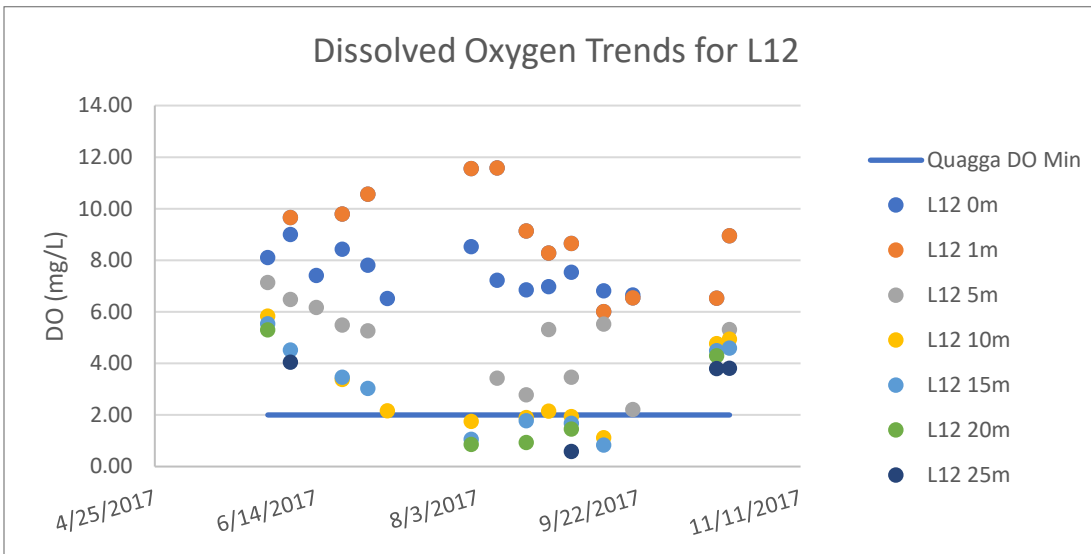
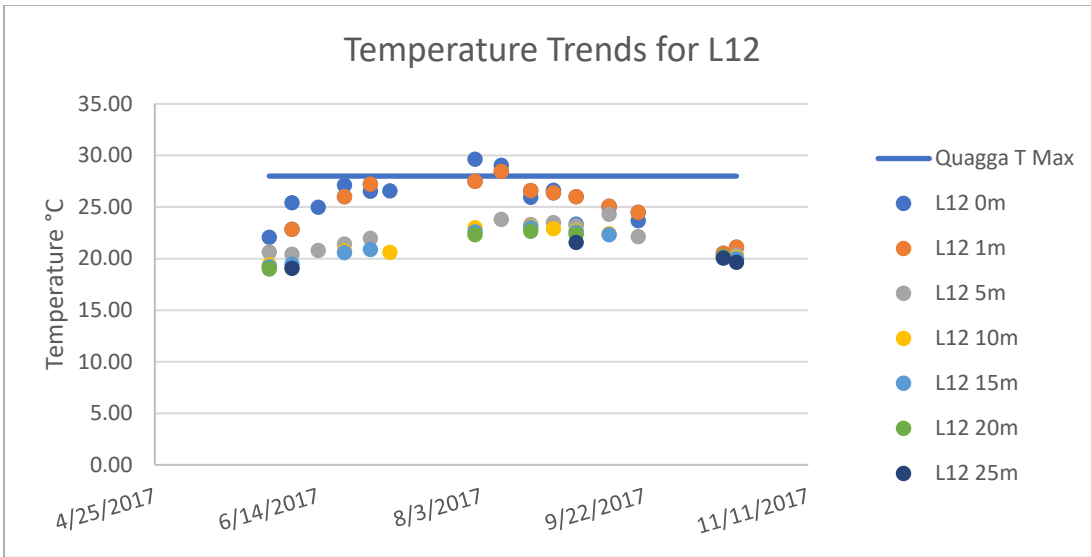


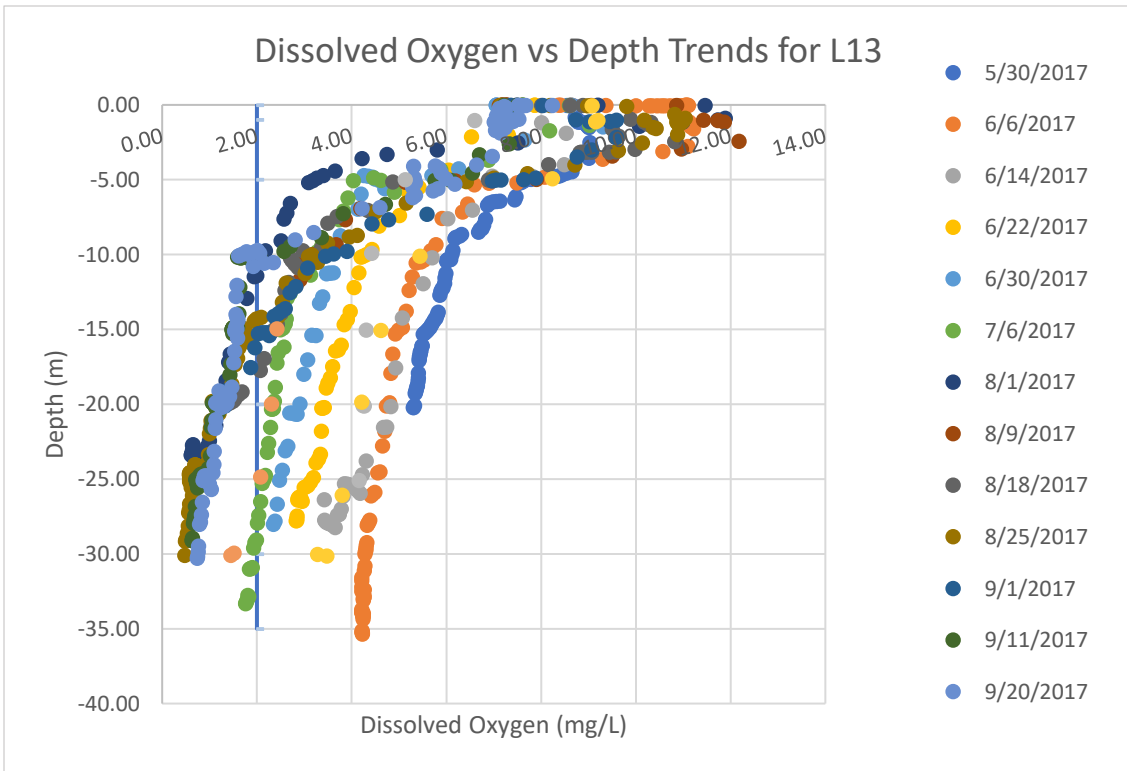
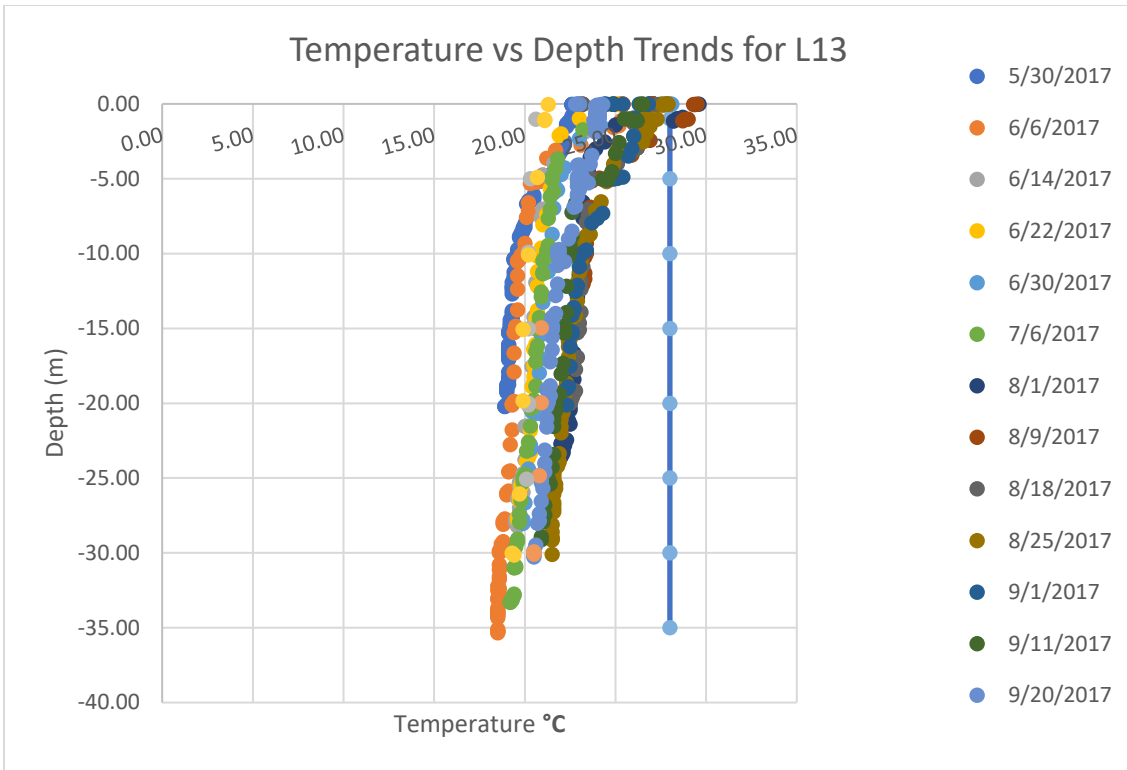


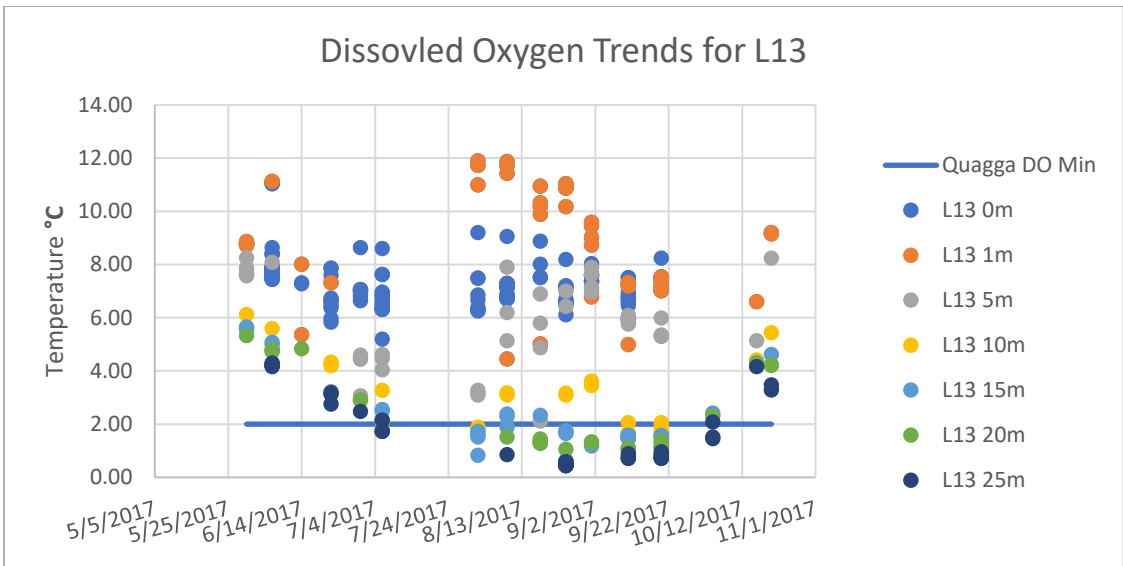
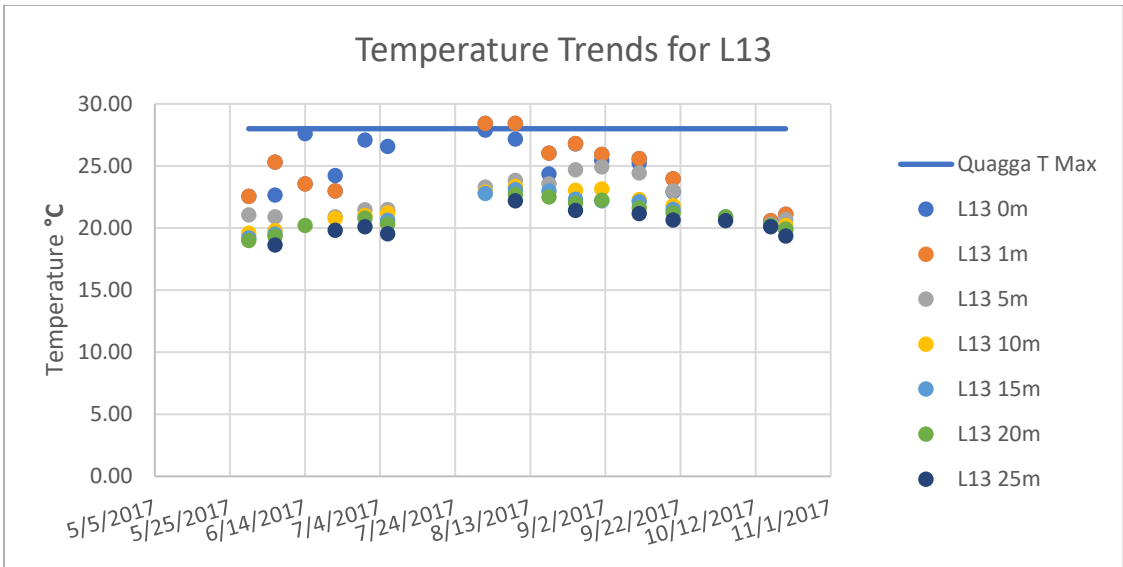


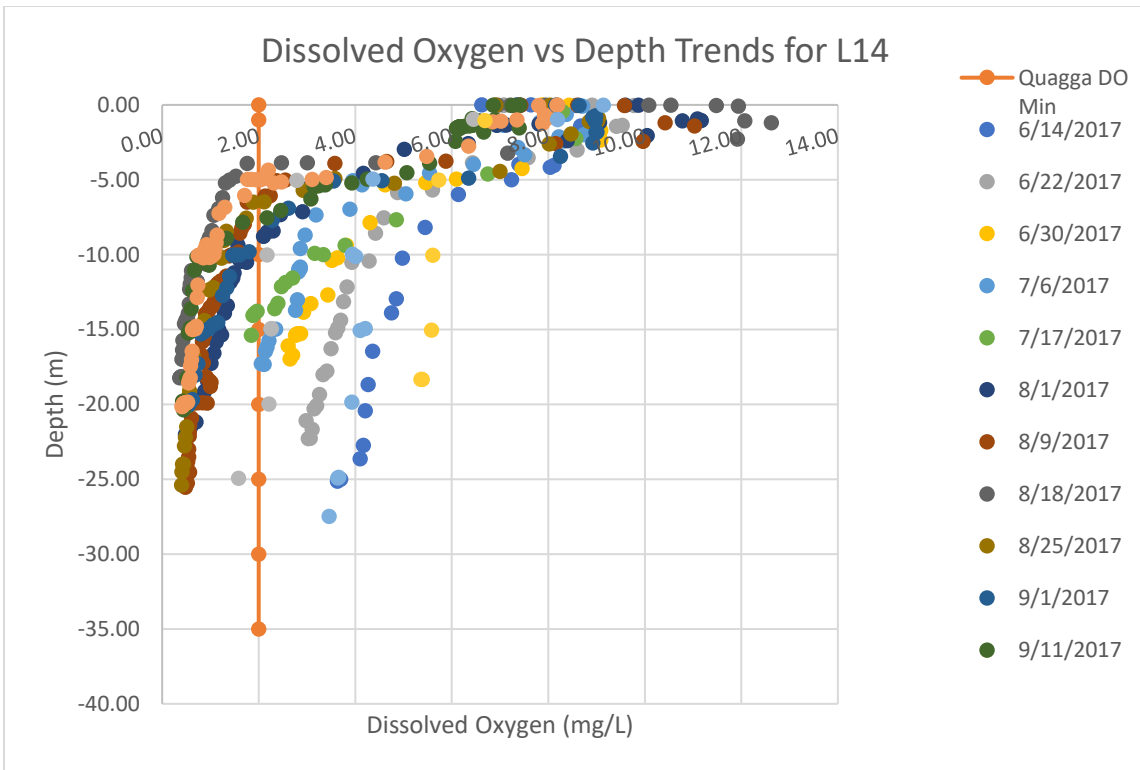
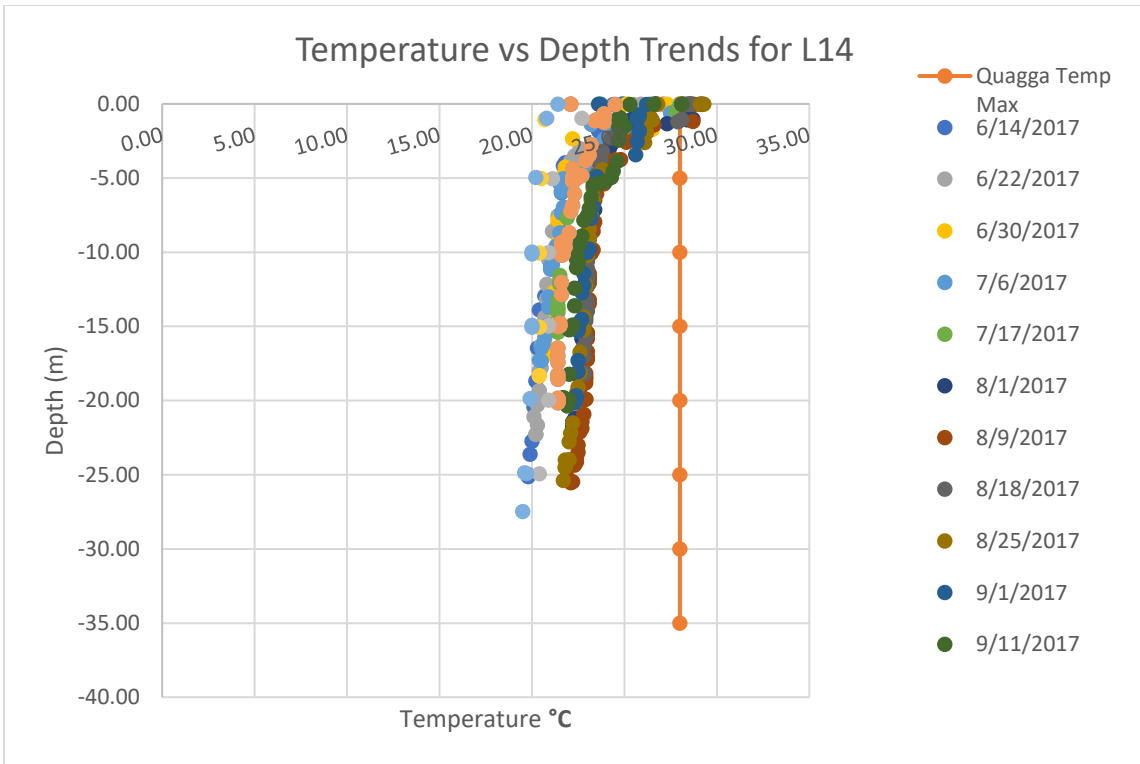


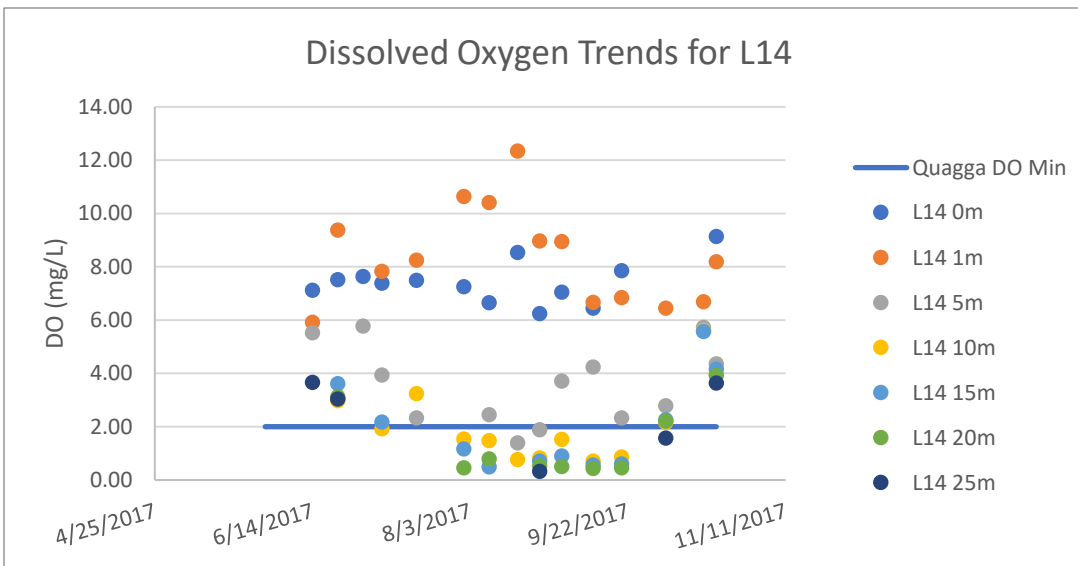
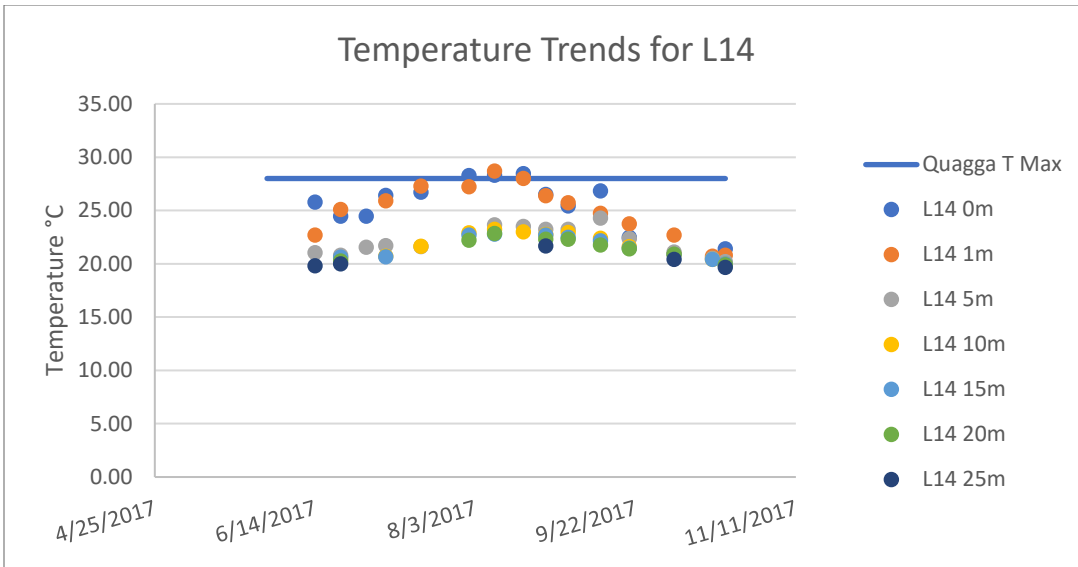


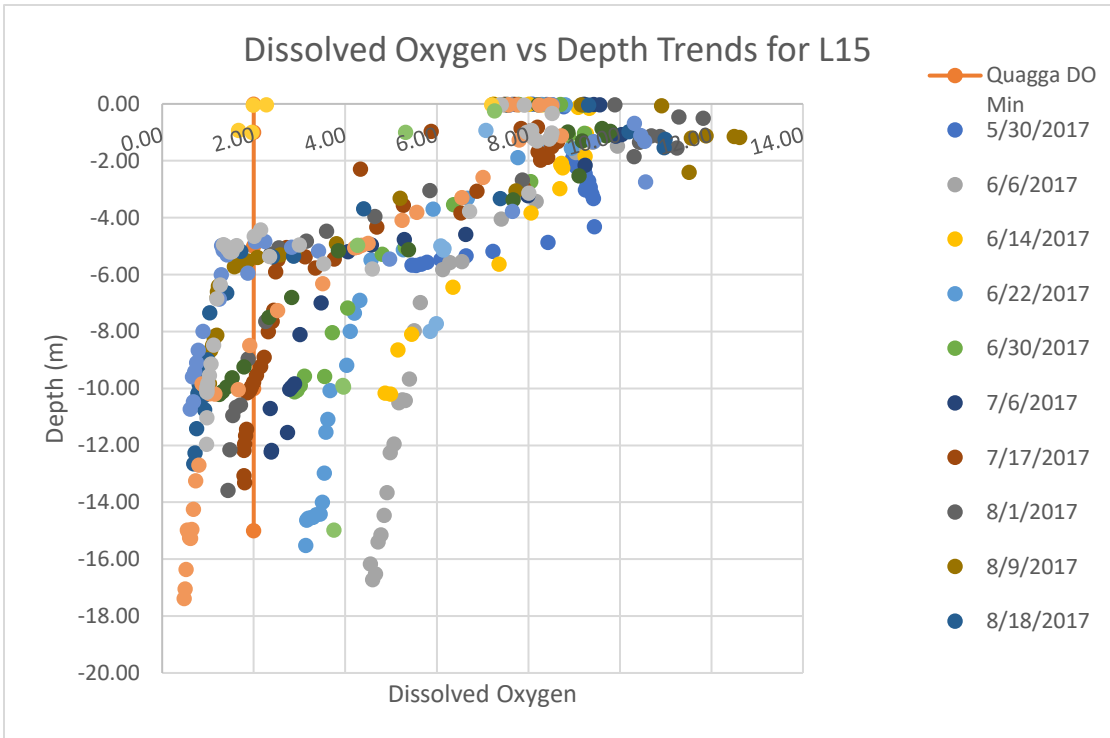
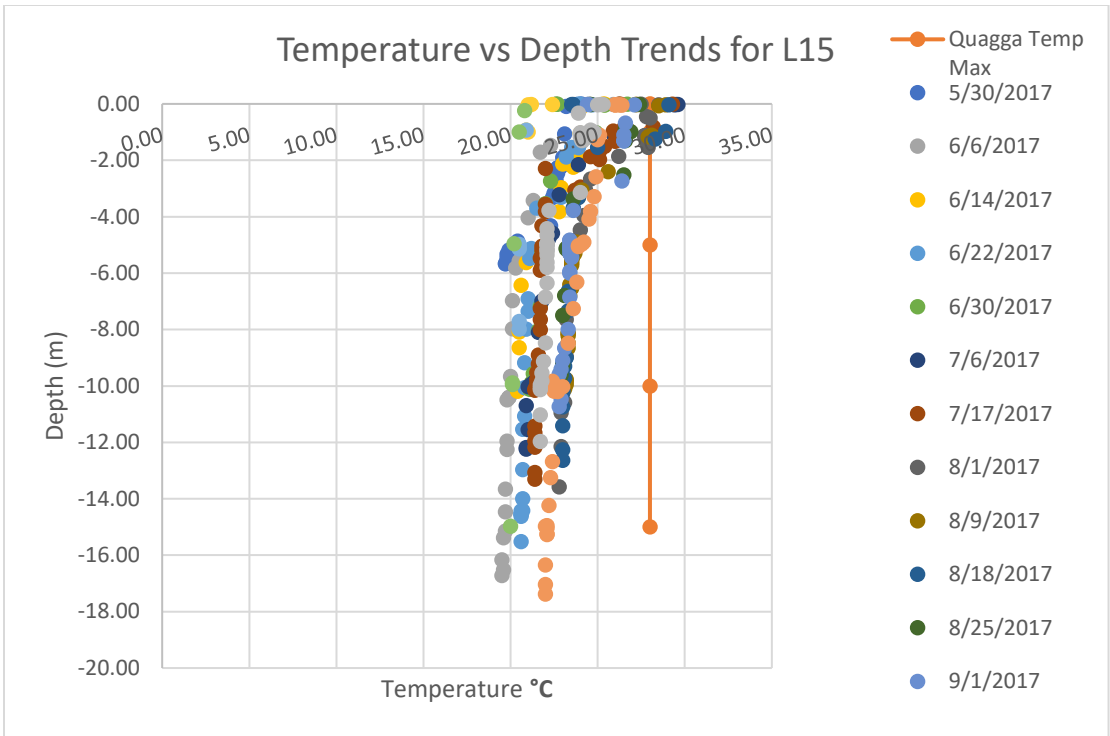


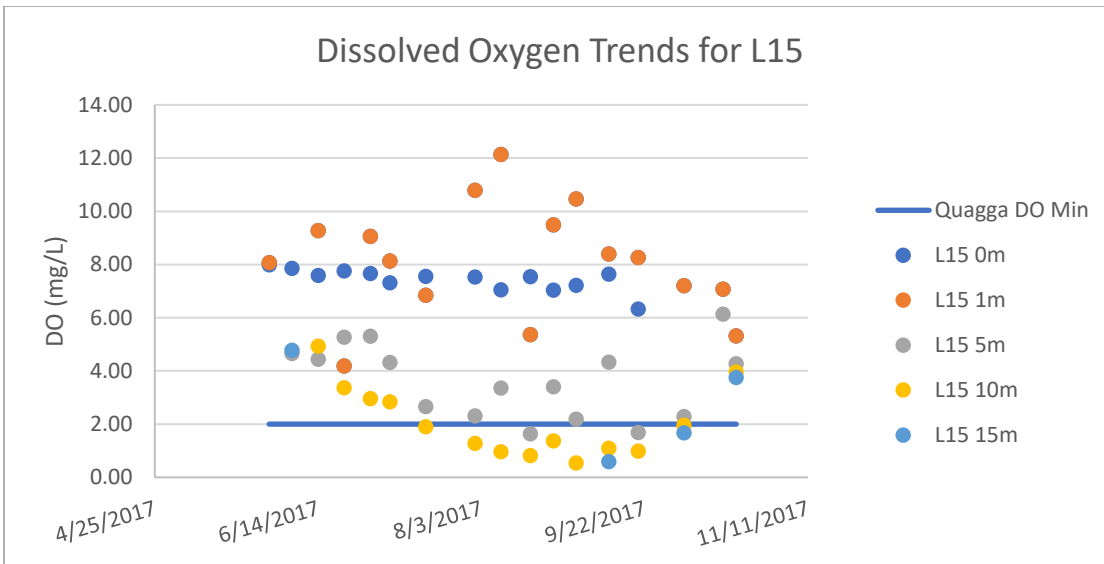
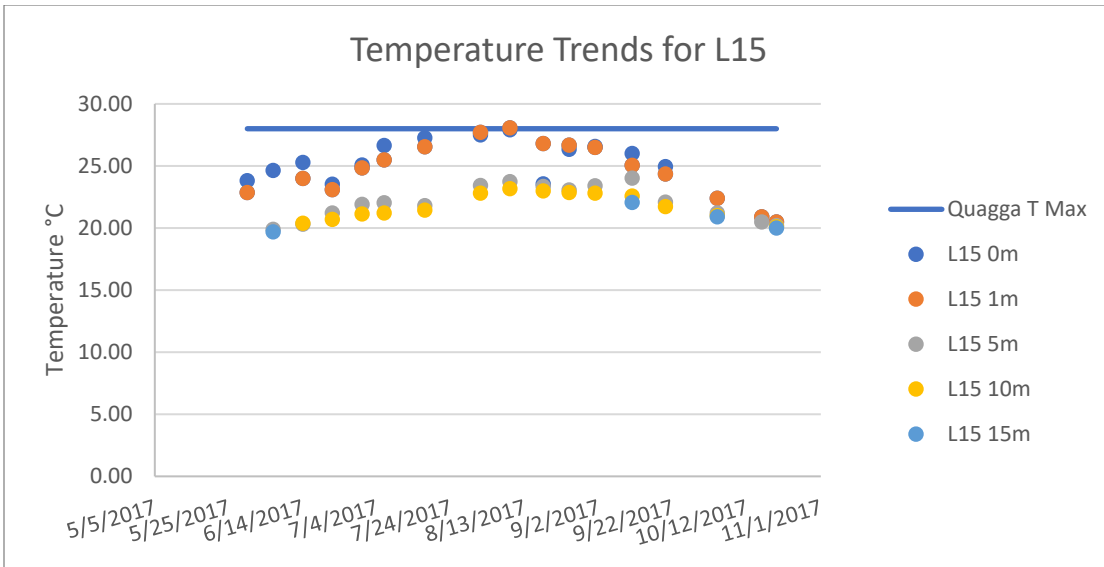


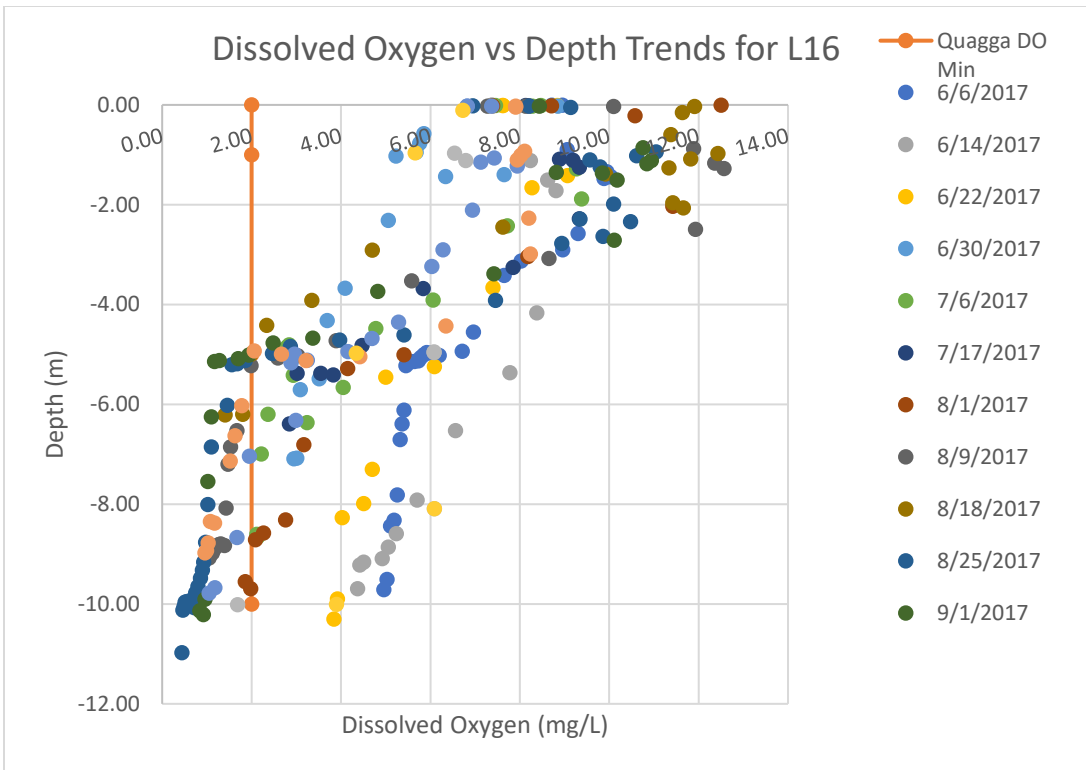
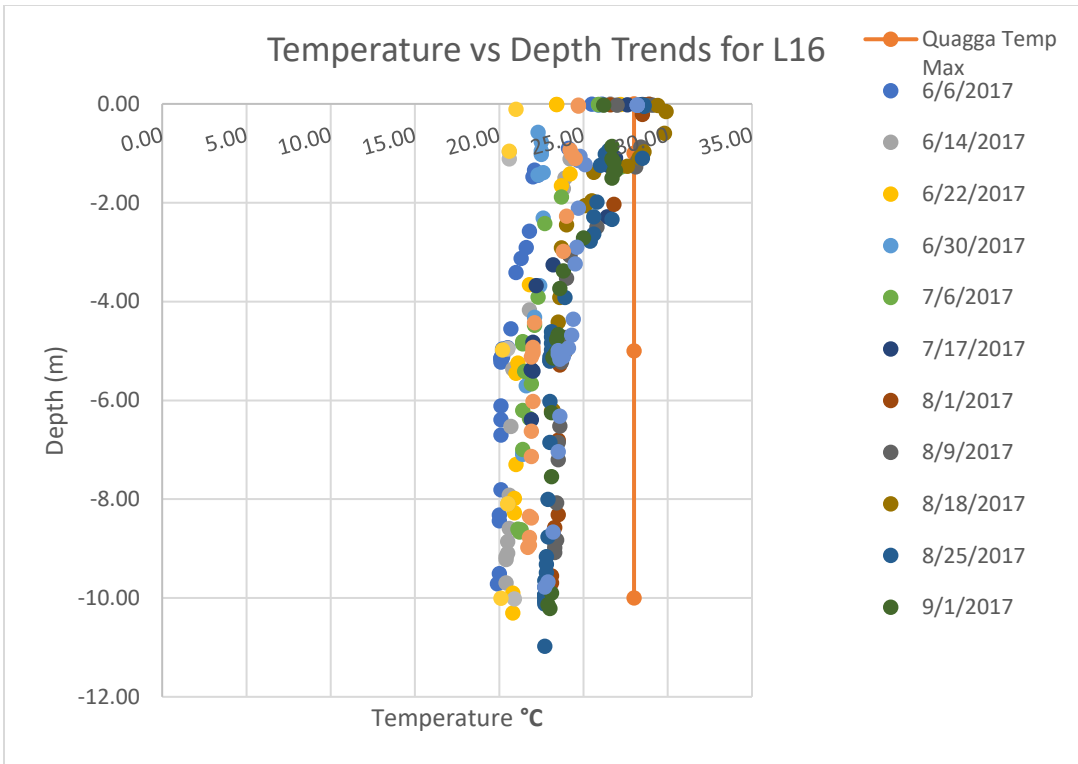


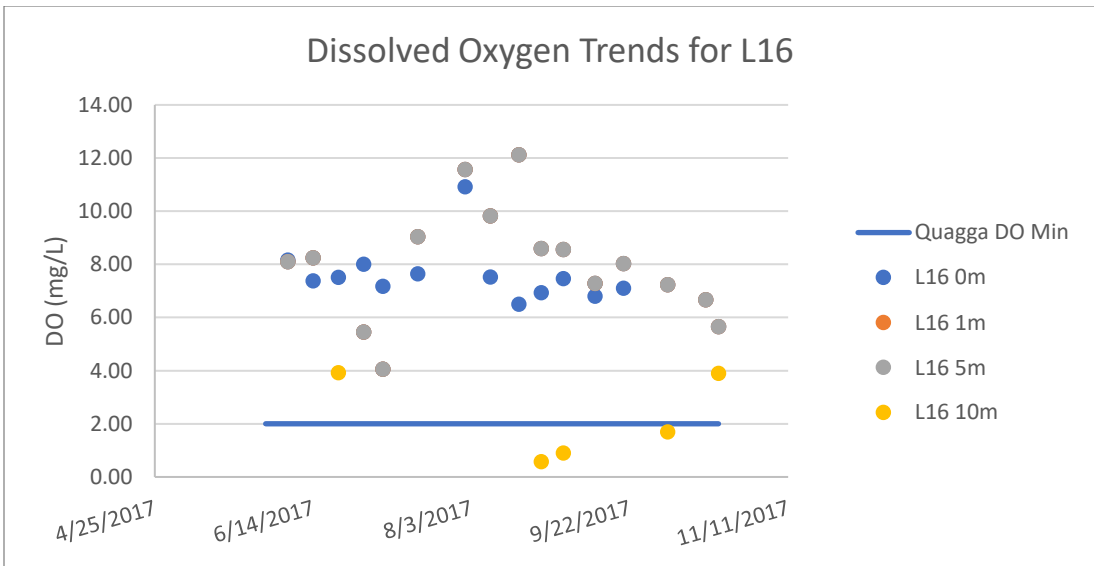
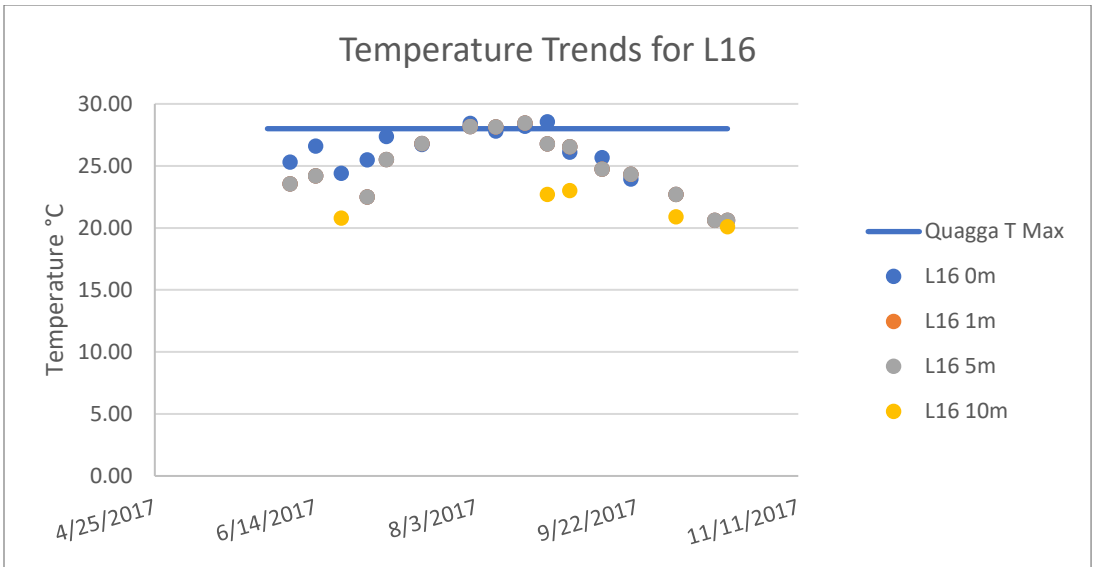


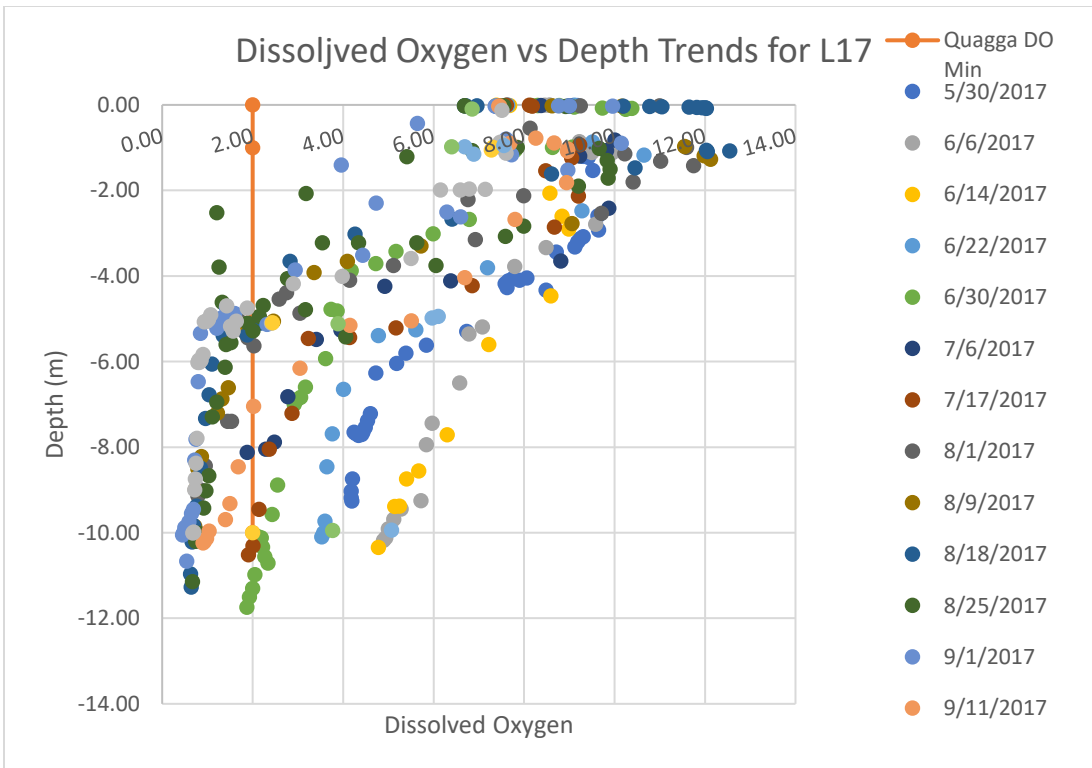
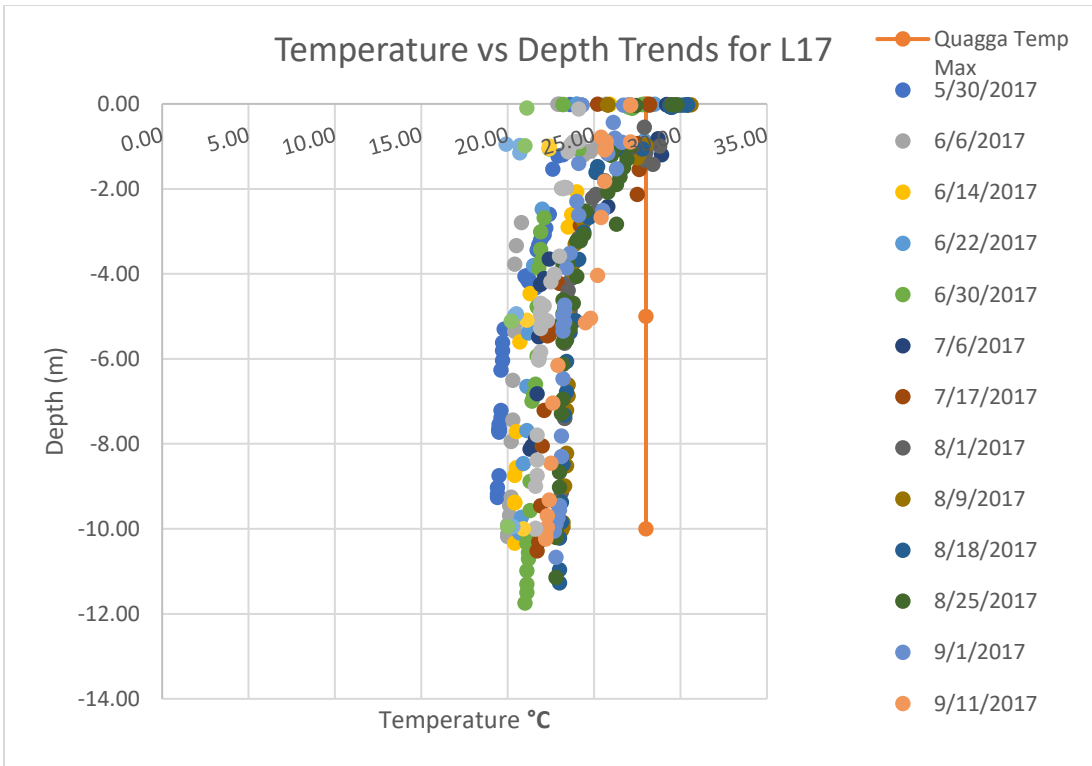


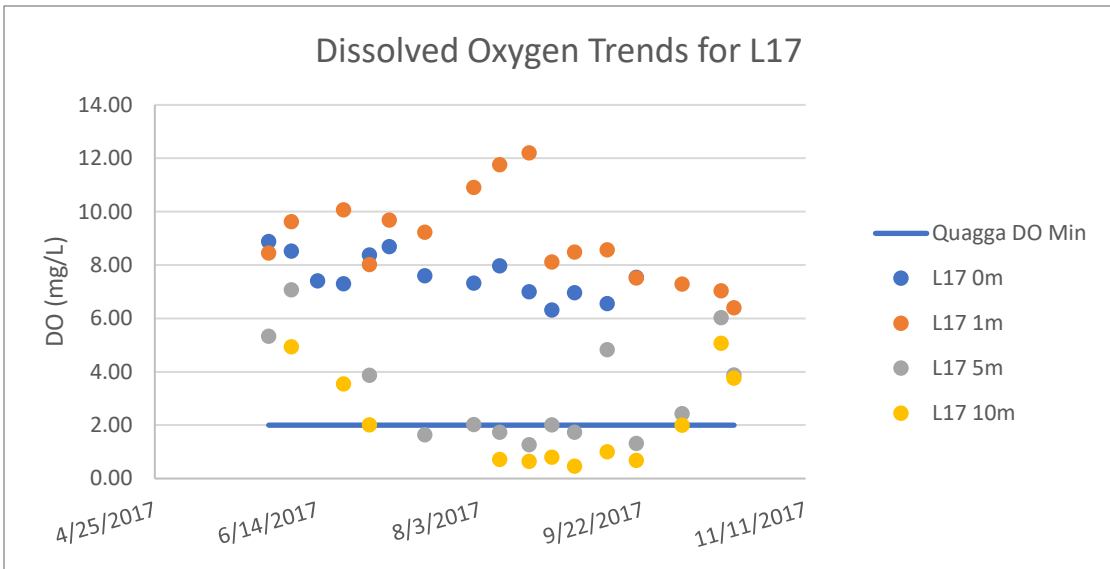
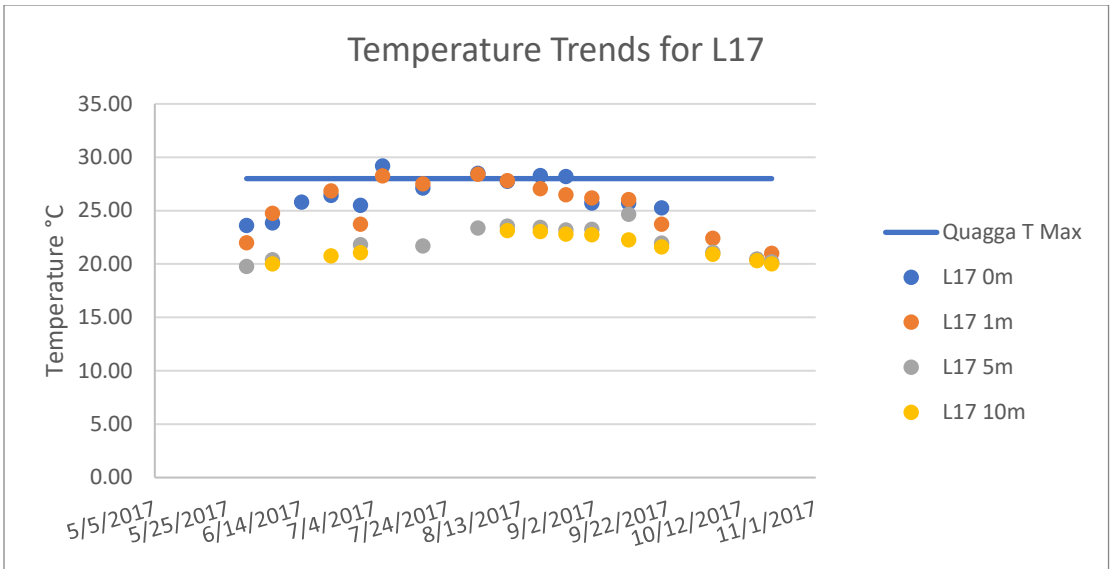


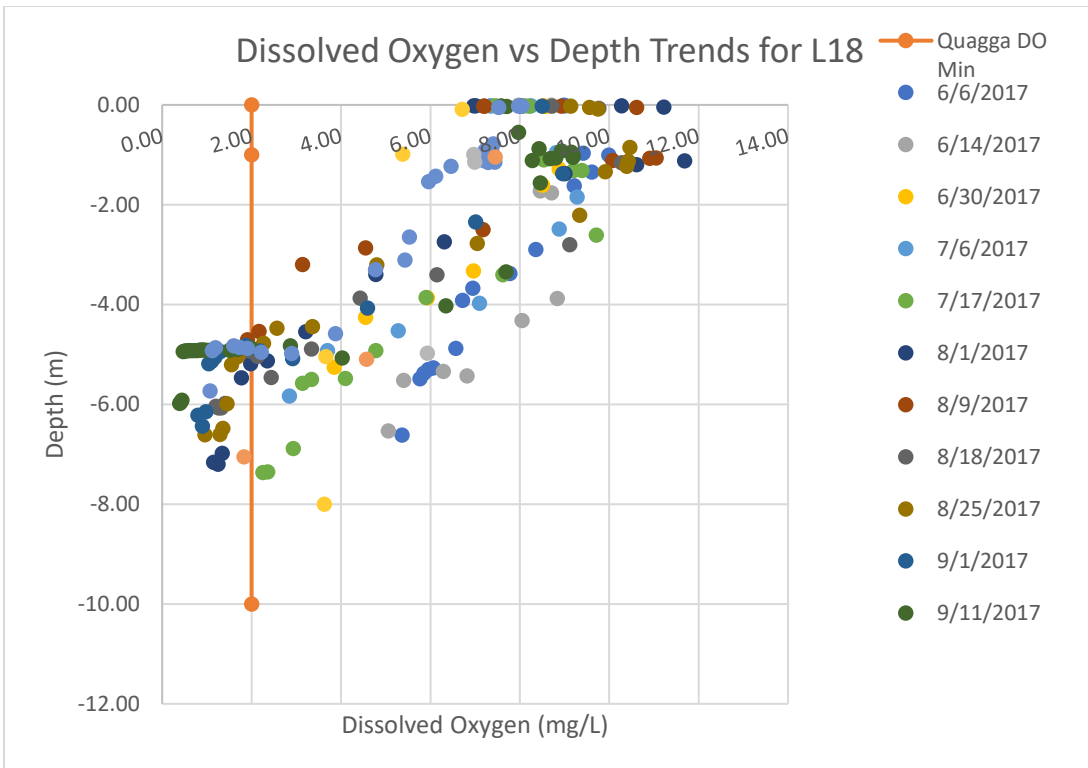
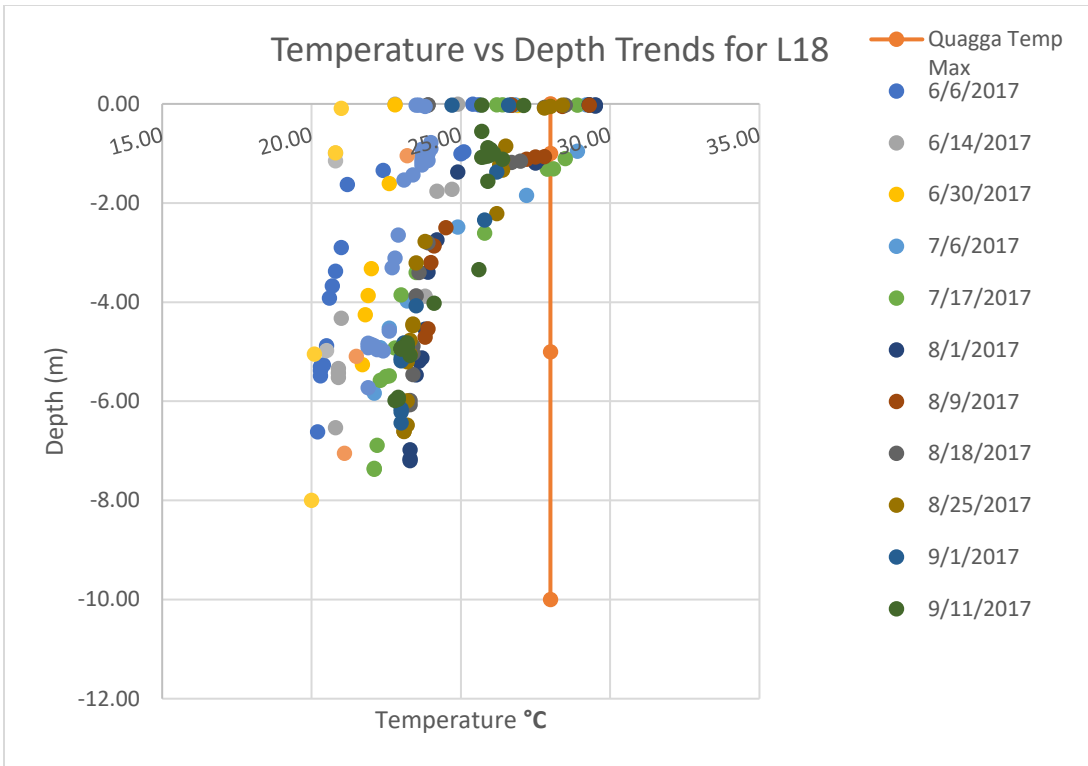


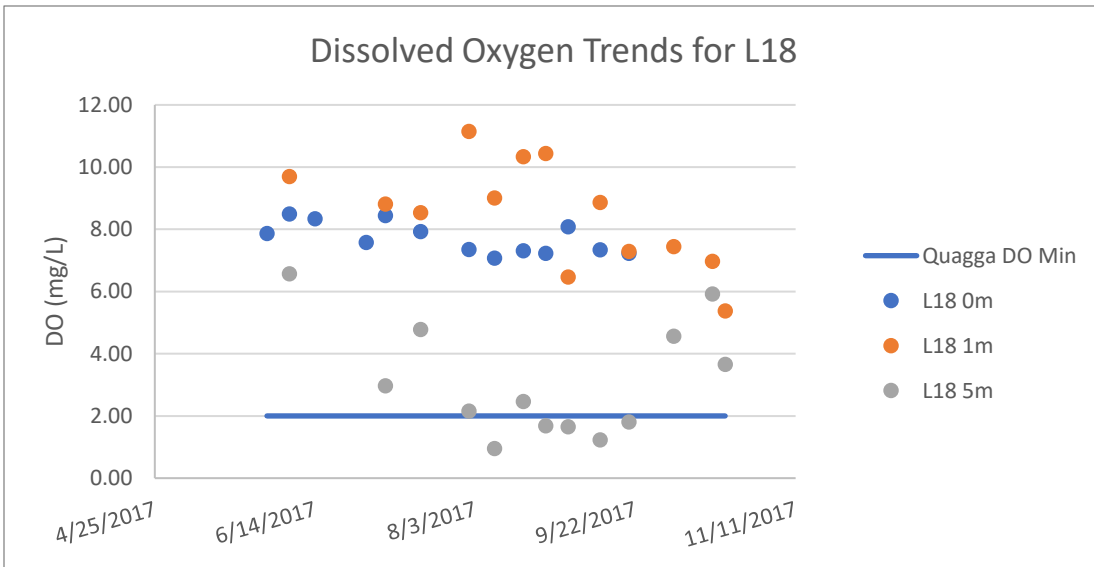
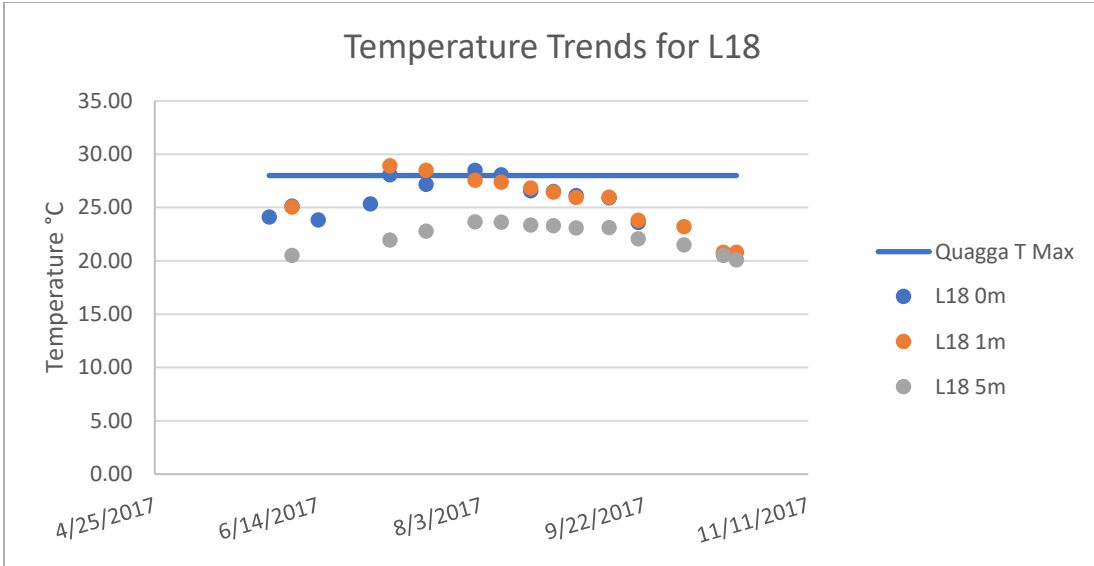


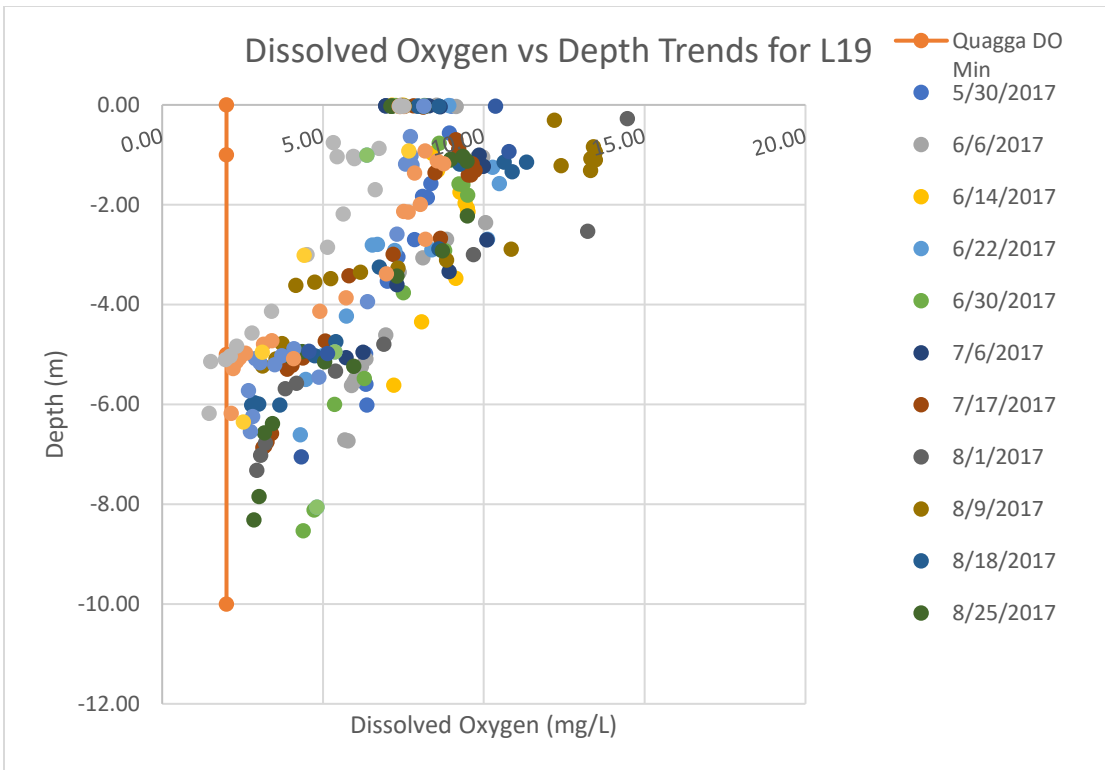
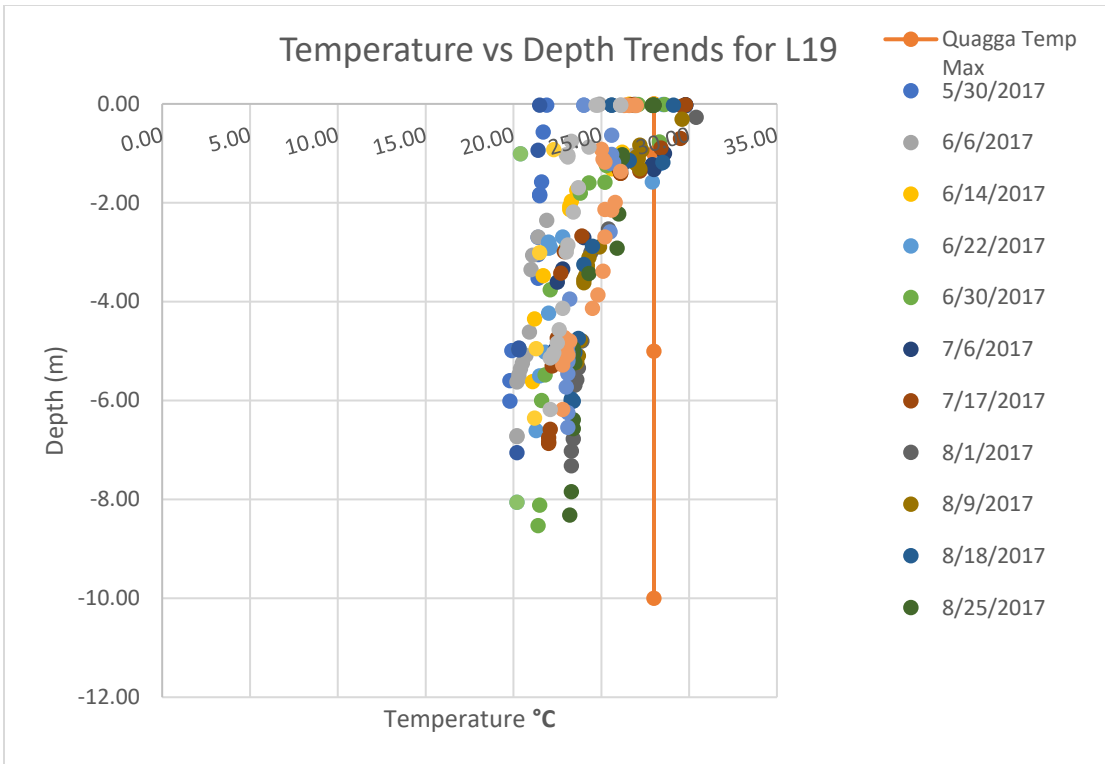


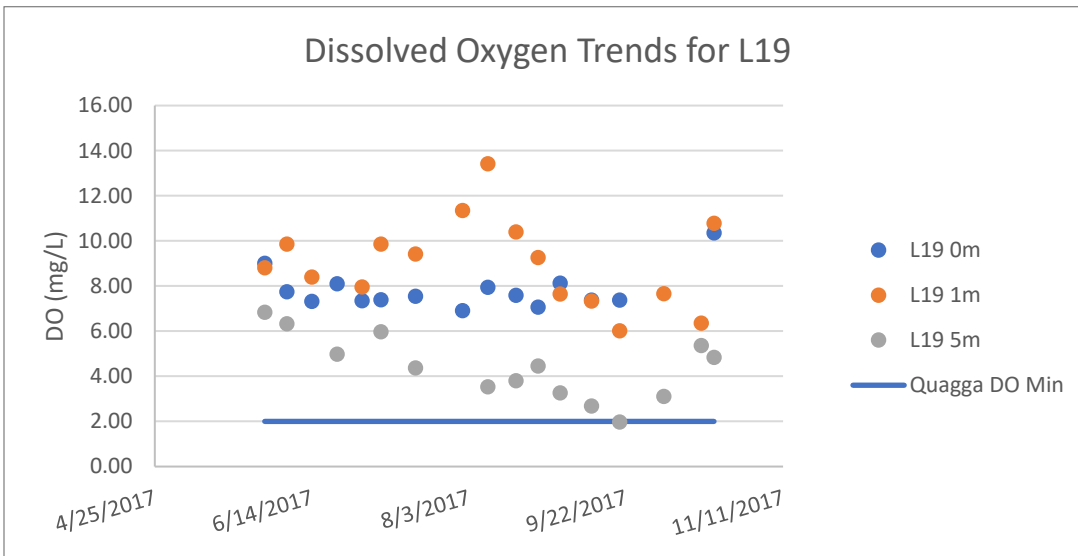
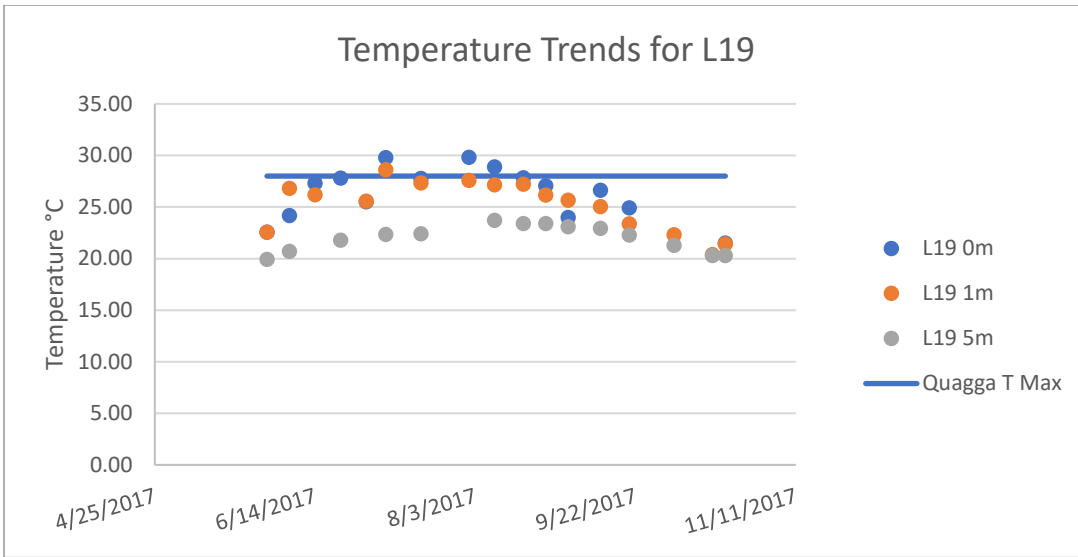


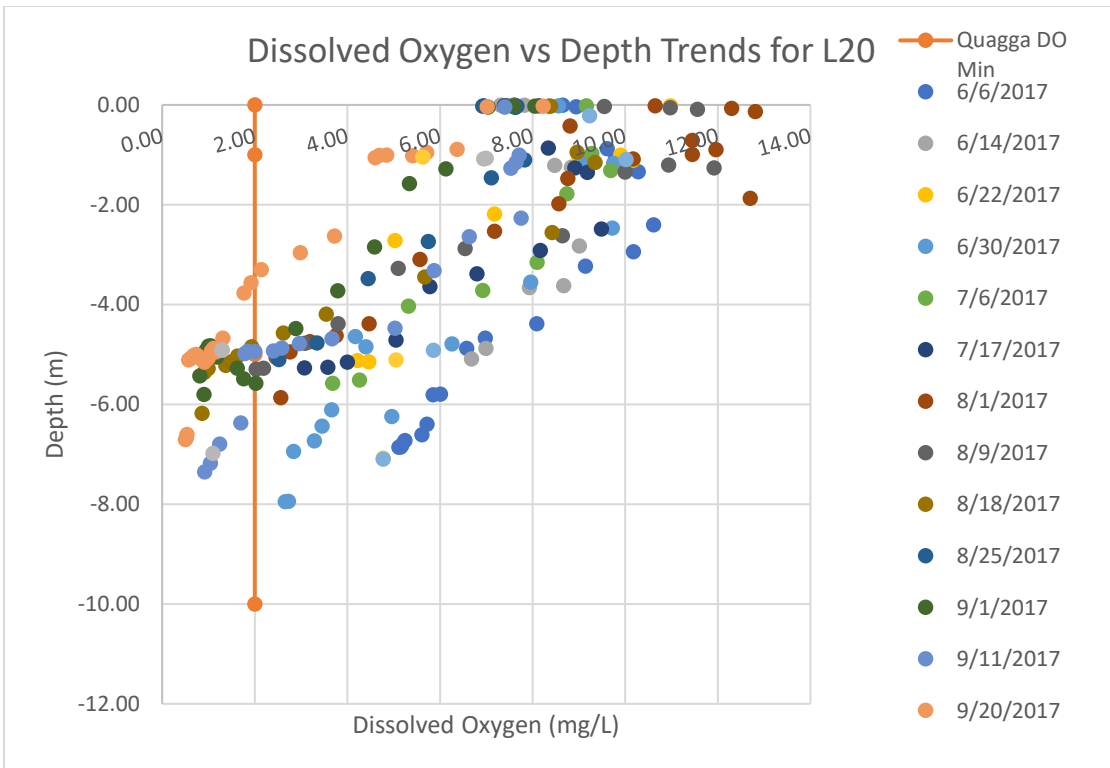
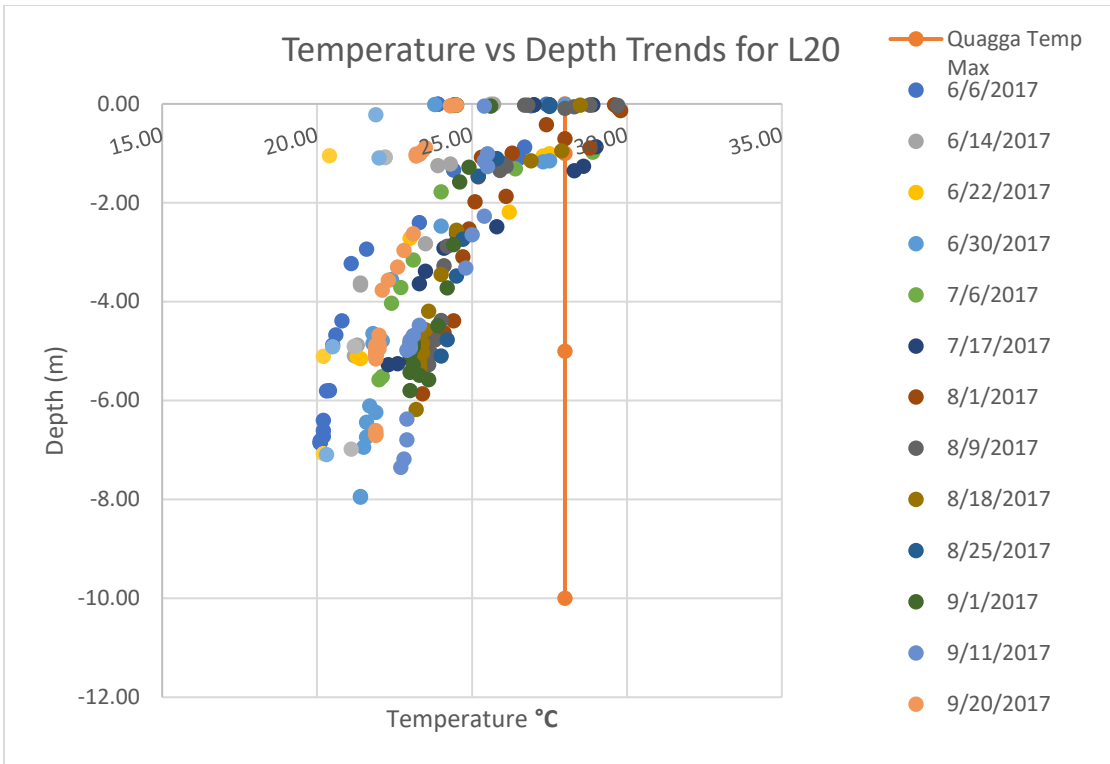


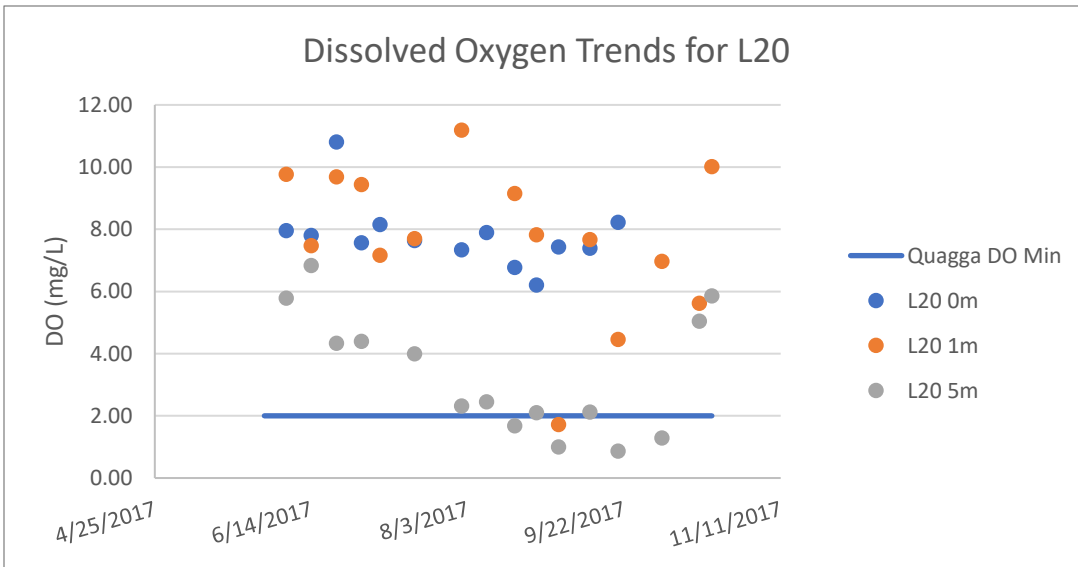
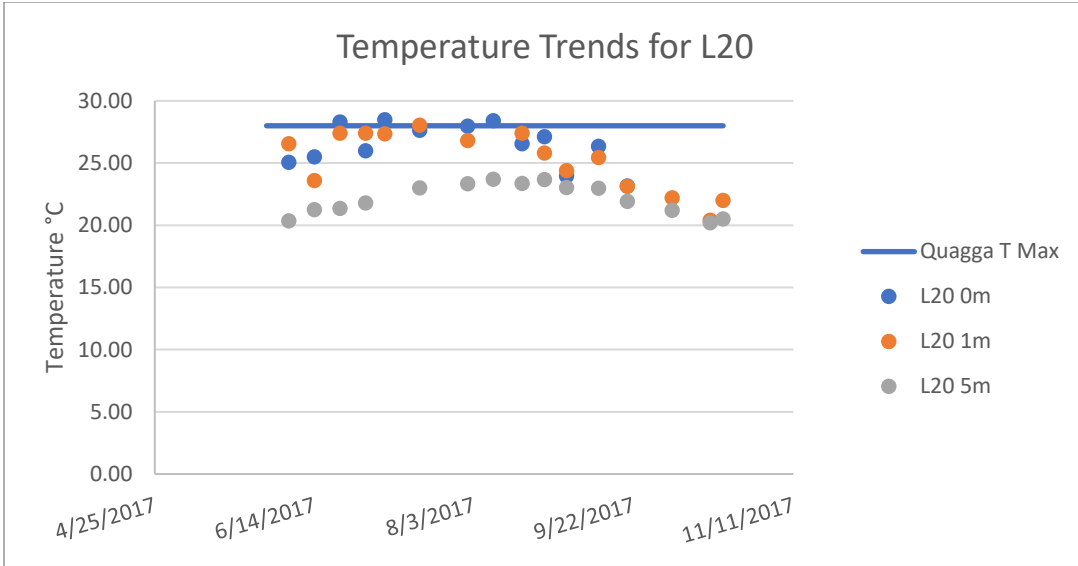


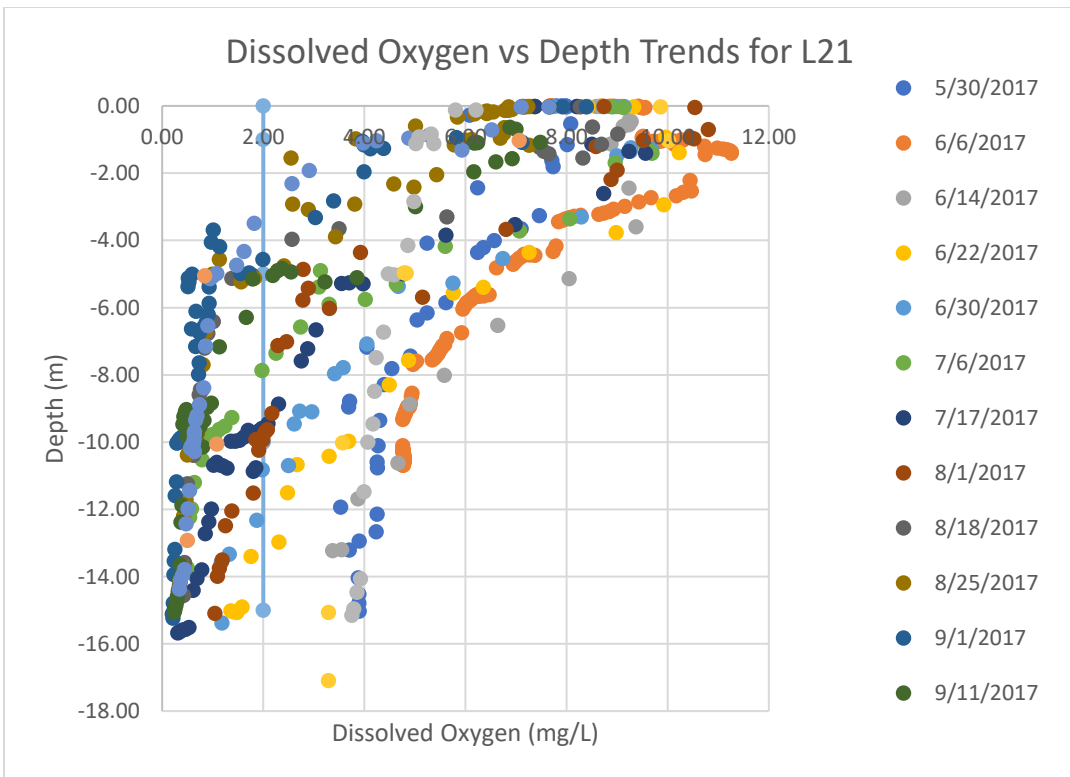
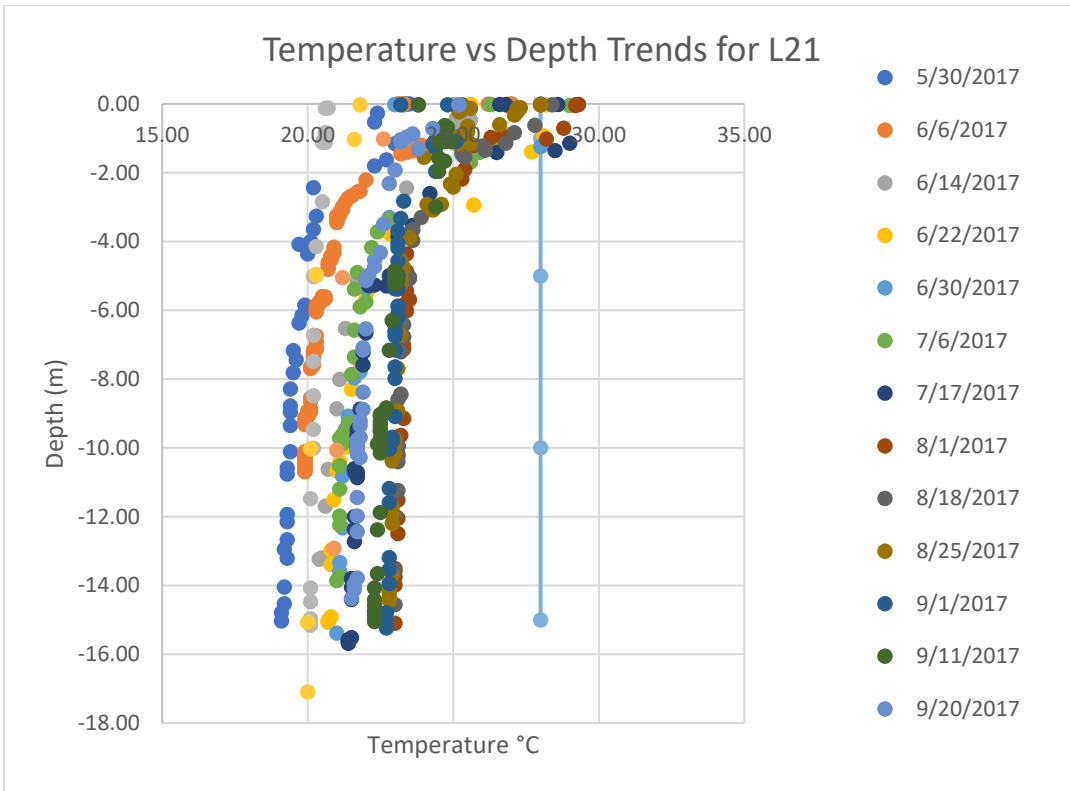


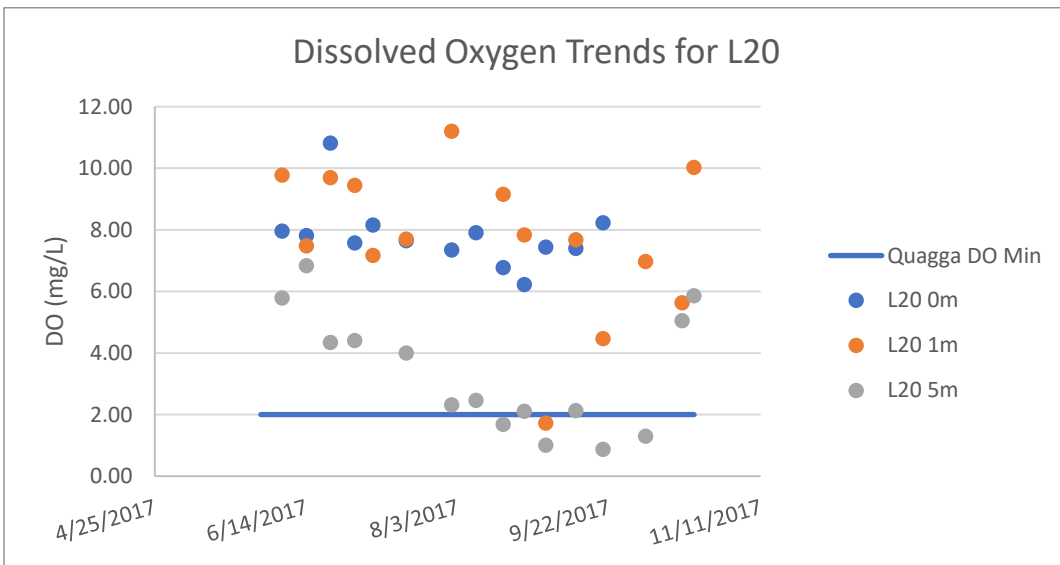
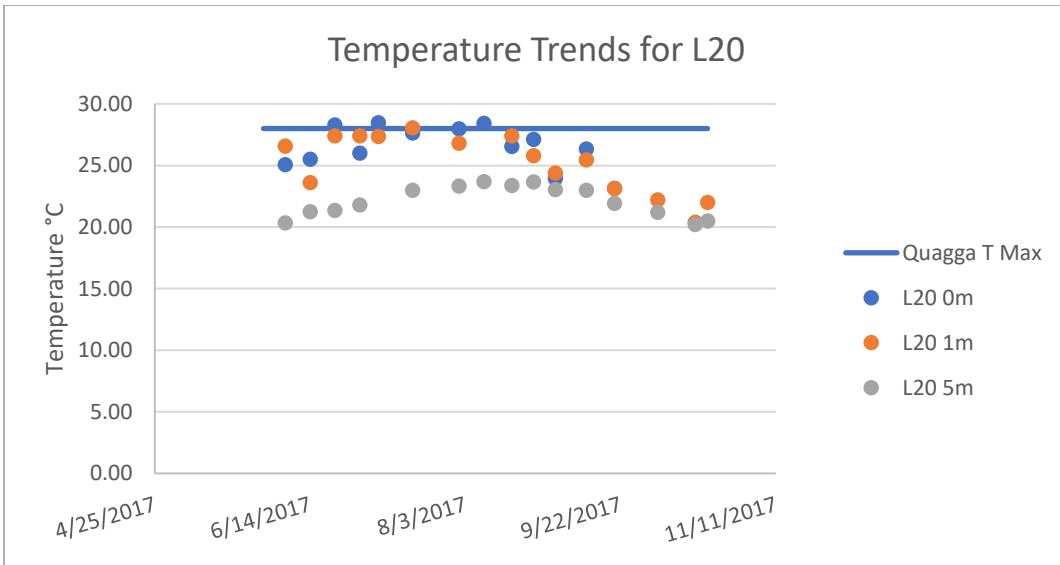












APPENDIX C

DATES OF QUAGGA-INHOSPITABLE CONDITIONS

L01	Date Start	Date End	Days
0m (T)	7/6/2017	7/17/2017	11
0m (T)	9/11/2017	9/27/2017	16
1m (T)			0
5m (DO)	8/18/2017	10/4/2017	47
10m (DO)	6/30/2017	10/4/2017	96
Greatest Depth, 11+ m (DO)	6/30/2017	10/4/2017	96

L02	Date Start	Date End	Days
0m (T)			0
1m (T)			0
5m (DO)	8/1/2017	10/4/2017	64
Greatest Depth, 9+ m (DO)	6/30/2017	10/4/2017	96

L03	Date Start	Date End	Days
0m (T)			0
1m (T)			0
5m (DO)	6/22/2017	7/6/2017	14
5m (DO)	8/1/2017	10/4/2017	64
Greatest Depth, 6+ m (DO)	6/22/2017	10/4/2017	104

L04	Date Start	Date End	Days
0m (T)			0
1m (T)			0
5m (DO)	8/1/2017	10/4/2017	64
10m (DO)	7/6/2017	10/4/2017	90
Greatest Depth, 11+ m (DO)	6/22/2017	10/4/2017	104

L05	Date Start	Date End	Days
0m (T)			0
1m (T/DO)			0
5m (DO)	8/9/2017	9/1/2017	23
5m (DO)	9/20/2017	10/4/2017	14
Greatest Depth, 6+ m (DO)	8/9/2017	10/4/2017	56

L06	Date Start	Date End	Days
0m (T)			0
1m (T)			0
5m (DO)	9/20/2017	10/4/2017	14
10m (DO)	8/1/2017	10/4/2017	64
15m (DO)	7/17/2017	10/4/2017	79
Greatest Depth, 16+ m (DO)	6/30/2017	10/4/2017	96

L07	Date Start	Date End	Days
0m (T)			0
1m (T)			0
5m (DO)			0
10m (DO)	8/9/2017	8/25/2017	16
10m (DO)	9/11/2017	10/4/2017	23
15m (DO)	7/6/2017	10/4/2017	90
20m (DO)	7/6/2017	10/4/2017	90
Greatest Depth, 23+ m (DO)	7/6/2017	10/4/2017	90

L08	Date Start	Date End	Days
0m (T)			0
1m (T)			0
5m (DO)			0
10m (DO)	8/18/2017	9/20/2017	33
15m (DO)	7/17/2017	9/20/2017	65
Greatest Depth, 16+ (DO)	7/17/2017	9/20/2017	65

L09	Date Start	Date End	Days
0m (T)			0
1m (T)			0
5m (DO)			0
10m (DO)	8/1/2017	8/25/2017	24
10m (DO)	9/11/2017	9/20/2017	9
15m (DO)	7/17/2017	10/4/2017	79
Greatest Depth, 16+ m (DO)	7/17/2017	10/4/2017	79

L10	Date Start	Date End	Days
0m (T)			0
1m (T)			0
5m (DO)			0
10m (DO)	8/9/2017	10/4/2017	56
15m (DO)	7/17/2017	10/4/2017	79
Greatest Depth, 16+ m (DO)	7/6/2017	10/4/2017	90

L11	Date Start	Date End	Days
0m (T)			0
1m (T)			0
5m (DO)			0
10m (DO)	7/17/2017	9/28/2017	73
15m (DO)	7/17/2017	10/4/2017	79
Greatest Depth, 16+ m (DO)	7/6/2017	10/4/2017	90

L12	Date Start	Date End	Days
0m (T)			0
1m (T)			0
5m (DO)			0
10m (DO)	8/1/2017	8/18/2017	17
10m (DO)	9/1/2017	9/20/2017	19
15m (DO)	8/1/2017	9/20/2017	50
Greatest Depth, 16+ m (DO)	8/1/2017	9/20/2017	50

L13	Date Start	Date End	Days
0m (T)	8/1/2017	8/9/2017	8
1m (T)	8/1/2017	8/9/2017	8
5m (DO)			0
10m (DO)	9/11/2017	9/20/2017	9
15m (DO)	8/25/2017	9/20/2017	26
20m (DO)	8/1/2017	9/20/2017	50
Greatest Depth, 23+ (DO)	7/6/2017	10/4/2017	90

L14	Date Start	Date End	Days
0m (T)	8/1/2017	8/18/2017	17
1m (T)	8/9/2017	8/18/2017	9
5m (DO)	8/18/2017	8/25/2017	7
10m (DO)	8/1/2017	9/20/2017	50
15m (DO)	7/17/2017	9/20/2017	65
Greatest Depth, 16+ m (DO)	7/17/2017	10/4/2017	79

L15	Date Start	Date End	Days
0m (T)			0
1m (T)			0
5m (DO)			0
10m (DO)	7/17/2017	10/4/2017	79
Greatest Depth, 13+ m (DO)	7/17/2017	10/4/2017	79

L16	Date Start	Date End	Days
0m (T)	8/1/2017	8/25/2017	24
1m (T)	8/1/2017	8/18/2017	17
5m (DO)			0
Greatest Depth, 9+ m (DO)	8/25/2017	10/4/2017	40

L17	Date Start	Date End	Days
0m (T)	8/18/2017	8/25/2017	7
1m (T)			0
5m (DO)	8/9/2017	8/18/2017	9
Greatest Depth, 9+ m (DO)	8/1/2017	10/4/2017	64

L18	Date Start	Date End	Days
0m (T)	8/1/2017	8/9/2017	8
1m (T)	7/6/2017	7/17/2017	11
5m (DO)	8/25/2017	9/20/2017	26
Greatest Depth, 6+ m (DO)	8/1/2017	10/4/2017	79

L19	Date Start	Date End	Days
0m (T)	8/1/2017	8/9/2017	8
1m (T)			0
5m (DO)			0
Greatest Depth, 6+ m (DO)			0

L20	Date Start	Date End	Days
0m (T)			0
1m (T)			0
5m (DO)	9/20/2017	10/4/2017	14
Greatest Depth, 5+ m (DO)	8/18/2017	10/4/2017	47

L21	Date Start	Date End	Days
0m (T)			0
1m (T)			0
5m (DO)	8/18/2017	9/1/2017	14
5m (DO)	9/20/2017	10/4/2017	14
10m (DO)	7/6/2017	10/4/2017	90
Greatest Depth, 10+ m (DO)	6/22/2017	10/4/2017	104